ALTERNATE STIMULI FOR THE ELICITATION OF EVENT-RELATED POTENTIALS

THESIS

Bryan V. Jackson, Captain, USAF

AFIT-ENV-MS-17-M-195

DEPARTMENT OF THE AIR FORCE
AIR UNIVERSITY

AIR FORCE INSTITUTE OF TECHNOLOGY

Wright-Patterson Air Force Base, Ohio

DISTRIBUTION STATEMENT A.
Approved for public release; distribution unlimited.

AFIT-ENV-MS-17-M-195

ALTERNATE STIMULI FOR THE ELICITATION OF EVENT-RELATED
POTENTIALS

THESIS

Presented to the Faculty

Department of Systems Engineering and Management

Graduate School of Engineering and Management

Air Force Institute of Technology

Air University

Air Education and Training Command

In Partial Fulfillment of the Requirements for the

Degree of Master of Science in Systems Engineering

Bryan V. Jackson, BS

Captain, USAF

March 2017

AFIT-ENV-MS-17-M-195

ALTERNATE STIMULI FOR THE ELICITATION OF EVENT-RELATED
POTENTIALS

Bryan V. Jackson, BS

Captain, USAF

Committee Membership:

Dr. Michael E. Miller
Chair

Dr. Brett J. Borghetti
Member

Lt Col Jeffrey C. Parr, PhD
Member

AFIT-ENV-MS-17-M-195

Abstract

Brain-Computer Interfaces (BCIs) are systems that leverage user-brain activity to identify

and perform specific functions. In applications requiring overt visual attention, focusing

on visual stimuli with known temporal variation can elicit measurable changes in brain

activity. However, elements of BCI applications can be intrusive. This research was

designed to determine if Event-Related Potentials (ERPs), to include Steady-State

Visually-Evoked Potentials (SSVEPs), could be elicited and interpreted from less

obtrusive stimuli. Specifically, this research explores the use of variable frequency and

long-wavelength (infrared) stimuli for SSVEP interpretation to explore the application of

less obtrusive stimuli for application in BCIs. It was determined that increasing the

primary wavelength of visual stimuli into the near infrared portion of the electromagnetic

spectrum negatively impacts the observation of ERPs in human subjects. Additionally,

the longer primary wavelengths of visual stimuli have a negative impact on the

observation of target frequency band powers in SSVEP experiments. However, each of

these signals were detected across the majority of participants for Light-Emitting Diodes

(LEDs) with center frequencies as high as 770 nm and across some participants and

conditions for LEDs with center frequencies as high as 830 nm.

Acknowledgments

To Dr. Michael E. Miller, Dr. Brett Borghetti, and Lt Col Jeffrey Parr, thank you for your patience, guidance, and support throughout the course of this thesis effort. To my colleague, Kevin Alexander, thank you for being just as dedicated to this endeavor as I am. Lastly, I thank my wife for being by my side on those very late nights.

<div align="right">Bryan V. Jackson</div>

Table of Contents

List of Figures

xi

List of Tables

ALTERNATE STIMULI FOR THE ELICITATION OF EVENT-RELATED

POTENTIALS

I. Introduction

Background

  Autonomy and automation are two of the Air Force Chief Scientist's focus areas

for increasing capabilities and cost savings by increasing manpower efficiencies and

reducing manpower needs (Endsley, 2015a). Challenges encountered in the

implementation of autonomous and automated agents are centered on system limitations

constrained by the designers' vision, programming, and limited data available to

understand the operating environment. This leads to the continued need for human

intervention to handle situations for which the autonomous or automated agent has not

been designed (Endsley, 2015b). The Air Force's Science and Technology vision aims to

capitalize on the agility, innovation, and intelligence of the human and the advanced

capabilities of autonomy to create effective teams able to accomplish mission activities

smoothly, simply, and seamlessly.

  To be successful, the approaches for creating these effective teams must be

human-centered and provide effective user interfaces that can support the operator's

requirements for informed trust, manageable workload, adequate situation awareness, and

ease of interaction. This flexible autonomy is critical to the performance of the human-

autonomy team, and the interfaces must address key design guidelines and

communication shortcomings.

One technology that may be useful in addressing the communication shortcomings of current human-autonomy teams is the Brain-Computer Interface (BCI). There are multiple reasons for wanting to connect a person's brain to a computer. For example, a person with Amyotrophic Lateral Sclerosis (ALS), also known as Lou Gehrig's disease, whose muscle control has decreased such that they can no longer speak, walk, or write may benefit from the use of a BCI to interact with their environment. Additionally, paraplegics and other persons with limited mobility or communication may find it more efficient or effective to use a BCI in any given situation than to rely on their own faculties. Persons with impaired muscular function, caused by degeneration of pathways from the brain to muscle, can have their brain activity amplified and fed into a computer with the appropriate algorithms to process them thereby providing another communication channel for the user (Prueckl & Guger, 2009). Visually-Evoked Potentials (VEP) have been used within the disabled community to create BCIs. VEPs are a voltage response, in the brain, to events or stimuli; therefore, they are considered Event-Related Potentials (ERP). BCIs that utilize ERPs "exploit the fact that the neural processing of a stimulus can be modulated by attention. In particular, attention to an event can enhance the positive and negative peaks of the ERP time-locked to this event. ERP-based BCIs attempt to detect these modulations to infer the stimulus that the user intended to choose," and systems which rely on this phenomena could be used to reflect user attention in various applications (Treder & Blankertz, 2010). Often, VEPs are generated when the user focuses their visual attention on localized flickering light sources to trigger programed responses in the BCI. By determining the particular visual stimuli

upon which the user is focused, the computer can activate a set response corresponding to that source.

Although this interface has not received acceptance by the broad user community due to distractions caused by the visible flickering of light, recent observations made by the National Aeronautics and Space Administration (NASA) suggest there may be room to improve the interface by using non-disruptive stimuli. In an experiment using VEP to understand user attention and fixation during flight simulation, NASA reported unexpected responses which they initially attributed to infrared emitters in a SmartEye Eye Tracking System. This observation raised the question of whether nonvisible or flickering lights could be used to invoke a VEP that could be measured and applied within a BCI, removing the distraction caused by visibly flickering lights associated with BCIs applying VEP (K. Kennedy, personal communication, August 16, 2016).

Current interfaces provide necessary communication channels between the users and the systems; however, there is room for improving many of the interfaces we take for granted. A computer mouse can be applied to complete a task such as selecting a button or icon within a user interface. However, this simple task typically requires the user to complete multiple subtasks including identifying an action to complete, grabbing the mouse, moving the mouse to translate the cursor to the desired location, and clicking on the mouse button to complete the task. During this process, it is not uncommon for a user to move the point of eye fixation from the button they wish to select on a display to the mouse and back multiple times. There is potential for this and other systems to be improved by reducing the number of subtasks and the time required to complete these subtasks through the use of BCIs. Such systems are those such as computer-based tasks

(even using the keyboard), home entertainment options like changing television channels, and replacing or compensating for disabilities. Even applications requiring near instantaneous decision-making, such as targeting tasks executed during military operations or selecting a person of interest during surveillance and reconnaissance missions, could benefit from reducing the number of subtasks and the associated time it takes to complete essential tasks.

Problem

Although current interfaces meet the needs of the users relying upon them to interface with their associated systems, there are many areas for improvement, which could benefit these user groups. Computer systems rely on the user interacting with keyboards or mice to communicate their desires to the computer, and these interfaces inject additional tasks into the process of completing any action with a computer. Other systems that use gaze trackers or muscle movements are also hindered by the lack of accuracy associated with determining the user's intentions/desires and by lacking depth of control, which would allow the user to communicate desires in three dimensions. Even the acceptance of current VEP-based interfaces is hindered by the disruption provided by the associated flashing lights.

Objective

This research sought to determine if Event-Related Potentials (ERP) can be elicited and measured with minimal intrusiveness and disruption to the user by using non-flickering visual stimuli or stimuli which emit energy outside the human visible range and an EEG to interpret the brain's responses to these stimuli. The stimuli of concern in

4

this research are near infrared or short wavelength infrared LEDs, and visible Light

Emitting Diodes (LED) operating at frequencies faster than humans can perceive.

Justification

A primary issue in the Human-Machine Teaming thrust within AFRL's

Autonomy Research Strategy is improving the bandwidth of communication between the

human and the machine. This barrier exists for multiple reasons including significant

differences in communication speed between the human and the system, the differences

in specificity of communication each element expects, and the machine's inability to

sense and respond to implicit human communication modes. Significant research has

been conducted towards reducing this barrier in recent years, often including methods to

assess human state information. For example, systems have been explored which

incorporate eye tracking, physiological monitoring, and monitoring and learning

relationships between changes in human behavior and psychological state. Despite this

research, each of these technologies has limitations that have slowed their adoption.

Scope

The research effort leverages past lessons learned in the development and

application of BCIs to investigate the use of VEP that do not suffer from the distraction

produced by today's flickering VEP BCI devices. The tasks essential to completing the

research and answering the research questions are the development of the test bed and

development of methods for evoking Event-Related Potentials, recording potential-

related signal data, and interpreting potential-related signal data.

Hypothesis

The hypothesis of this research is that Event-Related Potential energy can be generated in the human brain in response to non-flickering LEDs emitting light between 640 and 940 nm, and this response can be interpreted using EEG collected data. Additionally, frequencies as high as 60 Hz can be used to produce discernable Event-Relate Potentials when presenting peak wavelengths between 640 nm and 940 nm.

Research Questions

This research is focused on answering the following questions:

a) How does the wavelength of light emitted from Light-Emitting Diodes affect the signal characteristics of Event-Related Potentials produced in the human brain? More specifically, which wavelengths of light-emitting diodes can be used to elicit VEPs in the visual cortex?

b) How does the frequency of light produced by Light-Emitting Diodes affect the characteristics of Event-Related Potentials produced in the human brain? More specifically, can oscillatory frequencies above the human CFF be used to elicit oscillatory responses in the visual cortex without producing the visual perception of flicker?

Methodology

A literature review was conducted to determine the characteristics of past research efforts, which led to the successful production of Event-Related Potentials, successful signal feature extraction, and successful analysis of signal features able to be used in

6

practical BCI design. These design elements were incorporated into the design of research to reduce the likelihood of injecting error into the research and increase the likelihood of producing discernable results.

This literature review was used to guide the specification and construction of a test bed. This test bed includes signal elicitation, data acquisition, and signal analysis components. When the user focuses their attention on a temporally-varying stimuli, a temporally varying electrical response is created in the visual cortex. In turn, this response is captured using EEG and recorded as signal data and voltage readings within an EEG program. The data is then analyzed to determine if there is a neurological response to the stimuli.

A Human-in-the-Loop experiment is then conducted in which a group of participants were exposed to 5 breadboards equipped with visible, near-infrared, and short wavelength infrared LEDs. The EEG monitored signals from regions of the brain consistent with the VEP. Signal analysis was performed to reduce noise and isolate signal components to correlate the findings. Additional data analysis included plotting each subject's spectral results and topographical maps for visual inspection of brain responses.

Implications

This research demonstrates the potential for using non-obtrusive stimuli for evoking ERPs in human subjects. The findings could lead to the development of improved training systems and operational systems that can enable time-specific feedback to the user and communication to the other agents based on specific user

attention versus generalized 2-D observations of gaze and reliance on post event information recall to identify user attention. These systems could be integrated into DoD and civilian applications to improve the effectiveness and efficiency of the system.

Document Overview

The remainder of this document follows the format of a traditional five chapter thesis. Chapter II captures the review of literature deemed relevant to the design and execution of this research. Chapter III provides a summary of methods pursued in the research and a final approached used to collect and analyze data from participants. Chapter IV provides the results from the data collection and analysis processes with graphical representation of observations. Finally, Chapter V provides a summary of the findings and observations from the data collection and analysis efforts. Additionally, Chapter V provides a discussion of the limitations assumed in the completion of the research and some future research approaches that could reduce the impact of these limitations.

II. Literature Review

Chapter Overview

The purpose of this research was to explore the feasibility of using LEDs that produce long wavelength energy and LEDs oscillating beyond the Human Critical Fusion Frequency (CFF) as target stimuli in a Brain-Computer Interface-based experiment by evaluating the production of Event-Related Potentials (ERPs) and more specifically Visual Evoked Potentials (VEPs). This research is complementary to previous research that focuses on the use of flickering LEDs as stimuli to generate electrical potentials in a human subject's cerebral cortex. These flickering LEDs are typically used in laboratory environments and in situations where the flickering light does not impede task performance; however, the goal is to determine whether non-flickering LEDs could potentially be used as a tool to collect data with minimal intrusiveness to the subject.

The use of LEDs to generate VEPs in human subjects is well documented for visible light LEDs operating at frequencies between 1 and 100 Hz (Herrmann, 2001; Prueckl & Guger, 2009; Sakurada, Kawase, Komatsu, & Kansaku, 2015; C. H. Wu et al., 2011). This research is relevant to the design of experiments to assert the potential to generate VEPs with non-visible light from LEDs. The elements within the prior literature most relevant to the current research are VEP signal generating methods, signal reception methods, signal decoding methods, spectral analysis methods, experimental design, and experimental procedures.

This research effort hinged upon the design of experiments used to elicit VEPs; therefore, the focus of this literature review was peer-reviewed journal papers, books, and

9

test reports. Although the applicability of this research is geared toward the development of BCIs, this research is focused on identifying our ability to use unobtrusive stimuli to evoke cortical responses. To that end, this chapter focuses on imaging methods, stimulation methods, signal analysis methods, and test bed design.

Introduction

Event-Related Potentials are voltages occurring in the brain in response to sensory, perceptual motor, or cognitive events: "They are thought to reflect the summed activity of postsynaptic potentials produced when a large number of similarly oriented cortical pyramidal neurons fire in synchrony while processing information" (Sur & Sinha, 2009). Event-Related Potentials include any potential energy in the brain that is created in response to auditory, visual, tactile, motor, and cognitive stimuli (Teplan, 2002). ERPs that occur in response to any of the aforementioned stimuli are generally categorized according to the form of the stimuli that caused the response (e.g., Motor Evoked Potentials, Auditory Evoked Potentials, Visual Evoked Potentials, etc.). In the literature of primary interest, it was found that one term, Event Related Potential (ERP), was used to classify responses generated by visual, auditory, and tactile stimulation. (Landa, Leos; Krpoun, Zdenek; Kolarova, Martina; Kasparek, 2014; Sur & Sinha, 2009; Treder & Blankertz, 2010). Generally, the term "ERP" is used when neural potentials are discussed and examined in the time domain with the onset of the visual stimuli being represented at the origin and neural activity being represented after the onset of the stimuli. However, when stimulated by visual means and measured across the visual cortex the term Visual Evoked Potentials is used and represents the information that

highlights the function of the visual system (Kraemer, Abrahamsson, & Sjostrom, 1997).

A subset of the Visual Evoked Potential that is also relevant to this research is the Steady-State Visual Evoked Potential (SSVEP). The SSVEP is the periodic response to a periodic modulation of an exogenous visual stimulus (Gao, Wang, Gao, & Hong, 2014; Norcia, Appelbaum, Ales, Cottereau, & Rossion, 2015). Matching the stimuli's identified modulation frequency and the subject's associated frequency response to one another allow the identification of covert attention when multiple visual stimuli are present (Wang, Wang, Gao, & Hong, 2006). Actions such as fixating visual attention on an object in an environment can be interpreted as intent to select the item, permitting users to provide a response based on the associated stimulus by simply maintaining visual fixation and attention on that object. One system that can leverage the ERPs is a Brain-Computer Interface (BCI).

Types of Brain-Computer Interfaces

A BCI is a tool or system that enables information, in the form of electrical signals, to pass from the human brain to a computer or some other output device (Gao et al., 2014). A BCI that leverages the visually evoked ERP feature is considered a gaze dependent system because it requires the user to focus their attention on a desired stimuli (Wolpaw, Birbaumer, McFarland, Pfurtscheller, & Vaughan, 2002). The figure below provides a visual representation of a generic BCI concept. There are multiple reasons for wanting to connect a person's brain to a computer. For example, a person with Amyotrophic Lateral Sclerosis (ALS), also known as Lou Gehrig's disease, whose muscle control has decreased so much that they can no longer speak, walk, or write may

benefit from the use of a BCI to interact with their environment (Diez et al., 2013; Treder & Blankertz, 2010; Wang, Gao, Hong, Jia, & Gao, 2008). Additionally, paraplegics, other persons with limited mobility or communication ability, and persons without disabilities may find it more efficient or effective to use a BCI in any given situation than it is for them to rely on their own capacities (Graimann, Allison, & Pfurtscheller, 2010; Yin et al., 2013).

There are multiple methods for connecting the brain to computers and transmitting changes in brain activity, and some methods for applying BCIs, if highly effective, have the potential to increase the information exchange rate between humans and machines by reducing the need for complex motor movements required when interacting with a computer. These methods are easily organized into two groups, the invasive BCIs and the non-invasive BCIs. These two classes of systems are largely differentiated by the method used to image brain activity.
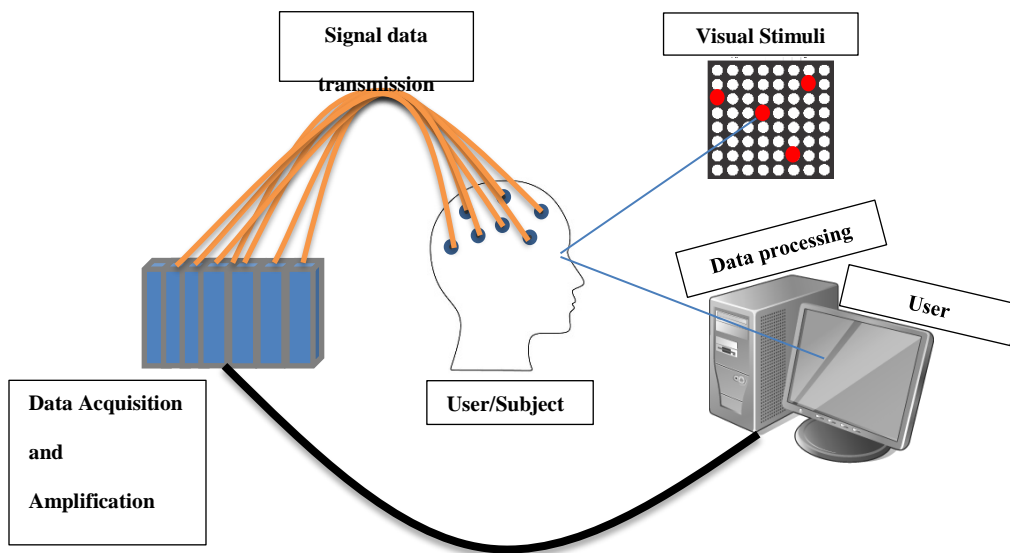
Figure 1 - Generic example of components necessary in a Visual Evoked Potential based Brain-Computer Interface

Imaging Methods

The changes in brain activity can be observed by using either electrocorticography (ECoG) or electroencephalography (EEG) to measure the voltage activity across different regions of the brain. The use of ECoG is not as common as EEG in research or practical applications because of ECoG is an invasive method for collecting data, and it is less acceptable than EEG to users (Wang et al., 2008). ECoG requires epidural electrode strips to be implanted over the regions of the brain of concern in applications. EEG, however, typically relies on electrodes in contact with the epidermis and is much less invasive to the user. In a BCI application, both EEG and ECoG are used to transmit the user's intent, via brain signal data, from the user to the signal processor.

ECoG-based BCIs are a rather invasive method for data collection because it relies on the subject consenting to the surgical application of sensors to the brain. The ECoG-based BCIs have a high signal to noise ratio, which is preferable in the application of BCIs (Lee et al., 2006; Singla, Khosla, & Jha, 2014; Z. Wu & Su, 2014). However, the EEG-based BCIs are more practical because they are more acceptable to subjects because of their non-invasiveness (Wang et al., 2008). It seems unlikely to encounter participants who are willing to consent to using ECoG unless they feel a dire need for it. The majority of research involving ECoG for the imaging of brain signal data employs persons with ALS (Wang et al., 2008). Figure 2 illustrates the placement of an EEG cap on a participant. In addition to the potential for causing irrevocable damage to a subject, it would be impractical to find persons who are qualified to apply these ECoG sensors to subjects for this experiment.

Figure 2 – Electroencephalogram (EEG)

It is believed that EEG works by measuring the summation of voltages generated when the release of neurotransmitters at dendrites of cortical pyramidal cells causes current flow between the apical dendrites and the cell walls to build up and to create dipoles at thousands of neurons at the scalp (Luck, 2005a; Sur & Sinha, 2009). While electrical fields are created whenever there is synaptic activity, the resultant voltages are only measurable with EEG when thousands of neurons exhibit this synchronous activity.

EEG can be an inexpensive solution for providing an imaging solution for BCI-type applications. Additionally, EEG systems do not require surgical procedures or extensive training to begin collecting data from human subjects. Compared to other systems, EEG provides an increased ability to distinguish between changes within specific time intervals in the signal data (Ferreira, Miranda, Miranda, & Sakamoto, 2013; Graimann et al., 2010; H. J. Hwang, Kim, Choi, & Im, 2013). However, EEG is not without limitations and is susceptible to noise artifacts at each sensor location that occur

14

because of the compounding brain activity occurring between neural networks and the scalp sensor locations (Burle et al., 2015; Cheng, Gao, Gao, & Xu, 2002).

Stimulation Methods

BCIs are constructed to leverage a variety of human senses (e.g., visual, auditory, physical, etc.) to generate evoked potentials related to external stimuli but also can leverage internal processes based on cognition and motor functions (Norcia et al., 2015). These evoked potentials are categorized based on the modality and features of the external stimuli, and the modality most relevant to this research is the visual-evoked potential. Some BCIs rely on VEPs to determine the signal that is being generated by any given stimulus (Cilliers & Van Der Kouwe, n.d.; Wang et al., 2006). VEPs are measurements of the brain's electrical activity in response to stimulation along the pathway of the optic nerve and are primarily captured in the occipital lobe of the brain. These measurements are used to understand a person's focus and, presumably, intent in order to provide a response based on the associated stimulus. There are numerous research efforts that have explored the influence of gaze and focal attention on VEP amplitudes and latencies (H.-J. J. Hwang et al., 2015; Treder & Blankertz, 2010). The paradigms under which experiments, relevant to this research, are frequently categorized are time-phased responses, steady-state visual evoked potentials (SSVEPs), and flash visual evoked potentials (FVEPs). Research regarding each of these responses are

covered in the following sections of this chapter (H. J. Hwang et al., 2013; Wang, Yijun; Gao, Xiaorong; Hong, Bo; Gao, 2010).

Time-phased responses to the onset or offset of visual stimuli are generally referred to as visual-P300 responses (Citi, Poli, Cinel, & Sepulveda, 2008; Donchin, Spencer, & Wijesinghe, 2000; Yin et al., 2013). P300 responses are thought to be caused by cognition in scenarios that follow the oddball paradigm, which include the random presentation of target stimuli to the human subject (Lenhardt, Kaper, & Ritter, 2008). However, the responses are ERPs whose waveforms are examined in the time domain for categorization and any of the features could be used to identify the brain's processing of the stimuli. In the time domain, these potentials are most frequently categorized according to the direction of their deflection (P = Positive and N = Negative), the latency of the amplitude (e.g., 100 = 100ms, 200 = 200ms, 300 = 300ms, etc.) occurrence relative to stimuli, or the order of the amplitudes occurrence (e.g., P2 = the second positive deflection) in a time-phased plot (Landa, Leos; Krpoun, Zdenek; Kolarova, Martina; Kasparek, 2014). Generally, a time-phased ERP plot would capture the ERP at some time point before the presentation of a stimuli all the way through and beyond the presentation of the stimuli and for a one second period as presented in the following figures (iMotions, 2016).
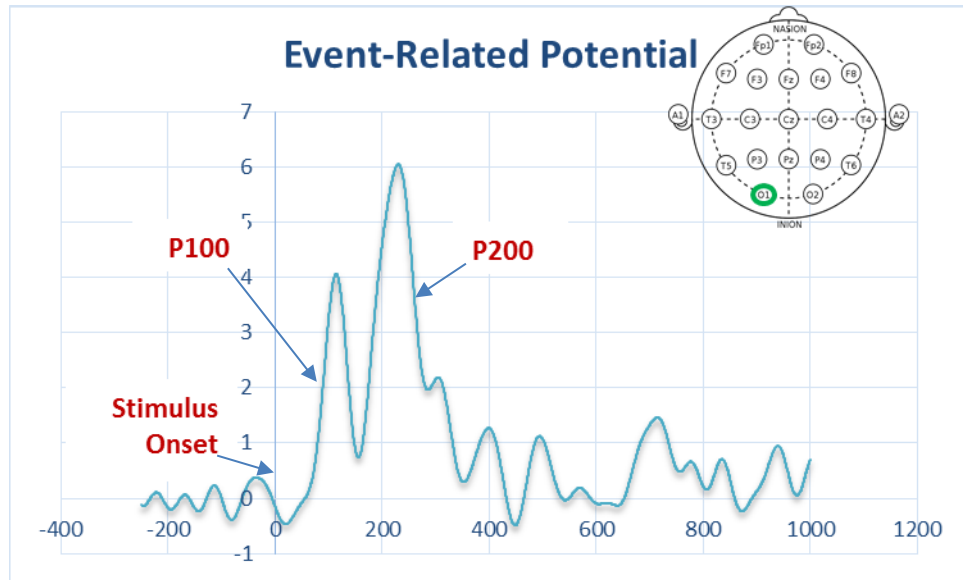
Figure 3 - Time-based ERP plot example showing categorization of response according to latency

An FVEP relies on the visual flashes of information (e.g., experiments using LEDs to generate flashes) to generate specific data while a subject focuses on one stimulus after another. The FVEPs are time and phase-locked to flashed onsets of the stimuli. This method was preferred in one study because it allowed the use of mutually independent flickering sequences generated by random ON–OFF durations and used the timing of flash onsets to segment EEG data followed by simple averaging (Lee et al., 2006). However, it does not appear to be a desired method for BCI applications, rather, it is used in situations when a person is unable to focus on specific stimuli or patterns or when conducting medical evaluations for disease identification (Tartaglione, Spadavecchia, Maculotti, & Bandini, 2012). Only peak-to-valley amplitudes, rather than

correlation values or power spectrum, are computed and compared to easily determine the target stimuli upon which the subject is focused.

A Steady-State Visual Evoked Potential (SSVEP) is an oscillatory cortical potential that occurs in response to visual stimulation at the same frequency as the observed stimuli (C. H. Wu et al., 2011). These signals may be triggered by any repeatedly flashing light, such as your computer screen refreshing every 60 Hz and have been observed at frequencies from 1 to 100 Hz (Herrmann, 2001; Z. Wu, 2016). By viewing a light flashing at a particular frequency, the visual pathway is stimulated and causes the frequency to radiate throughout affected areas of the brain. This stimulation produces electrical signals at both the base frequency and multiples thereof (Wang et al., 2008). Oscillations occurring after and phase-locked to the on/offset of the stimuli are categorized as evoked oscillations (Herrmann, 2001). Additionally, the use of SSVEP-based systems can allow the system to distinguish between the user's intent when multiple stimuli are present because the neural response to events or stimuli can be increased by attending to the stimuli versus observing the event through one's periphery (Treder & Blankertz, 2010). SSVEPs also enable the reduction of false positive identification of stimuli through identification of the stimulus frequency (Wang et al., 2006). SSVEP-based methods require control of the oscillations of the light source (e.g., controlling update rate of a stimulus area on a monitor, power level and oscillation of LEDs, etc.) and do not require much training. However, SSVEP experiments may be impacted by random alpha rhythm noise artifacts that may arise at frequencies below 14 Hz (Lee et al., 2006). Additional features called harmonics may occur in the amplitude spectrum associated with SSVEPs due to nonlinear information transference in the visual

system (Wang et al., 2008). Harmonics can be identified as the summation of sinusoidal waveforms that are equivalent to integer multiples of one another. In a periodic SSVEP function, the harmonics may be captured at these integer multiples of the base frequency when analyzing the PSD of the measured neural activity. This method is often preferred when creating BCIs because of the minimal training requirements relative to other BCI methods (Yu Zhang, Zhou, Jin, Wang, & Cichocki, 2015).

Signal Analysis

Generally, the analysis of ERPs involves steps to emphasize the elicited response over surrounding noise artifacts, identify the relative density of the response power of a window of frequencies, identify signal-to-noise ratios, and categorize the components of the identified response. For time-based responses, analysis includes visual inspection of the measured waveforms to include, component identification, amplitude measurement, latency measurement, and ordinal identification. The component measurements facilitate the identification of specific types of brain responses, such as the recognition of object in an oddball task by identifying the P300 component in the ERP. Frequency-based responses almost always include some form of Power Spectral Density analysis to separate and identify amplitudes of responses occurring at multiple frequencies. Additional analysis for both response types include statistical analysis of the factors affecting the experiment and its outcomes by using the Analysis of Variance (ANOVA) tests against each factor; however, no literature capturing the use of statistical analysis to identify responses against noise were identified, and it appears that visual inspection is the primary method for identifying responses to stimuli.

19

Independent Component Analysis (ICA) is associated with FVEPs and is employed to decompose measured EEG and associated data for data reconstruction (Lee et al., 2006). This method is used to separate the FVEP portion of data from the EEG recordings (Lee et al., 2006). "Electrical signals from the brain are decomposed into independent components (ICs) by means of solving a matrix in which each column represents a spatial map tailoring the weights of the corresponding temporal component at each EEG sensor. Task-related ICs are screened and identified by correlating their spatial maps with a pre-defined spatial template, which is created based on the spatial weight distribution of the P2 peak in a conventional FVEP obtained from each individual" (Lee et al., 2006). This method relies on the averaging of VEPs from peripheral and directed stimuli to determine where the subject's attention is directed. Additionally, this method is also appropriate for ERP and SSVEP experiments because the underlying assumptions of EEG data representing linearly mixed signals still hold, and ICA is targeted at separating and analyzing these mixed components (Urigüen & Garcia-Zapirain, 2015).

Canonical Correlation Analysis (CCA) is used to measure the relationship of one multi-dimensional data set to another (Urigüen & Garcia-Zapirain, 2015; Yu Zhang, Jin, Qing, Wang, & Wang, 2012). "CCA is a multivariable statistical method for seeking linear combinations that maximize the correlation between two sets of data" (Yangsong Zhang, Xu, Cheng, & Yao, 2014). CCA can be leveraged by correlating one or more input signals to an electrical signal of concern where the input signal with the highest correlation to the electrical signal can be identified as the signal to which the user is responding. CCA has proven appropriate for analysis of SSVEP experiments and often

outperforms Power Spectral Density (PSD) analysis, but CCA may suffer from over-fitting due to the lack of data relevant to the trial being included in the pre-constructed sine and cosine waveforms used as references (Yu Zhang et al., 2015).

PSD analysis is a type of frequency-domain analysis in which a structure is subjected to a probabilistic spectrum of harmonic loading to obtain probabilistic distributions for dynamic response measures and is most frequently used to detect SSVEP responses (Middendorf, McMillan, Calhoun, & Jones, 2000; Wang et al., 2008). A root-mean-square (RMS) formulation translates the PSD curve for each response quantity into a single, most likely value. Because PSD curves represent the continuous probability density function of each response measure, most of the integrated area will occur near the resonant frequencies of the structure. This means that the average power of the signal over the chosen frequency band will be calculated, and the stimulated frequency may be identified as the frequency with the highest average power. Fast Fourier Transform (FFT) changes a wave from the time domain to the frequency domain and is a method for analyzing the signals generated by SSVEPs (Singla et al., 2014). Additional, complex, methods for leveraging an FFT can be used to reuse stimulation frequencies in singular experiments by identifying phase shifts in the frequency-based neural response through phase information detection. It is worth noting that the design of the stimuli for a phase-locked SSVEP experiment is important and requires a stable phase for each of the stimuli (Wang et al., 2008).

Test Bed Design

In addition to using an EEG based test bed, it is important, for reflection of practical systems, to design a system that is affordable. Computers are typically used to address all of the processing requirements associated with the experiments; however, Digital Signal Processors (DSP) can be used to relieve the user/subject of the requirement to have a computer that has the cost associated with functionality required for analysis (Wang et al., 2008). To further reduce cost, EEG use can be limited to the occipital region of the brain, limiting the number of channels of data that must be processed. This limitation is acceptable as the occipital region is nearest the visual cortex and, therefore, is the area most likely to reflect VEP activity (Wang et al., 2008).

Another cost cutting method employed is the use of computer monitors and embedded components to execute experiments. The majority of SSVEP-based experiments used the visual display and color ranges already existing in computer monitors. The known refresh rate associated with common computer monitors (i.e., Liquid Crystal Displays (LCDs), Cathode Ray Tube (CRT), LED, and Thin-Film Transistor (TFT)) enables researchers to easily account for it in the data collection and signal analysis stages of experiments (Treder & Blankertz, 2010; Wang et al., 2008). LEDs have been used in a number of BCI-based ERP experiments to provide visual stimulation for the subject (Herrmann, 2001; Prueckl & Guger, 2009; Sakurada et al., 2015; C. H. Wu et al., 2011). LEDs provide an inexpensive and controllable stimuli to which subjects can attend and come in a variety of sizes, colors, and power levels that can be controlled with simple adjustments to circuits. It is common to control the oscillations of the LEDs, when not using a computer monitor as a stimuli, by programming

microcontrollers to provide precise control of the timing of the LEDs' oscillations (H.-J. J. Hwang et al., 2015; Kuś et al., 2013; Wang et al., 2008; C. H. Wu et al., 2011). LEDs are an attractive choice for experiments that require precise and independent control of multiple stimuli.

Conclusion

The accuracy associated with both SSVEP and FVEP are above 80%, so either would be considered reliable for the purpose of this research (Lee et al., 2006; Singla et al., 2014). Based on the reviewed literature, an ERP experiment focused on evaluating the observed time-locked response to visual stimuli and SSVEP-based oscillatory response seems to be able to best address the proposed research questions. Although there are a number of methods frequently used to generate and analyze ERP signals, the use of PSD analysis, FFT, and ANOVA appear to be most useful for this effort. Additionally, these analysis methods should make the signal analysis more of a signal matching effort (ensuring consistency and discernable results) than a mathematical excursion in this offline experiment. Another beneficial finding from the existing literature associated with ERP-based BCIs is the identification of useful data and the locations most applicable to this data collection. Most of the literature associated with SSVEPs has highlighted the most identifiable and useful data as coming from the occipital lobe. This makes sense because the occipital lobe is the portion of the brain that handles and processes visual information. Additionally, the findings make a case for focusing data collection efforts on the occipital regions when using the EEG for data collection. By leveraging the lessons learned from existing literature associated with

23

ERP-based BCIs the experiment should be in a good position to produce consistent results at a relatively low setup cost. Because the research will focus on an area of this topic that has yet to be explored, it is anticipated that benefits of ERP-based BCI literature will be limited to test design and signal generation and analysis methods.

III. Methodology

Chapter Overview

The purpose of this research is to determine the feasibility of generating Event-Related Potentials (ERP), specifically Visual Evoked Potentials (VEP), in human subjects by using visual stimuli producing light 1) outside of the visible wavelengths and 2) modulating at frequencies beyond the human Critical Fusion Frequency (CFF). This chapter is intended to capture the plan for making these determinations. The method used follows the Institutional Review Board approved protocol (Protocol: FWR20170014H; Approved 10 January 2017) for evoking ERPs with unobtrusive stimuli. The approval letter for this protocol is attached in Appendix C.

Overview of Research Method

The premise of the research is that there is a phase locked response between the stimuli used to evoke a response in the brain and the brain's response to the stimuli. The approach pursued in this research follows the design of many steady-state visual evoked potential (SSVEP) electroencephalogram (EEG) based brain-computer interface (BCI) studies by presenting frequency modulated visual stimuli to a participant, monitoring the participant's brain activity across different channels, recording that brain activity, removing undesired artifacts in the collected activity, and analyzing the recorded brain activity to identify anticipated responses.

Data collected addressed the following variables 1) the peak wavelength of light emitted from the each LED; 2) the frequency of the LED's modulation; 3) the intensity of the energy; 4) the perception of the illumination; 5) perception of flicker from the LED;

and 6) measured neurological response to stimuli. Of the variables, the independent

variables are the peak wavelength of the light emitted from the LED and the frequency of

the LED's illumination. The dependent variables are the subjective determination of

perceived illumination, subjective determination of perceived flicker, and the measured

biological response to the stimuli. The power output for the LEDs was controlled across

the group of participants to facilitate a better understanding of the relationships between

each of the other variables.

Participants

This research was conducted with a group of participants that included 1 female

and 5 males ranging in age from 23 to 57. Participants were volunteers who were

solicited locally via coordination of the experimental protocol and campus intranet

advertisements. Participants were not offered any form of compensation to participate in

the research effort. There were 6 participants recruited for this research and although

data collection issues such as excessive blinking or signal dropout were anticipated, there

were no data collection issues encountered during the experiment. There were no special

considerations for gender, age, or corrective lenses because there are neither anticipated

impacts to any of these populations nor were these populations expected to produce

varying results in the research. However, participants were expected to be able to focus

on 5mm LEDs at a minimum viewing distance of 18 inches, and the age range of

participants and use of corrective lenses was recorded for completeness. Additionally, it

was anticipated that the participants would include a diverse group of people due to the

potential participants available at the Air Force Institute of Technology and the Air Force

Research Laboratory. Similar research efforts, eliciting Visual Evoked Potentials, have used participant groups comprised of 1 to 20 participants to provide confidence in the research (Cilliers & Van Der Kouwe, n.d.; Lee et al., 2006; Nakanishi, Wang, Wang, Mitsukura, & Jung, 2014b; Prueckl & Guger, 2009; Singla et al., 2014). For example, a standard set of EEG signal data was collected from 7 participants to determine the LED upon which the participants were focused (Cilliers & Van Der Kouwe, n.d.). Additional experiments relied on participant pools of 3 or 10 people to present diverse data for analysis (Nakanishi, Wang, Wang, Mitsukura, & Jung, 2014a; Prueckl & Guger, 2009).

Additional screening of participants included self-identification of medical history experiencing epileptic seizures, photosensitive epilepsy, and compromises to the participant's central or peripheral nervous systems. Photosensitive epileptic seizures can be triggered when visual stimuli are oscillated between 5 and 30 times per second, and these seizures can present a risk to the welfare of the participants ("Photosensitivity and Seizures," 2013). Also, participants with impeded central and peripheral nervous systems may present uncertainties that cannot be identified or mitigated. Therefore, participants who reported exhibiting these characteristics were excluded or asked to exclude themselves from the experiment.

Laboratory Environment

The research was conducted at the Air Force Institute of Technology, building 640, room 340 on Area B of Wright-Patterson Air Force Base. The laboratory in which the experiment was conducted is approximately 30ft x 20ft with desktops and partitioned cubicles. The experiment was conducted in a 7ft x 8ft cubicle within this laboratory by

setting up the LED displays on top of a stationary desk. The laboratory was warm at times and a stationary fan was used to keep the participants cool enough to prevent perspiration because it could lead to noise in the EEG data collected during the experiment. The cooling fan was angled in a manner such that the movement of air across the participant's face did not encourage blinking. An additional fan was placed near and angled away from the participant to provide noise abatement. The laboratory's primary source of light consisted of overhead fluorescent lighting and residual LED lighting from computer monitors. Both of these sources had the potential to inject noise artifacts into the data collected and were removed by turning them off and creating other means of ambient light in the laboratory. An incandescent lamp was used to create ambient light in the room to reduce safety hazards and aid the participant in attending to the specific LED for which energy was being emitted.

The incandescent lamp contains one 60 W bulb and was aimed away from the participant in a manner such that the illuminance at the surface of the display was 1.4 lux, and the illuminance at the surface of the desk is 0.7 lux. Based on trial studies, the illuminance measured at the display has the potential to impact the participants' ability to identify the stimulus and attend to it. The illuminance maintained during the experiment was intended to facilitate the participant's ability to attend to a fixation pointed located adjacent to each of the target stimuli during each of the experiment's tasks. The

illuminance measurements were obtained by using a Konica Minolta T-10 Illuminance

Meter, shown in Figure 5.

Figure 4 - Konica Minolta T-10 Illuminance Meter

The illuminance meter was placed on the desk that supported the LED display or

held by hand at the surface of the LED display and all lighting other than the

incandescent lamp was turned off when measurements were taken. Measurements were

recorded when the digital display of the illuminance meter reached its highest value

under a given condition. The illuminance meter was capable of recording measurements

between 0.01 and 900 lux and was not expected to impose any limitations on the

illuminance measurements of the data collection environment.

Apparatus

There were several pieces of equipment used to conduct this experiment. This

includes a BIOPAC MP150 data acquisition system, EEG100C electrode caps, a laptop

for signal processing and analysis, LED displays, and three Arduino Mega 2650

microcontrollers.
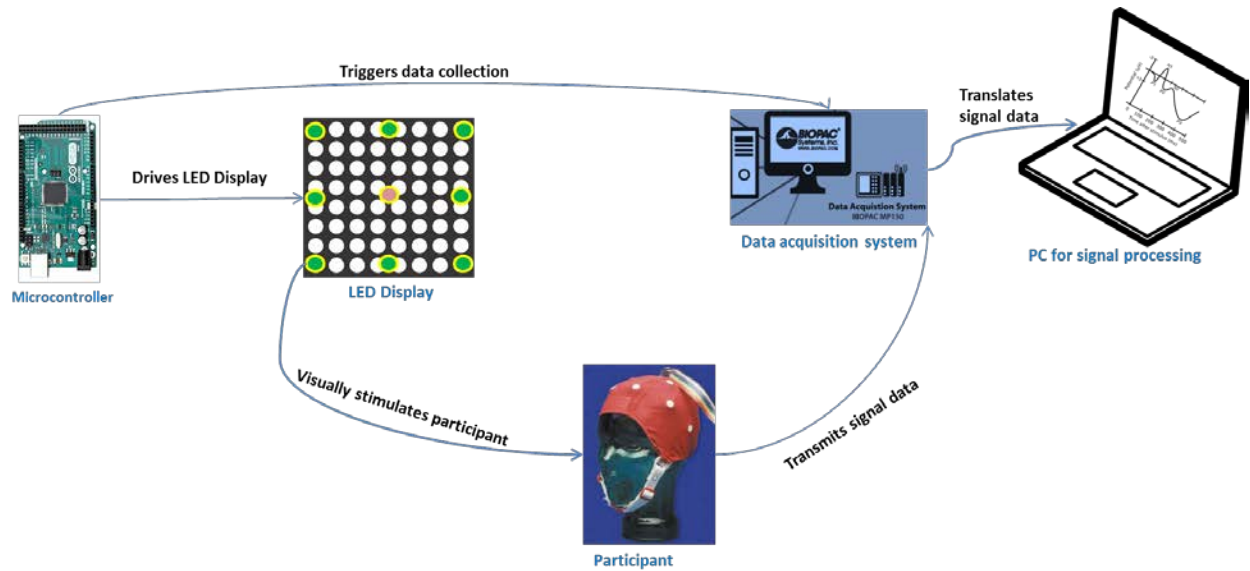
Figure 5 - Flow of Experiment

LED Display

The LED display consisted of 5 groupings of 9 LEDs arranged in a grid with each grid of 9 LEDs containing LEDs of the same wavelength and the 5 groupings having wavelengths ranging from 640 nm to 940 nm. Each of the groupings was powered and controlled by an independent Arduino Mega 2650 microcontroller that was programmed to supply power at 5V (HIGH) or 0V (LOW) to each identified digital pin at specific time intervals. That is to say that each of the digital pins used in the experiment were identified as a variable in the Arduino program code and called out via that variable in order to program high and low periods into the power cycles of each digital pin. The effect intended by this method was the oscillation of LEDs in each grouping at defined frequencies every second. The oscillations, written in milliseconds, were 500 high and low (1 Hz at 50% duty cycle), 25 high and 225 low (4 Hz at 10% duty cycle), or 12.5

high and 12.5 low (40 Hz at 50% duty cycle). A resistor was placed in series with each

of the LEDs to reduce the relative steady-state power output of each LED to near the

same level. This was consistent for each LED group except for the 640 nm grouping,

which was reduced until the intensity of the light output was low enough for a participant

to focus on the light without feeling the urge to blink continuously.
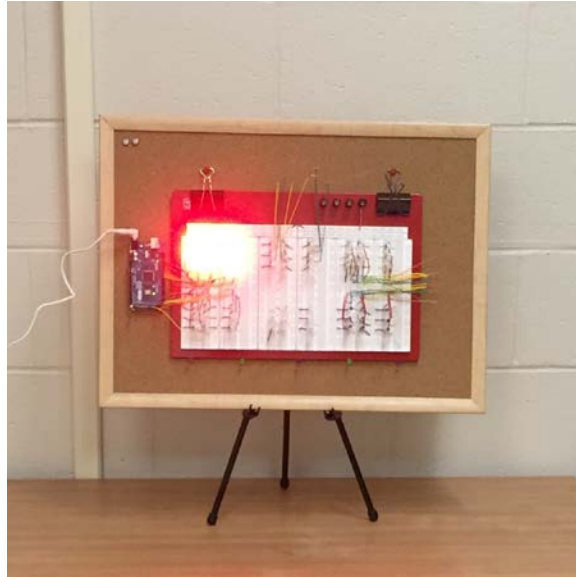
Figure 6 - 640nm LEDs at 3mW
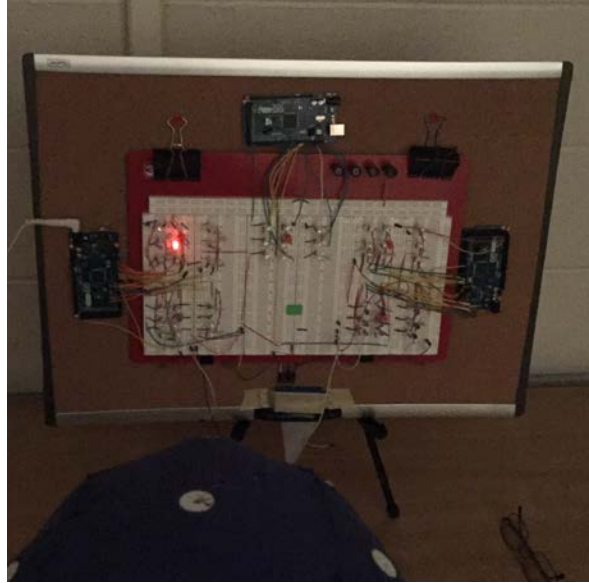
Figure 7 - 640nm LED at 50nW

Although the LEDs were grouped together, only the center LED was actively

powered during the experiment. One LED was used, vice the entire LED grouping, in the

experiment because overt attention has been shown to result in stronger ERP responses in

human subjects than covert attention (Treder & Blankertz, 2010). Each of the 640nm

LEDs output approximately 50 nW of optical power with 10 kΩ resistors in series as

measured by using a Coherent Fieldmaster in a dimly lit room and with the LED placed

beneath the measurement hood of the instrument. This produced a luminance of

approximately 79 cd/sq m when measured with a photometer from a point approximately

perpendicular to the LED substrate.

Table 1 - Peak wavelengths and resistor values of LEDs used in experiment

Peak Wavelength (nm)	Spectral Bandwidth (nm)	Product ID Number	Manufacturer	Resistor Used
640	Not noted	297	Adafruit Industries	10 kΩ
770	25	MTE1077N1-R	Marktech Optoelectronics	330 Ω
810	40	MTE2081-OH5	Marktech Optoelectronics	220 Ω
830	40	TSHG8200	Vishay Semiconductors	370 Ω
940	45	IR333-A	Everlight	220 Ω

The 770 nm, 810 nm, 830 nm, and 940 nm groupings' outputs were approximately 3 mW with 330 Ω, 220 Ω, 370 Ω, and 220 Ω resistors in series respectively. Each of the LEDs was measured with the Coherent Fieldmaster to determine a baseline power output from which they could be modulated. It was anticipated that the changes in the output of the LEDs would follow $Po = \frac{D_p}{T}$ (where P_o is power output, D_p is duty cycle of the pulse, and T is the period of the signal) and result in lower current and power output as the duty cycle was decreased from 100% to 10%.
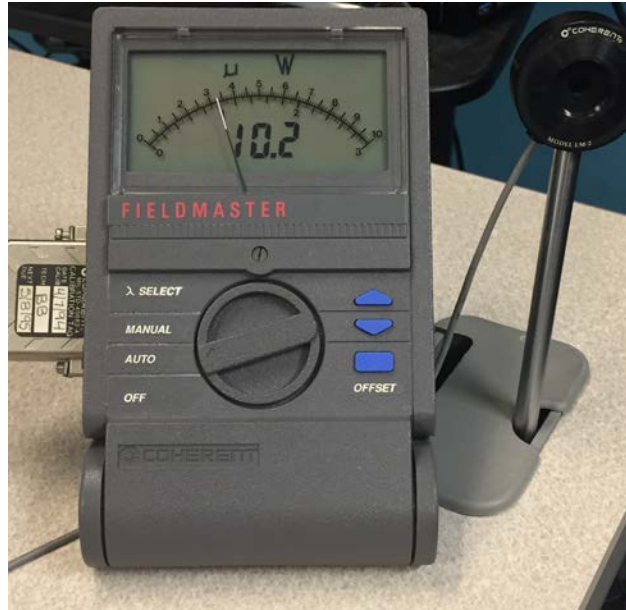
Figure 8 - Coherent Fieldmaster Power Measurement Device

The Arduino Mega 2650 microcontroller has 54 digital input/output pins (of which 15 can be used as PWM outputs), 16 analog inputs, a USB connection, and a power jack being used in this research. Power was supplied to the microcontroller by using a 12V power supply, and the regulator on the microcontroller reduced this voltage to provide 5V outputs to each circuit board for the experiment. All electric leads from the breadboard were powered at 5V with a maximum current of 100 mA.
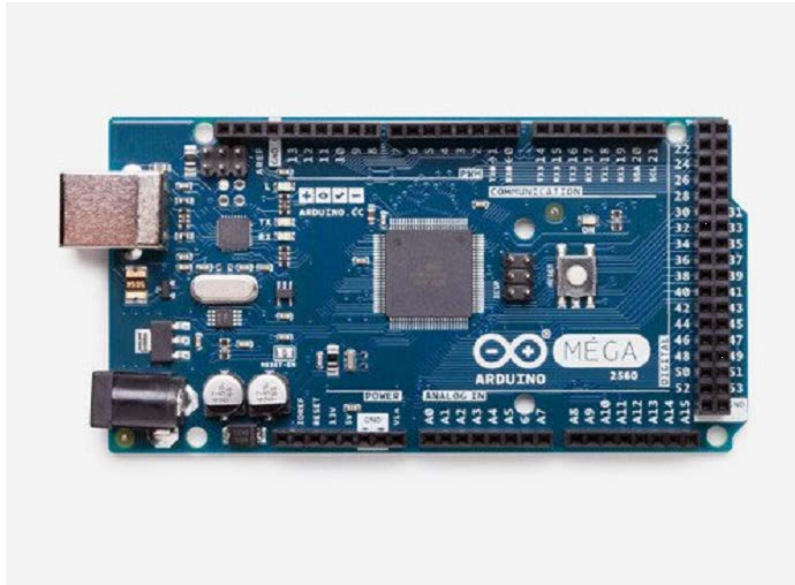
Figure 9 - Arduino Mega 2560 Microcontroller

The microcontroller was also interfaced to the Biopac MP150 to provide a timing signal indicating the onset of the flickering source. The timing signal facilitated the segmentation of EEG data, which isolated the EPOCHS within the human participant data at which a VECP was expected. Care was also taken to ensure the electrical limitations of the microcontroller were not exceeded.

Data Collection Equipment and Setup

In addition to the LED display as an external stimulus, there were components of the experiment that facilitated the collection and processing of data to identify the effects of the stimulus on the participant. These elements were the BIOPAC MP150 data acquisition system shown in Figure 10 and the EEG CAP100C.

Figure 10 - BIOPAC MP150

The BIOPAC MP150 data acquisition system consisted of 15 digital signal amplifiers, each represented by its own channel in the data acquisition software and connected to the data analysis laptop via ethernet cable. The data acquisition system was powered by a 12V wall-plugged power supply, which introduced line noise into the signal at 60 Hz. However, the risk of this line noise impacting the experiment was avoided by oscillating the visual stimuli at frequencies a minimum of 20 Hz lower than the line noise. Additionally, bandpass filters were used to remove the observations of noise above 50 Hz from the signal data before analysis. The signal data was amplified and then recorded in the Acknowledge 4.0 software to give the investigator realtime feedback of the data collection so that visible errors in the data collection could be captured and resolved. A sample of the data collected through the Acknowledge software is shown in Figure 11.
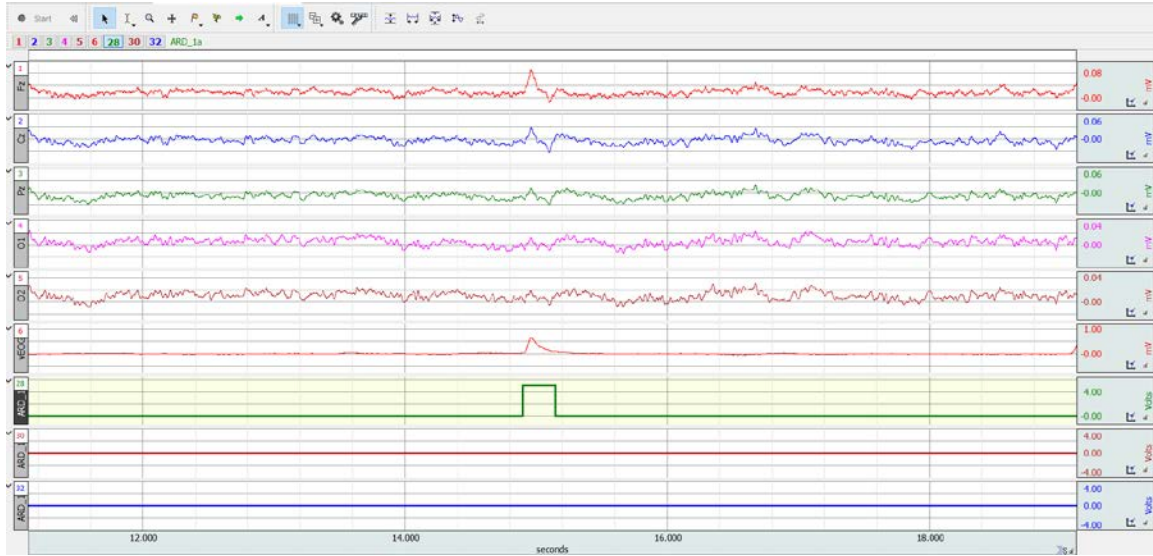
Figure 11 - Sample Filtered EEG Recording from Acknowledge Software

Additionally, the Acknowledge 4.0 software allowed the investigators to reduce the risk of data collection errors and incompatabilies with other programs because it allowed the investigators to record data and save it with the MATLAB file extension, specifically, and other file extensions. MATLAB would serve as the primary means of signal data analysis, so files were saved with its file extension.

In order to transmit the participant's signal data to the data acquisition system, the EEG CAP100C electrode cap was used as shown in Figure 12.

Figure 12 - CAP100C Electrode Cap

The electrode cap has preplaced electrodes installed at set intervals around the cap and connects to the data acquisition system via a wiring harness that is prewired with color coded wires that correspond to electrodes that are installed into the electrode cap. This electrode placement is based on the International EEG 10 – 20 Electrode Placement configuration, which spatially defines the locations for each electrode based on measurements of the participants' skull and relative distances between adjacent electrodes based on them being placed either 10% or 20% of the measured distance from nasion to inion and ear to ear.
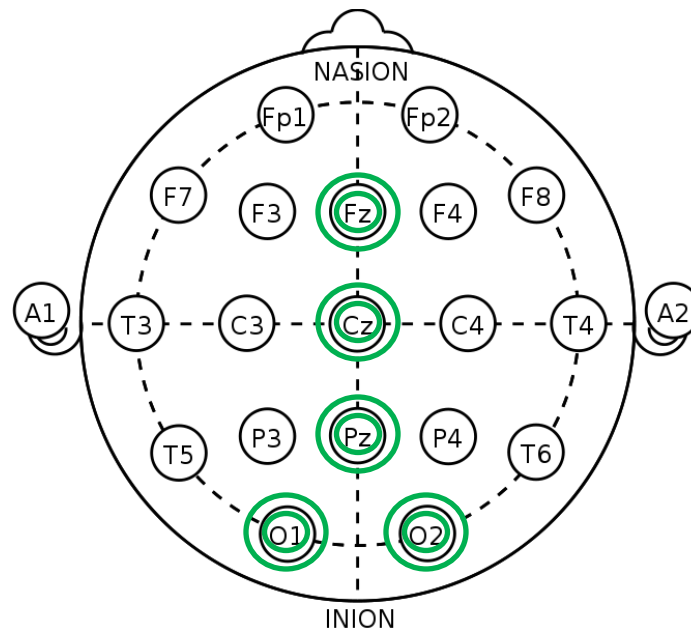
Figure 13 - International EEG 10 - 20 scalp electrode placement with experiment collection locations identified (Fz, Cz, Pz, O1, O2 with linked mastoid reference)

Experimental Procedure

The participants were seated in the chair used for the length of the experiment for their experiment preparation. To prepare the participant for the experiment, the investigator provided a written description of the experiment and explained each step of the experiment preparation and execution to the participants. Next, the participant's skull was measured from nasion to inion and the circumference of the skull was measured. Additionally, the participants scrubbed their left and right mastoids with an abrasive pad, then wiped both areas with alcohol pads. After the mastoid areas were cleaned, the investigator used a cotton swab to apply Nuprep skin preparation gel to the mastoid areas and applied one electrode to each mastoid with additional conductive electrode gel. These electrodes served as the reference for the EEG. After the electrodes were applied

to the mastoid areas, the participant used an alcohol pad to clean the areas directly above and below their right eye. Nuprep skin preparation gel was then applied to the areas directly above and below the participant's right eye and one electrode was applied to each location with conductive gel. This electrode was used to measure a vertical electrooculogram (EOG) signal, which was used to identify eye blinks during the experiment. After the electrodes were placed, the impedance at each location was verified to be below 10kΩ at EOG electrode locations and 5kΩ at EEG electrode locations with the BIOPAC EL-CHECK electrode impedance checker.

Figure 14 - BIOPAC Brand Electrode Impedance Checker

After verifying the impedances at the previous locations, the electrode cap, chosen based on previous skull measurement, was placed on the participant's head ensuring that the Cz electrode was placed in the center of the measured distance between the participant's nasion and inion. Next, a blunt tipped syringe was used to abrade the

40

scalp and apply electrode gel at GND, Fz, Cz, Pz, O1, and O2, and the impedance was verified to be below 5 kΩ at each location. After the impedances were verified, the data acquisition system was powered on, and the participant was asked to complete a series of tasks (i.e., clench teeth, blink, and close eyes) to verify the system was capturing expected activity before beginning the experiment.

The experiment was divided into three tasks, conducted against each of the LED display types, with independent goals, and each task was followed by a 15 second break before beginning the next task. Additionally, data collection for each display type started with a 65 second period recording of baseline activity in which the participant was seated still, and quietly while staring at the LED display while it was not actively powered. After the baseline period elapsed, the user was given a 15 second break, then the first task in the experiment was started. After the baseline period, each task was completed using the 640nm first, then proceeding to progressively longer wavelengths until completing the experiment with the 940 nm LED display. The first task was designed to saturate the participant's visual field with the target stimuli and elicit a time-based cortical response to the onset of the target stimuli. The target stimuli were oscillated at a 1 Hz frequency by modulating the width of each pulse at 500 milliseconds on and 500 milliseconds off each second. This cycle continued for approximately two minutes to capture up to 125 events to calculate the mean amplitude of the components over the range of events for each LED stimulus. The number of events was necessary to reduce the size of noise the average of events as reflected in the function $(1/\sqrt{N}) \times R$ where N is the number of events and R is the amount of noise in a single trial (Luck, 2005b). The impact of this function is that it may take 9 trials to triple the signal to noise ratio in a given experiment (by $\sqrt{9} =$

3). A digital timing signal was transmitted directly from the microcontroller to the data acquisition system at each onset of the target stimuli.

The second task was designed to elicit a cortical response by using a target steady-state oscillating frequency of 4 Hz for the target stimuli. The target stimuli were on for 25 milliseconds and off for 225 milliseconds, 4 times in each second. This cycle continued for 1 minute, before the 15-second break was reached. A digital timing signal was transmitted directly from the microcontroller to the data acquisition system at every fourth onset of the target stimuli, starting with the first onset (i.e., 1, 5, 9…). After completing the experiment, the oscillating frequency of the target LED was determined to be approximately 4.3 Hz.

The third task was designed to elicit a cortical response using a steady-state frequency beyond the anticipated Critical Fusion Frequency (CFF) of 40 Hz for the target stimuli. The target stimuli were on for 12.5 milliseconds and off for 12.5 milliseconds 40 times each second for 1 minute before the end of task set for each display. A digital timing signal was transmitted directly from the microcontroller to the data acquisition system at every fortieth onset of the target stimuli, starting with the first onset (i.e., 1, 41, 81…). After completing the experiment, the oscillating frequency of the target LED was determined to be approximately 39.8 Hz.

Initial Methods

The initial attempts to conduct Power Spectral Density (PSD) analysis on the data collected from experiments were based on code that attempted to identify the relative power captured at each frequency across the entire 60 second trials and was anticipated to

reveal an increase in 4 Hz power with harmonic features occurring at 8 Hz and 12 Hz. However, the power increase seemed to be most dense at 8 Hz and 12 Hz in the Occipital region. This method did reveal responses that may have been generated by the target stimuli; however, the signal was mostly obscured by noise and other methods to reduce noise and extract the signal were pursued.
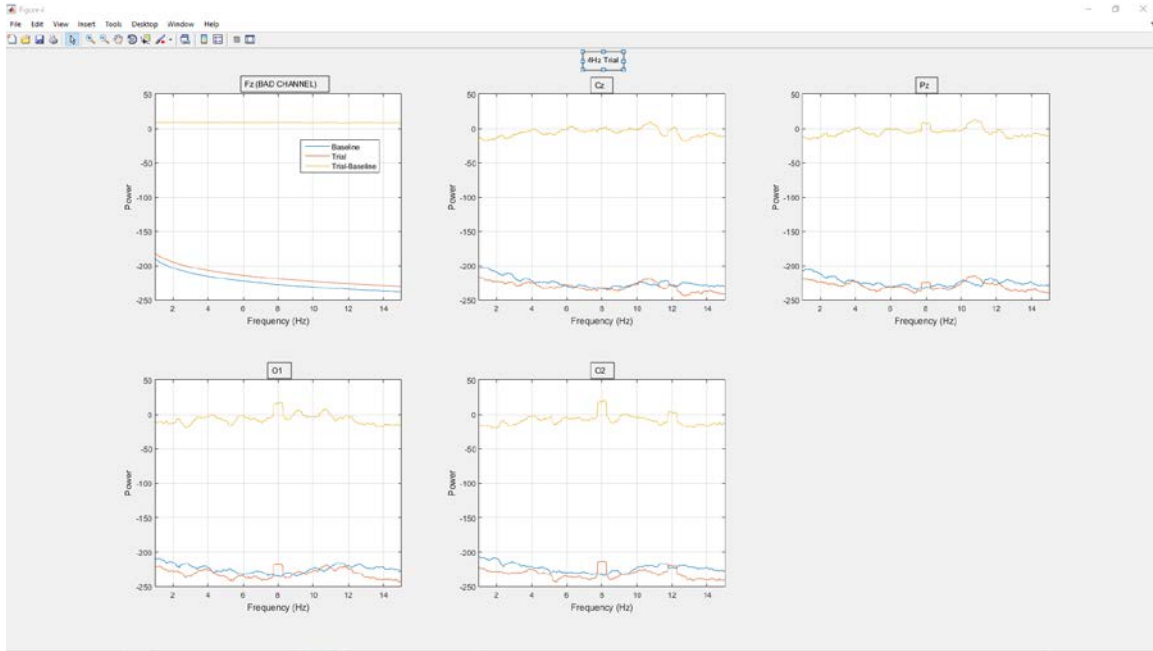
Figure 15 - Initial PSD Plots against sample 4 Hz Trial

The same approach was used at 50 Hz and appeared to show a response at the target frequency without additional power increases at other frequencies presented in earlier trials (i.e., 4 Hz). The line noise encountered at 60 Hz due to the data acquisition system power supply became apparent through this approach.
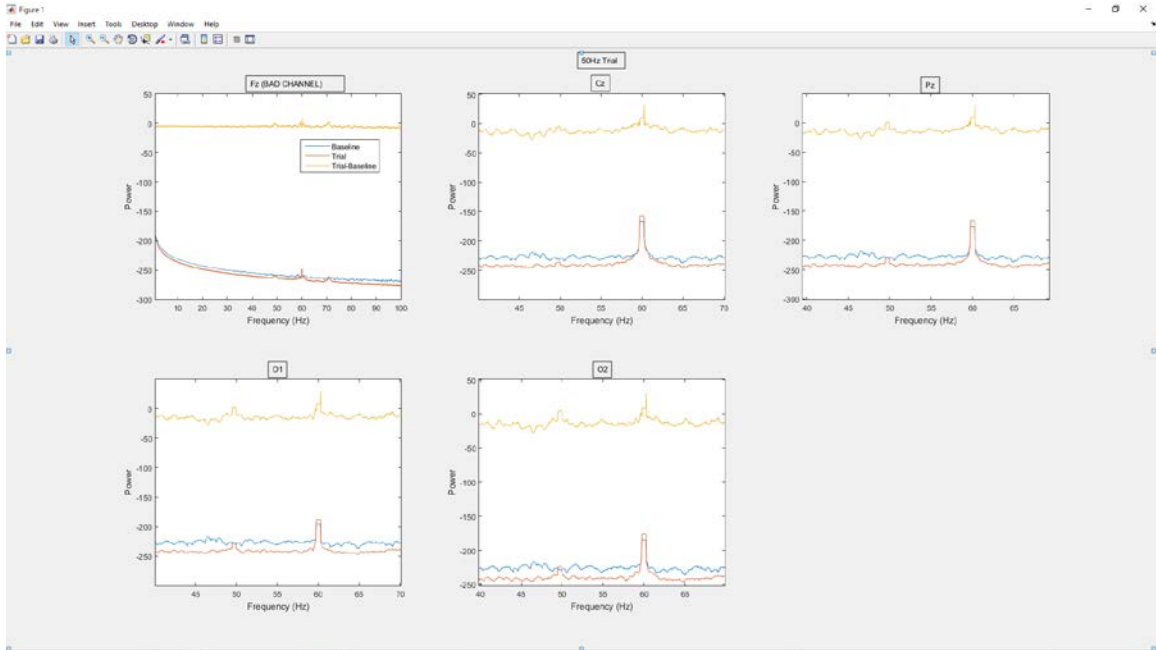
Figure 16 - Initial PSD Analysis against sample 50 Hz trial

Next, a Complex Morlet Wavelet was convolved with the EEG signal data at the integer frequencies from 2-25 Hz. This band passes the data and returns the time-series power of that frequency as the square of the absolute value of the complex signal. The following figure is an example of the result at 8 Hz example.
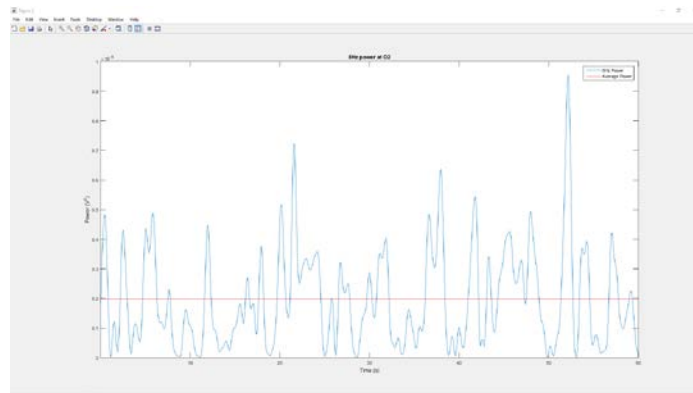
Figure 17 - Morlet Wavelet Convolution at 8 Hz for example

Next, the average power at each frequency was taken for both the baseline and trial data, and the decibel changes were computed for all frequencies, and plotted in the Figure 18.
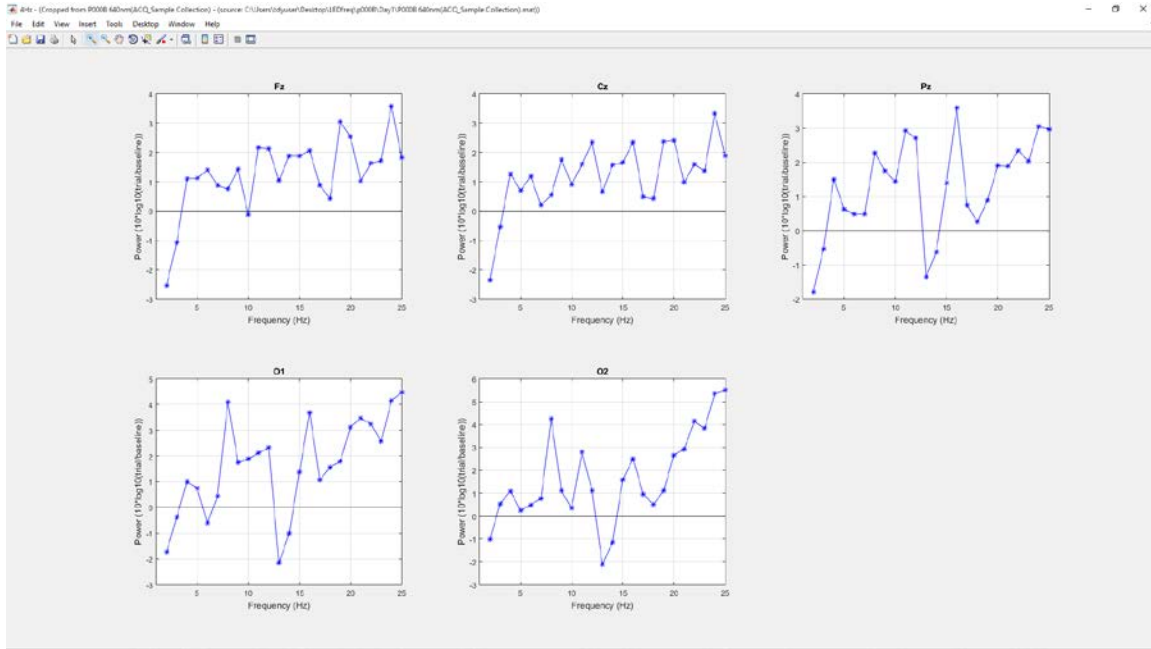
Figure 18 - Decibel change in power between sample trial and baseline periods

In the 4 Hz trial both O1 and O2 reveal power increases around 4 Hz and its harmonics around 8 Hz, 12 Hz and 16 Hz.

Final Methods

The data acquisition system and Acknowledge software were used for signal data acquisition. The MATLAB software (code attached in Appendix A) was used to complete the signal data processing (i.e., epoching, averaging, & spectral density analysis) and noise reduction through signal averaging and blink removal.

In Task 1, the data collected from each participant was segmented into at least 87, 1-second epochs to produce plots of each time-based ERP in Microsoft Excel and MATLAB for visual inspection and measurement of the ERP. Epochs were removed

when blinks were indicated by a vertical EOG signal which exceeded 250 µV. Because the neural activity is time-locked to the stimulus, the occurrence of activity post stimulus onset reflects the participant's response to the stimulus; however, it was necessary to identify additional criteria to objectively determine the presence of the response.

Qualitative measures of the response's validity include visual comparison of the pre-stimulus period and post-stimulus period and their associated voltage deflections for each participant. The voltage deflections were compared to determine if the activity measured from the two periods is different. If there was a significant difference in magnitude of the signal compared to the noise, the response was assumed to be valid and not valid otherwise. To support the determination of response validity, the root-mean-square (RMS) of the pre-stimulus (samples from 200 ms before the onset of stimuli to stimuli onset) and post-stimulus (samples from onset of stimuli to 500 ms after onset of stimuli) periods of the 1 Hz task are calculated to provide unbiased estimates of the variance of the neural activity for both periods. The RMS values are calculated using the following equation:

$$RMS = \sqrt{\frac{\sum_{t=1}^{n}(\hat{y}_t - y_t)^2}{n}} \qquad (1)$$

Where $\hat{y}_t$ is the expected voltage (V) of each sample (equaling zero), y_t is the measured voltage of each sample, and n is the number of samples (1401) measured in the 700 ms window.

The resultant pre-stimulus and post-stimulus RMS values are compared to one another (Equation 2) to provide a ratio of the participant's neural response to the stimulus and their baseline activity that evaluates each deflection of the activity and not just the

46

positive or negative deflections. This ratio, where S_T is the RMS value obtained from the post-stimulus data points and S_B is the RMS value from pre-stimulus data points, is used to determine a signal-to-noise ratio that accurately reflects the sum of measured brain activity at the subject electrode. A signal-to-noise ratio of 1.5 or higher was said to support a claim of response validity and a lower signal-to-noise ratio supported claiming the lack of a response to the stimuli.

$$SNR = \frac{S_T}{S_B} \qquad (2)$$

Before analysis, the neural signal data from Task 1 was segmented into 700 ms epochs (200 ms before to 500 ms after onset of stimuli) each second over the length of the task by referencing the digital event timing signal triggered by the microcontroller. That is, the epochs represent the neural signal data from the initial onset of the visual stimuli (e.g., at time = 0) to the next onset of the visual stimuli (e.g., at time = 1000 ms) for 87 – 125 epochs. These epochs were then averaged across the trials that were not obstructed by blinks. This segmentation and averaging process is reflected in Figure 19.

This process was used to generate outputs for all collected scalp locations, but only data referenced from O1 and O2 were used to conduct data analysis.
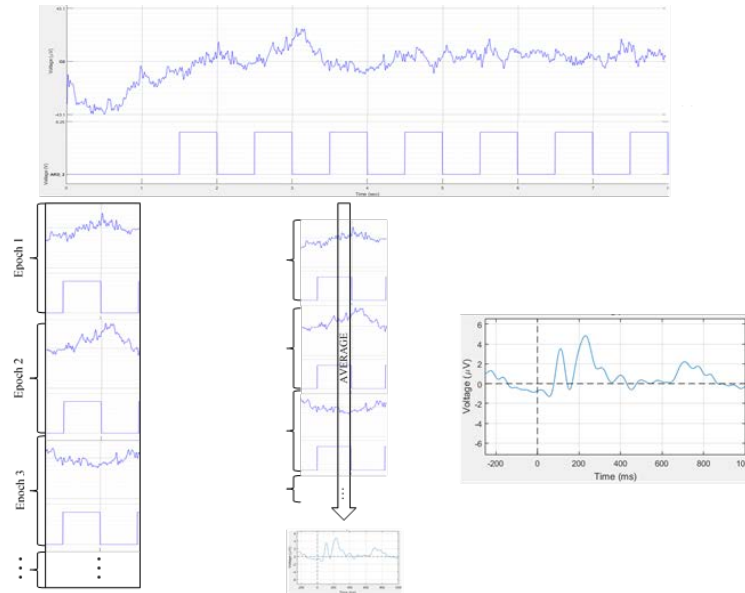
Figure 19 - Depiction of Segmentation and Averaging Method

Data collected from Task 2 and Task 3 followed a similar segmentation processes as Task 1; however, the neural signal data collected from each participant in each, Task 2 and Task 3, was segmented into 65 3-second epochs. The epochs were collected at every 4th onset of the stimuli (Task 2) and every 40th onset of the stimuli (Task 3) from the initial onset of the visual stimuli to the final offset of the visual stimuli (each epoch either overlapped or was overlapped by another). These epochs were averaged after removing the first 3 and last 3 samples removed to capture the centralized response for each participant (i.e., it was assumed that the participants could require up to 3 seconds to adjust to the stimuli and control blinking), and there were no blinks removed from samples in Tasks 2 and 3. The neural signal data was processed using spectral density analysis to examine the power as a function of frequency for each participant. In BCI

applications the window of frequencies analyzed for response are usually specific to the range of frequencies used in the experiment; however, a wider window was used in this experiment to evaluate a larger field of frequency band powers reflected in the measurements. Additionally, to emphasize the response occurring across the visual cortex and normalize the measurements, the frequency powers measured at O1 and O2 were multiplied together, multiplied by the frequency at which the power was observed, and divided by the maximum measured frequency power. The power associated with the frequency spectrum of EEG data may decrease as the frequency is increased and follow a 1/f power scaling, where f is the frequency at which the power is observed (Cohen, 2014). Therefore, the frequency powers are multiplied by the associated frequencies to account for the power scaling. Additionally, normalizing the amplitudes of the frequency data facilitated the comparison of power data against the same scales.

The goal for Task 2 was to identify the target stimuli frequency of approximately 4.3 Hz or its first harmonic as the predominant frequency band powers in the subject trial. However, if the frequency power did not rise to at least 0.4 in amplitude, the response was determined to be commensurate to noise and not an elicited signal.

In Task 3, the goal was to identify the target stimuli frequency of approximately 39.8 Hz as either the predominant or secondary frequency band power above 0.4 in amplitude (below 0.4 was determined to be commensurate with noise) in the subject trial. The frequency window used for analysis did not include the range of potential harmonic features, so the target stimuli frequency was the only frequency evaluated.

IV. Analysis and Results

Chapter Overview

This chapter will provide a collection of results derived from the analysis of the signal data collected from each participant in this research effort. The analysis of the signal data follows the methods outlined in Chapters II and III. Additionally, the results are displayed in the order in which each of the 3 tasks occurred and the data from each of the participants is grouped together for each task.

Results of Simulation Scenarios

Task 1 – 1 Hz Condition

In task 1, the signal data from each participant was filtered using a low pass finite impulse response (FIR) filter with a passband frequency of 15 Hz, stopband frequency of 20 Hz, passband ripple of 0.5 dB, and stopband attenuation of 65 dB. The time-locked responses, for each participant and target stimuli (640 nm – 940 nm), from this task are reflected in the figures which follow in the next section of this report. Additionally, a grand average for the group has been produced, and it highlights the trend of responses occurring between 100 to 200 ms after the onset of the target stimuli at time zero. However, it is worth noting that the grand average reduces the variance in responses seen across participants, but it is useful for highlighting the consistency based on the latency of the responses for each participant. The table below is intended to highlight each participant's observation of illumination and flicker from the target stimuli. A table will precede each of the analysis sections to identify participant observations of the target stimuli. The data in these tables is used to determine if there is a correlation between the

observations and the resultant ERPs and frequency powers collected from each

participant and task. Table 2 reflects each participant observed both illumination and

flicker in the 640 nm portion of Task 1.

Table 2: Participants observation of stimuli at 640 nm portion of Task 1

Participant Number	Observed Illumination	Observed Flicker
P001	Yes	Yes
P002	Yes	Yes
P003	Yes	Yes
P004	Yes	Yes
P005	Yes	Yes
P006	Yes	Yes

Task 1 – 640 nm

In Figure 20, the Grand Average of the measured ERPs demonstrates the

overarching responses with latencies of approximately 100 ms to 250 ms after the onset

of the visual stimuli. The noise from the pre-stimulus baseline is low relative to the

averaged peak response in the ERP which has an amplitude near 3 µV.

Figure 20 - Grand average across participants for 640nm portion of Task 1

Figure 21 demonstrates that ERPs were captured in each of the participants from this task and the latency of the response for each participant was identified between approximately 100 and 250 ms after the onset of the target stimuli. The responses measured at each location, O1 and O2, were synchronized even though there was variation between the voltage measurements. Examination of each participant demonstrates a response to the stimuli. The SNRs for participant 1 were 3.15 (O1) and 4.43 (O2), participant 2 were 2.42 (O1) and 3.98 (O2), participant 3 were 3.49 (O1) and 3.87 (O2), participant 4 were 1.70 (O1) and 2.89 (O2), participant 5 were 2.07 (O1) and 1.85 (O2), and participant 6 were 4.52 (O1) and 4.74 (O2). The SNRs suggest relatively (compared to pre-stimulus period) pronounced response to the onset of the target stimuli.

Additionally, the peak amplitude of the response is greater than 2μV for each participant

in this task.

Figure 21 - Task 1: ERPs for each participant to the 1Hz, 640 nm target stimuli

Task 1 – 770 nm

Each participant observed both illumination and flicker of the LED in the 770 nm portion of Task 1. The participant observations are reflected in Table 3.

Table 3: Participant target stimuli observations at 770 nm

Participant Number	Observed Illumination	Observed Flicker
P001	Yes	Yes
P002	Yes	Yes
P003	Yes	Yes
P004	Yes	Yes
P005	Yes	Yes
P006	Yes	Yes

The Grand Average in Figure 22 demonstrates relatively low noise in the pre-stimulus baseline period relative to the peak voltage measured in the ERP. The average latency of the main component was approximately 200 ms after the onset of the stimuli and has a peak amplitude near 4μV.

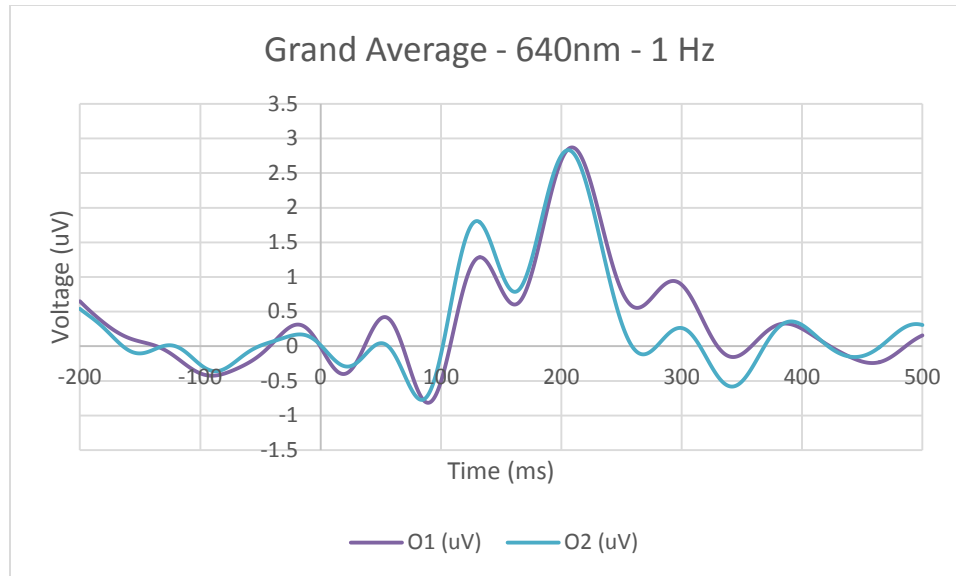**Figure 22 - Task 1: Grand average across participants for 770 nm portion of Task 1**

Figure 23 demonstrates that the ERPs captured from each of the participants from this task had latencies of approximately 100 and 250 ms after the onset of the target stimuli. The responses measured at each location, O1 and O2, were predominately synchronized even though there was variation between the voltage measurements and slight variation between the phase of some O1 and O2 measured components, and each participant demonstrates a response to the stimuli. The SNRs for participant 1 were 2.29 (O1) and 2.64 (O2), participant 2 were 2.84 (O1) and 3.36 (O2), participant 3 were 8.42 (O1) and 6.98 (O2), participant 4 were 4.48 (O1) and 4.68 (O2), participant 5 were 4.19 (O1) and 3.58 (O2), and participant 6 were 3.89 (O1) and 2.93 (O2). The SNRs suggest relatively (compared to pre-stimulus period) pronounced response to the onset of the target stimuli. Additionally, the peak amplitude is greater than $2\mu V$ for each participant in this task. Participant 2 appears to have a lower response at O1 than O2; however, there is clearly a response at O2.
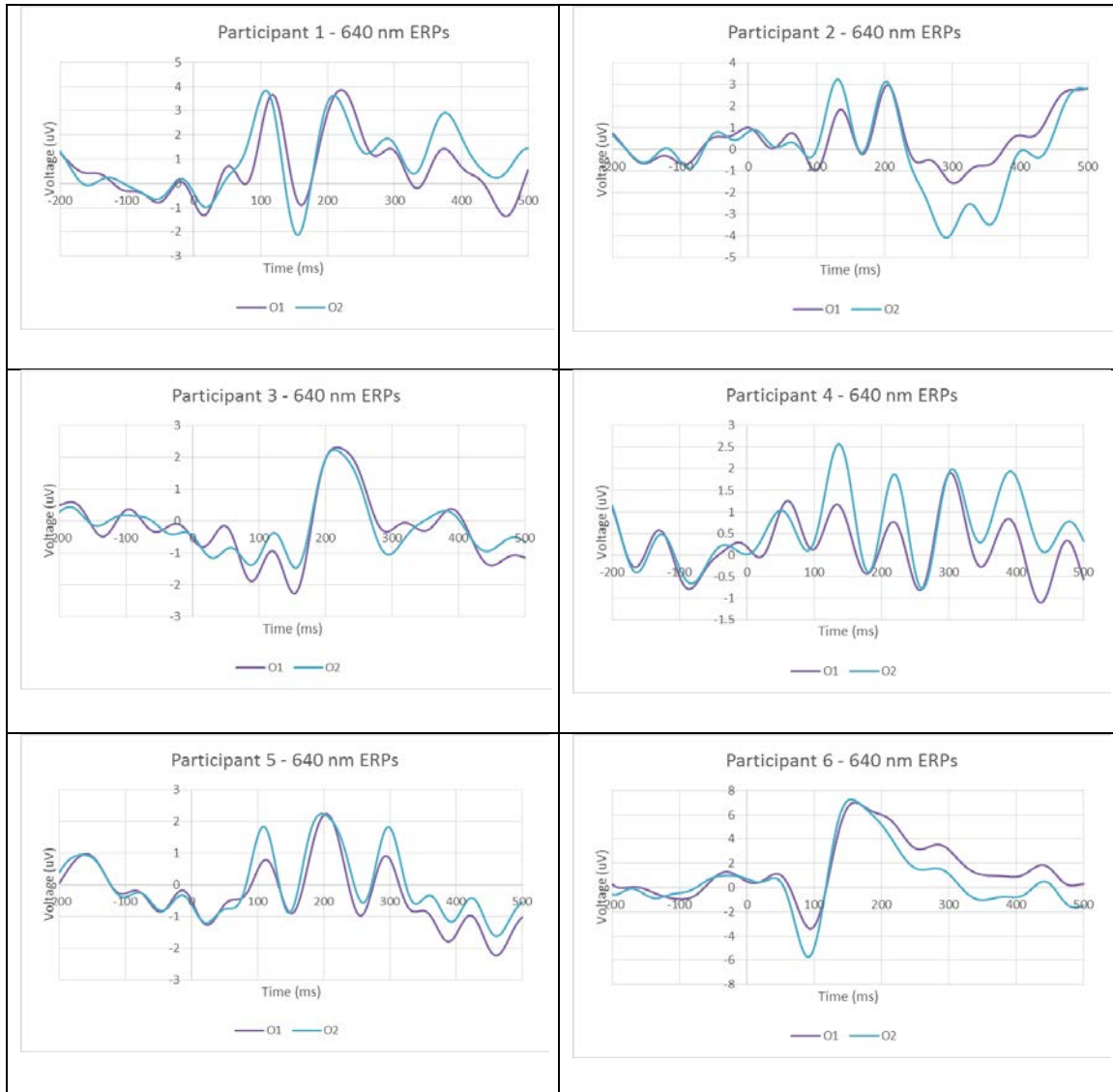
Figure 23 - Task 1: ERPs for each participant to the 1Hz, 770 nm target stimuli

Task 1 – 810 nm

Each participant observed both illumination and flicker of the LED in the 810 nm portion of Task 1. The participant observations are reflected in Table 4.

Table 4: Participant observations of 810 nm target stimuli in Task 1

Participant Number	Observed Illumination	Observed Flicker
P001	Yes	Yes
P002	Yes	Yes
P003	Yes	Yes
P004	Yes	Yes
P005	Yes	Yes
P006	Yes	Yes

Figure 24 demonstrates the Grand Average of ERPs measured across participants in the 810 nm portion of Task 1. It reveals an indication of responses with latency between 200 ms and 300 ms after the onset of the stimuli; however, it also reveals that the amplitude, maximum near 1μV, of the responses have decreased considerably with the brightness of the visual spectrum associated with the stimuli.
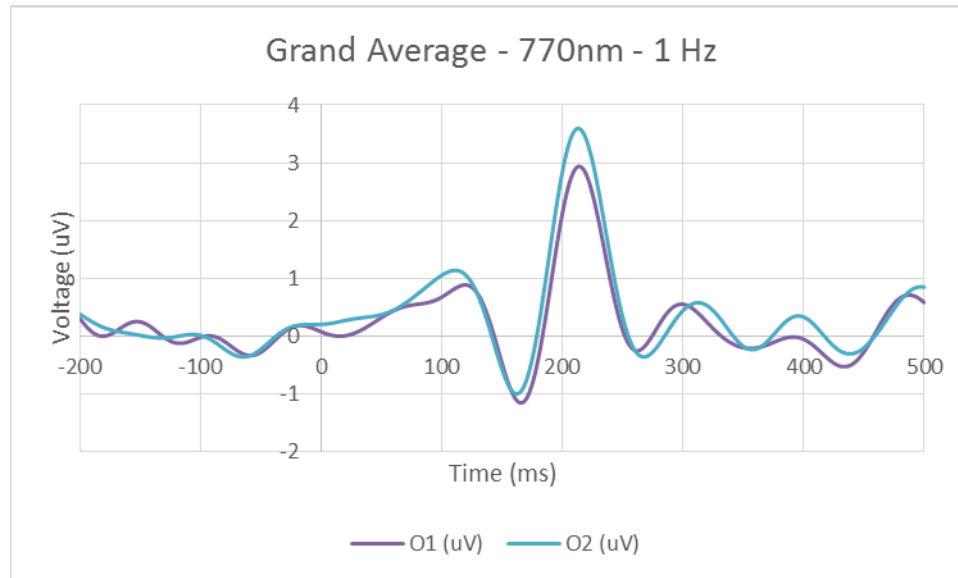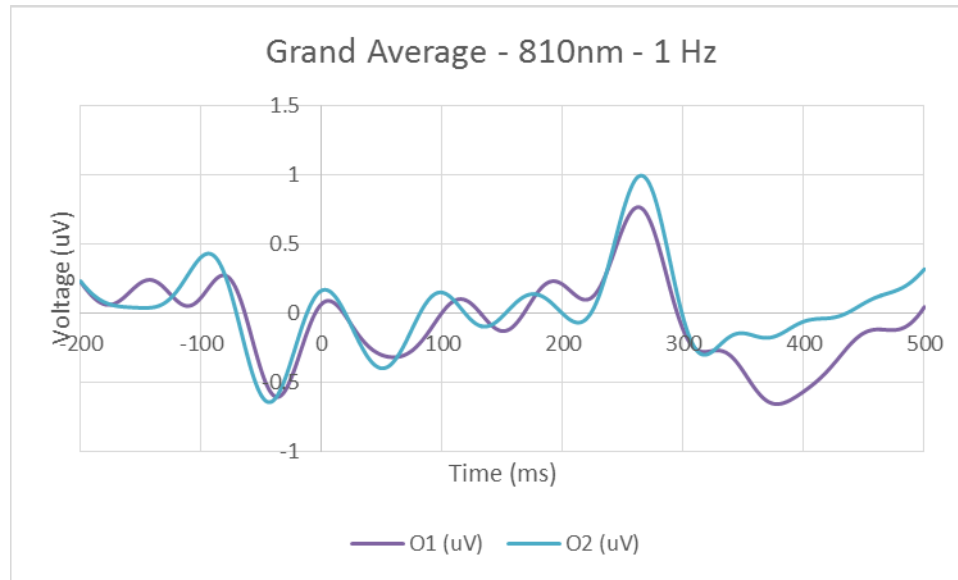
Figure 24 - Task 1: Grand average across participants for 810nm portion of Task 1

Figure 25 demonstrates the preponderance of the participants did not have responses distinguishable from the pre-stimulus baseline. The lacking responses are indicated by the level of noise being nearly the same in the pre-stimulus baseline and the post-stimulus periods. The exception was Participant 4 who had a considerable increase in activity from approximately 100 ms to 300 ms after the onset of the stimuli with a peak amplitude higher than 2μV in response to the stimuli. The responses measured at each location, O1 and O2, were predominately synchronized even though there was variation between the voltage measurements and slight variation between the phase of some O1 and O2 measured components. The SNRs for participant 1 were 1.04 (O1) and 1.85 (O2), participant 2 were 1.21 (O1) and 1.23 (O2), participant 3 were 0.63 (O1) and 1.32 (O2), participant 4 were 4.47 (O1) and 4.70 (O2), participant 5 were 1.99 (O1) and 1.45 (O2), and participant 6 were 0.70 (O1) and 0.68 (O2). Additionally, the peak amplitudes of the component waveforms are less than 1.5 μV for all participants except participant 4.

The target stimuli were much more difficult for each participant to observe and attend to during this task, and this may have contributed to the lacking responses across participants in this task.

Figure 25 - Task 1: ERPs for each participant to the 1Hz, 810 nm target stimuli

Task 1 – 830 nm

        Each participant observed both illumination and flicker of the LED in the 830 nm portion of Task 1. The participant observations are reflected in Table 5.

Table 5: Participant observations of 830 nm target stimuli in Task 1

Participant Number	Observed Illumination	Observed Flicker
P001	Yes	Yes
P002	Yes	Yes
P003	Yes	Yes
P004	Yes	Yes
P005	Yes	Yes
P006	Yes	Yes

        The Grand Average for the 830nm portion of Task 1, Figure 26, implies there was a clear response across the group in this task. It reveals pronounced components around 100 ms to 250 ms in latency with relatively low noise. Again, it was anticipated that the dimness of the stimuli would result in lower amplitudes for any measured response although the 830 nm stimuli was brighter than the 810 nm stimuli, it was dimmer than the 640 and 770 nm stimuli presented in Task 1.
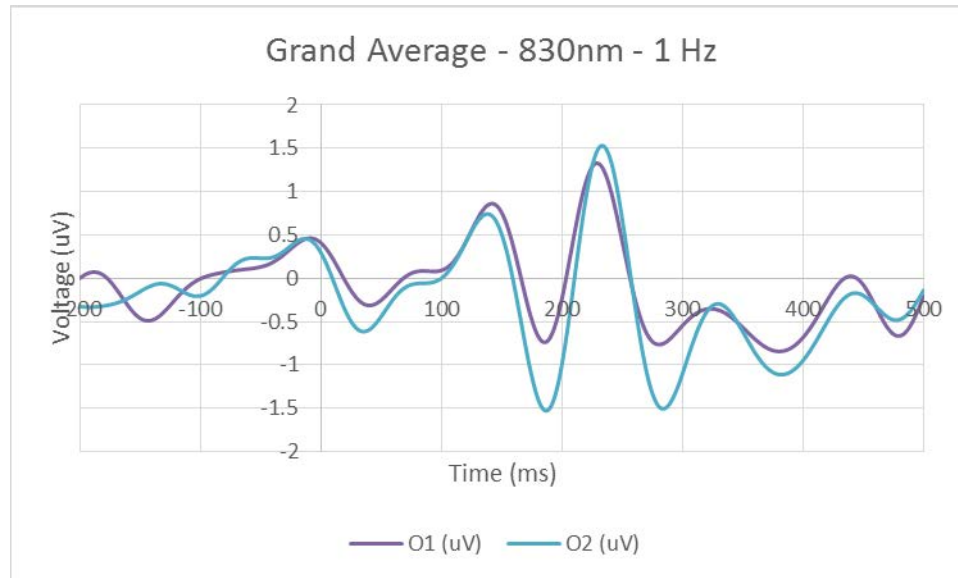
Figure 26 - Task 1: Grand average across participants for 830nm portion of Task 1

ERPs were captured from each participant in this task (Figure 27) and the latency of the response for these participants was identified between approximately 100 and 250 ms after the onset of the target stimuli. The responses measured at each location, O1 and O2, were predominately synchronized even though there was variation between the voltage measurements. The SNRs for participant 1 were 1.74 (O1) and 3.03 (O2), participant 2 were 4.99 (O1) and 6.15 (O2), participant 3 were 2.04 (O1) and 2.61 (O2), participant 4 were 2.21 (O1) and 2.69 (O2), participant 5 were 2.12 (O1) and 1.71 (O2), and participant 6 were 1.39 (O1) and 1.78 (O2). The grand average of the waveforms and their SNRs suggest relatively (compared to pre-stimulus period) pronounced response to the onset of the target stimuli; however, the measurements at O1 and O2 for participants 1, 2, 4, 5, and 6 appear to be obscured by surrounding neural activity and not distinct with respect to the noise. The ERPs from participants 4, 5, and 6 also appear to reveal a response that is not locked to the onset of the stimuli (indicated by the increase in

activity just before the onset of the stimuli). There is, however, a more defined response
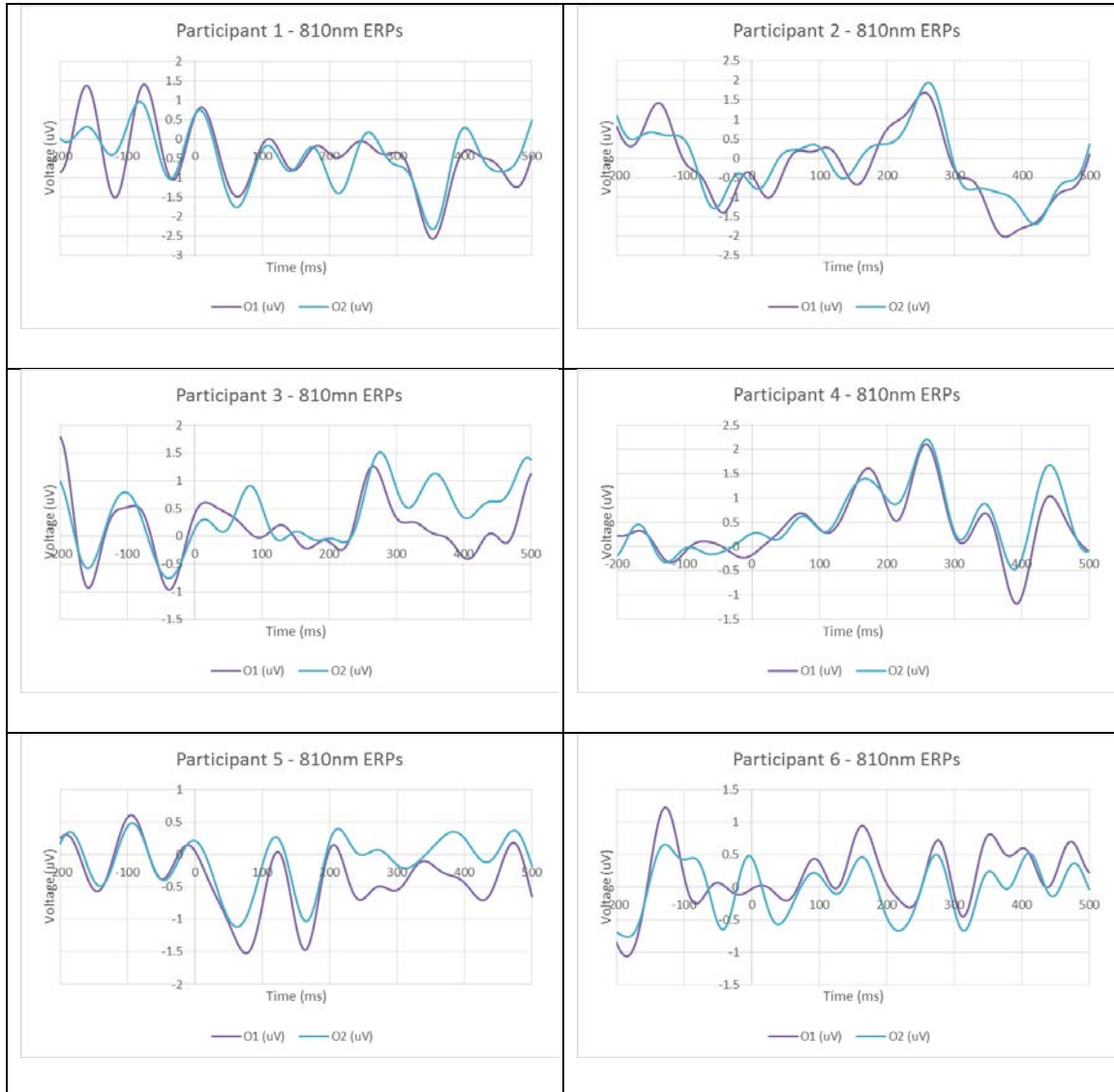
for participant 3 in this task.

Figure 27 - Task 1: ERPs for each participant to the 1Hz, 830 nm target stimuli

Task 1 – 940 nm

Each participant observed both illumination and flicker of the LED in the 940 nm

portion of Task 1. The participant observations are reflected in Table 6.

Table 6: Participant observations of 940 nm target stimuli in Task 1

Participant Number	Observed Illumination	Observed Flicker
P001	No	No
P002	No	No
P003	No	No
P004	No	No
P005	No	No
P006	No	No

The Grand Average of the 940 nm portion of Task 1 (Figure 28) captures neural activity around the onset of the stimuli that is approximately 3 times as strong at O1 as the pre-stimulus baseline period. As anticipated, the amplitude of the ERP is low compared to the shorter wavelength stimuli, and the components of the response appear from approximately 50 ms to 200 ms after the onset of the stimuli without any increases in activity before the onset of the stimuli.
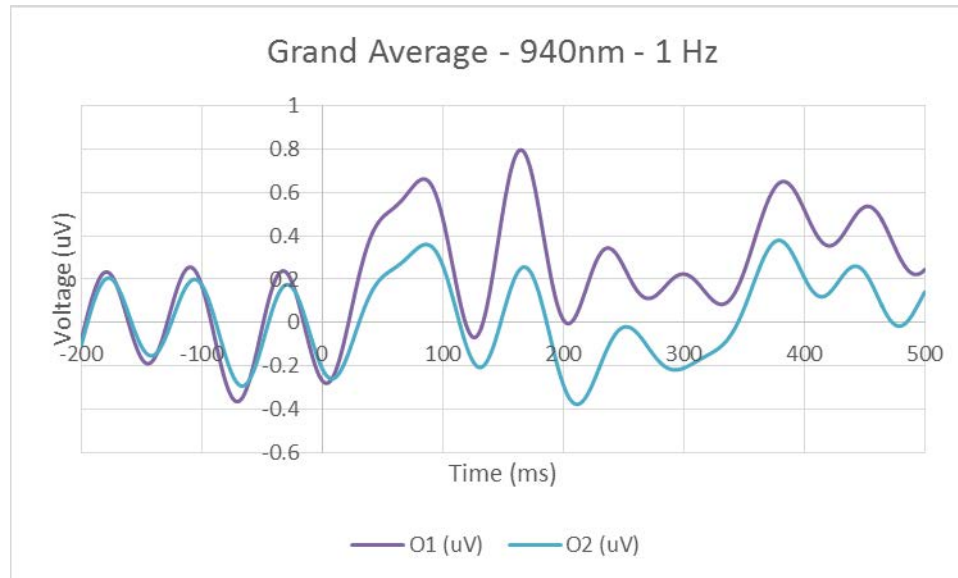
Figure 28 - Task 1: Grand average across participants for 940nm portion of Task 1

ERPs (Figure 29) were captured in each of the participants from this task, and although the responses are sporadic, the latency of the responses for each participant appear to begin approximately 50 ms after the onset of the target stimuli and randomly diminish at O1 and O2. The responses measured at each location, O1 and O2, were predominately synchronized even though there was variation between the voltage measurements and slight variation between the phase of some O1 and O2 measured components. The SNRs for participant 1 were 1.34 (O1) and 2.31 (O2), participant 2 were 1.75 (O1) and 2.03 (O2), participant 3 were 1.72 (O1) and 2.45 (O2), participant 4 were 1.78 (O1) and 1.69 (O2), participant 5 were 1.99 (O1) and 1.09 (O2), and participant 6 were 2.88 (O1) and 3.25 (O2). The SNRs suggest relatively (compared to pre-stimulus period) pronounced response to the onset of the target stimuli; however, the sporadic neural activity and peak amplitudes suggest the observed activity is noise and not responses to the target stimuli.
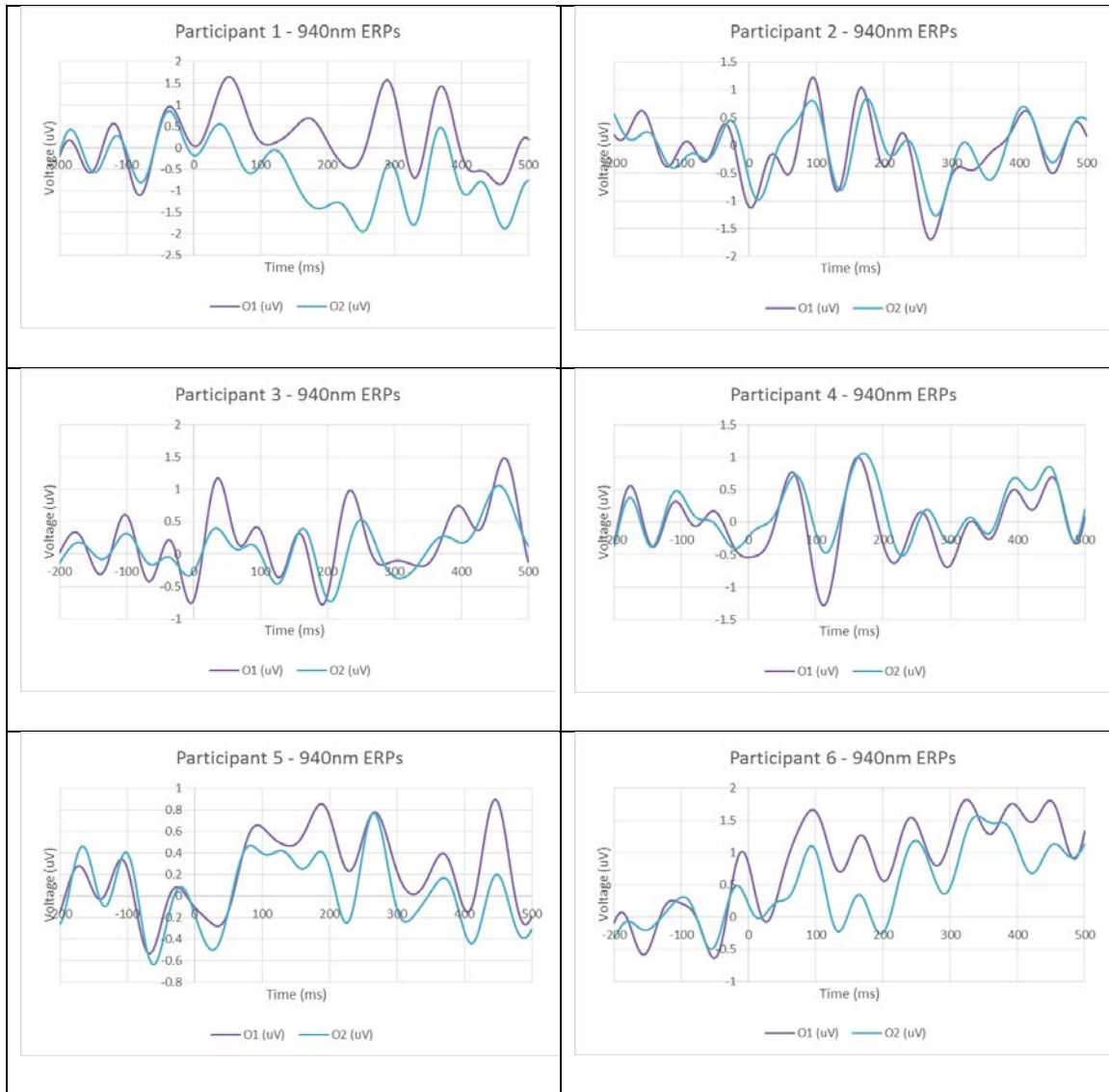
Figure 29 - Task 1: ERPs for each participant to the 1Hz, 940 nm target stimuli

Task 2 – 4 Hz Condition

The oscillatory responses for each participant, in task 2, were calculated by using spectral density analysis. The responses for each participant were plotted referencing a normalized amplitude against the frequency window extending from 2 Hz to 12 Hz. The normalized amplitude is used to extract the frequency containing the highest power density occurring over the observed period of 65 seconds, and it is represented as the

product of the measured power at O1 and O2, for each observed frequency, divided by the maximum observed power across the frequencies. No blinks were removed from the data collected; however, the first 3 and last 3 epochs were removed from the data before analysis, in an effort to capture a centralized period in which the participant was most attentive to the task. Additionally, a bandpass FIR filter with cut off frequencies of 2 Hz to 12 Hz were used to filter each 3 second epoch from the collected data.

Through each trial there was at least one prototypical observation of the frequency band power expected at the target and harmonic frequencies (primary feature at 4 Hz and secondary at 8 Hz). Additionally, each task for the group revealed responses at the apparent harmonic of the target frequency. The specificity of each of the 4 Hz and 8 Hz responses indicates that they were exogenous responses caused by the stimuli and not endogenous responses resulting from internal processes in each participant. Table 7 depicts the frequency measured post task for each of the target stimuli, the observed 4 Hz response frequency, and the observed 8 Hz response frequency from the task. The Target Frequency was calculated by measuring the change between approximate time hacks of each onset of the digital event signal and dividing the value by 4. By dividing 1 by the obtained value the frequency of the target stimuli could be approximated. Additionally, the frequency resolution of the spectral density windows provided in tasks 2 and 3 are limited to .244 Hz, therefore, the observed frequencies may be off by $\pm$ .244 Hz. The aforementioned frequencies are referenced in the sections which follow this introduction.

Table 7: Frequencies observed during Task 2

Target Frequency	Observed 4 Hz Frequency	Observed 8 Hz Frequency
4.28 Hz	4.3945 Hz	8.5449 Hz

Task 2 – 640nm

Both flicker and illumination were observed by each participant in the 640nm portion of Task 2. The participant observations are annotated in Table 8.

Table 8: Participant observation of 640 nm target stimuli in Task 2

Participant Number	Observed Illumination	Observed Flicker
P001	Yes	Yes
P002	Yes	Yes
P003	Yes	Yes
P004	Yes	Yes
P005	Yes	Yes
P006	Yes	Yes

Although Participant 3 was the only participant to have a predominant increase in power at the target frequency (approximately 4.3 Hz), participants 2, 4, and 6 also had predominant increases in power at approximately twice the target frequency (8.5 Hz).

The observed power at approximately 8 Hz may represent harmonics of the 4 Hz target frequency because it occurs at approximately an integer multiple (approximately 8.5 Hz) of the target frequency of 4.4 Hz. Additionally, the observed increase at 8 Hz occurs at exactly the same frequency across participants. The increased 8 Hz activity does not preclude the observed power increase at the target stimuli from being considered a positive response to the target stimuli. Figures 30 and 31, below, compares the baseline measure of frequency band power at the same frequencies from the 1 Hz task to the 4 Hz task. The baseline measures were epoched and averaged in the same manner as the 4 Hz task period. The intent of this figure is to show the target frequencies are not present in other trials for the participant. Participant 5 is the only participant who has an amplitude that appears to peak near the targeted frequencies in the baseline period, and it is actually peaking at 9 Hz.

Figure 30 - Task 2: Normalized PSD for Participants 1 - 3 for the 4Hz 640nm target stimuli compared to baseline

Figure 31 - Task 2: Normalized PSD for Participants 4 - 6 for the 4Hz 640nm target stimuli compared to baseline

Task 2 – 770nm

Both flicker and illumination were observed by each participant in the 770nm portion of Task 2. The participant observations are annotated in Table 9.

Table 9: Participant observations of 770 nm target stimuli in Task 2

Participant Number	Observed Illumination	Observed Flicker
P001	Yes	Yes
P002	Yes	Yes
P003	Yes	Yes
P004	Yes	Yes
P005	Yes	Yes
P006	Yes	Yes

The participants to see a predominant increase in power at the target frequency (approximately 4.3 Hz) were participants 2 and 3; however, Participant 5 also had an observed increase in power at the target frequency at a lower amplitude than the 8 Hz power increase. Participants 1, 4, 5, and 6 had a predominant increase in power at the same frequency, 8.5 Hz. Participants 2 and 3 also had secondary power increases at 8.5 Hz. The observed power at approximately 8.5 Hz may represent harmonics of the 4.4 Hz target frequency because it occurs at approximately an integer multiple of the target frequency. Figures 32 and 33, below, compare the baseline measure of frequency band power at the same frequencies from the 1 Hz task to the 4 Hz task. The baseline measures were epoched and averaged in the same manner as the 4 Hz task period. The intent of these figures is to show the target frequencies are not present in other trials for the participant. In the baseline for Participant 3, the increase in power near 8 Hz is at approximately 8.1 Hz.
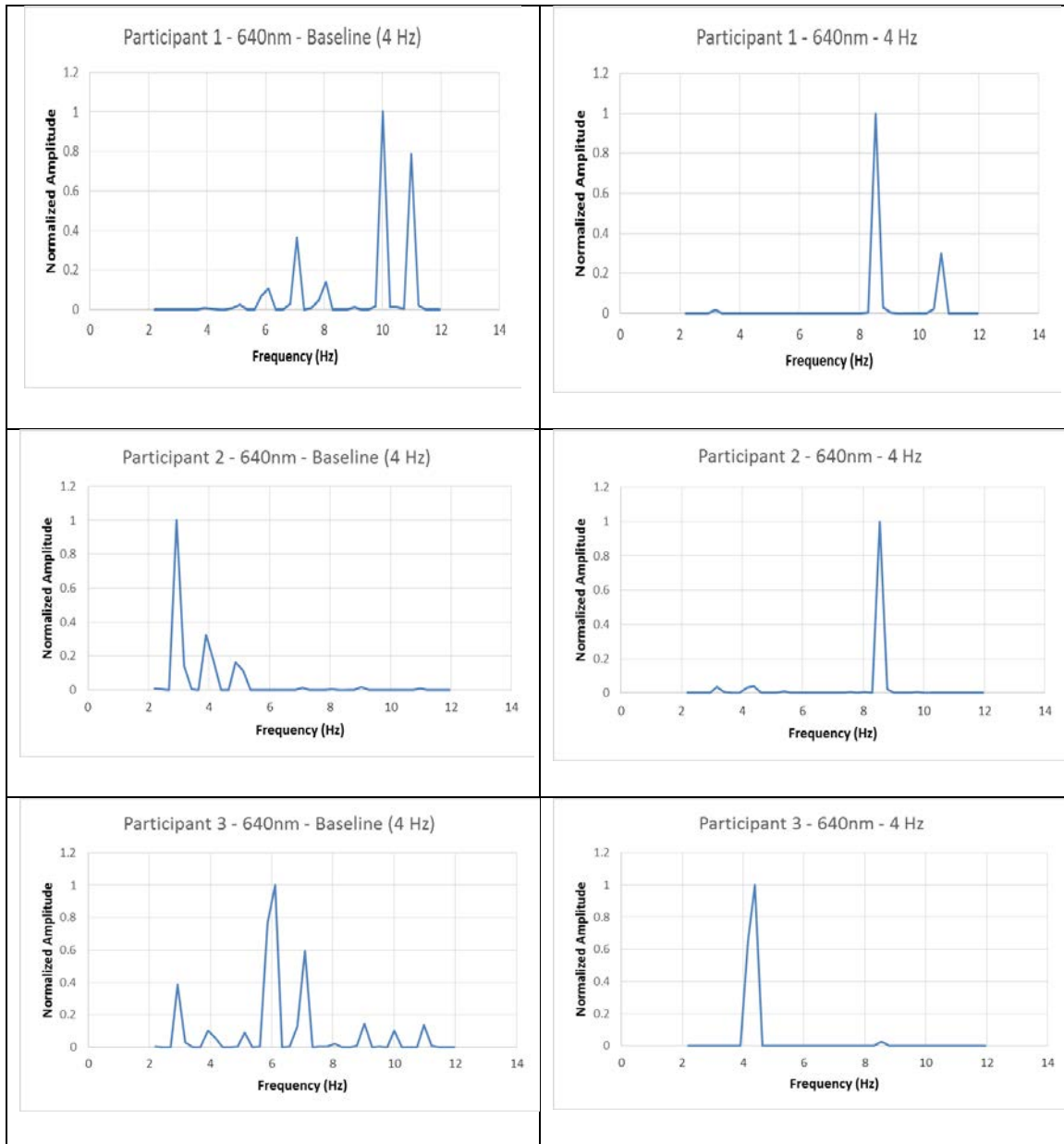
Figure 32 - Task 2: Normalized PSD for Participants 2 - 3 for the 4Hz 770nm target stimuli compared to baseline
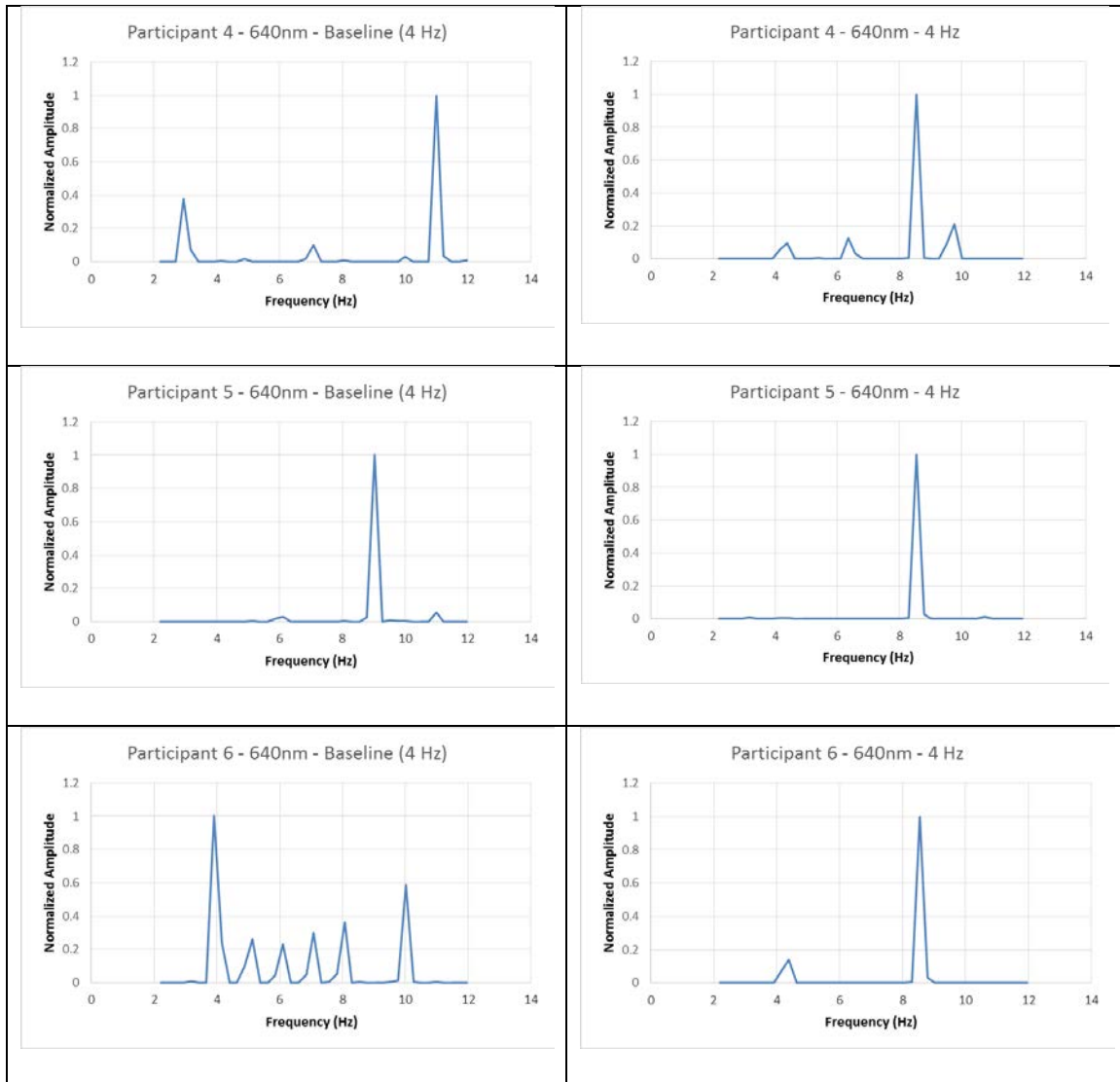
Figure 33 - Task 2: Normalized PSD for Participants 4 - 6 for the 4Hz 770nm target stimuli compared to baseline

Task 2 – 810nm

Both flicker and illumination were observed by Participant 2 but not by participants 1, 3, 4, 5, and 6 in the 810nm portion of Task 2. The participant observations are annotated in Table 10.

73

Table 10: Participant observations of 810 nm target stimuli in Task 2

Participant Number	Observed Illumination	Observed Flicker
P001	No	No
P002	Yes	Yes
P003	No	No
P004	No	No
P005	No	No
P006	No	No

The only participant to see a predominant increase in power at approximately the target frequency was Participant 4. Participants 1 and 5 had predominant power increases at approximately 8.5 Hz and Participant 4 also had a secondary increase at approximately 8.5 Hz. Participants 2 and 6 did not have an observed power increase around either the target frequency or its harmonic. Figures 34 and 35, below, compare the baseline measures of frequency band power at the same frequencies from the 1 Hz task to the 4 Hz task. The baseline measures were epoched and averaged in the same manner as the 4 Hz task period. The intent of this figure is to show the target frequencies are not present in other trials for the participant. The baseline, again, reflects that no occurrences of either the target frequency or its harmonic exist before the 4 Hz target stimuli were presented.

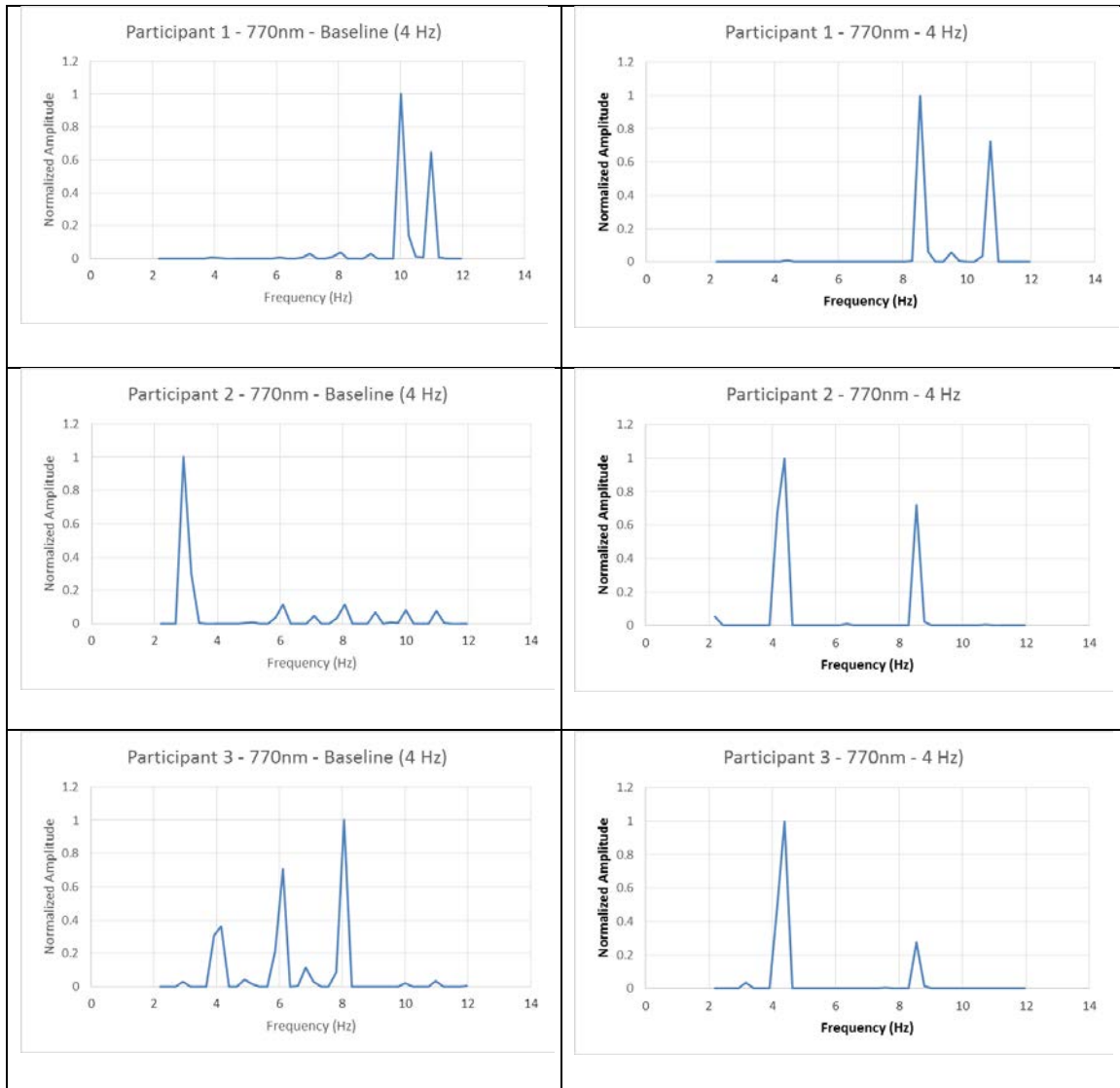**Figure 34 - Task 2: Normalized PSD for Participants 1 - 3 for the 4Hz 810nm target stimuli compared to baseline**
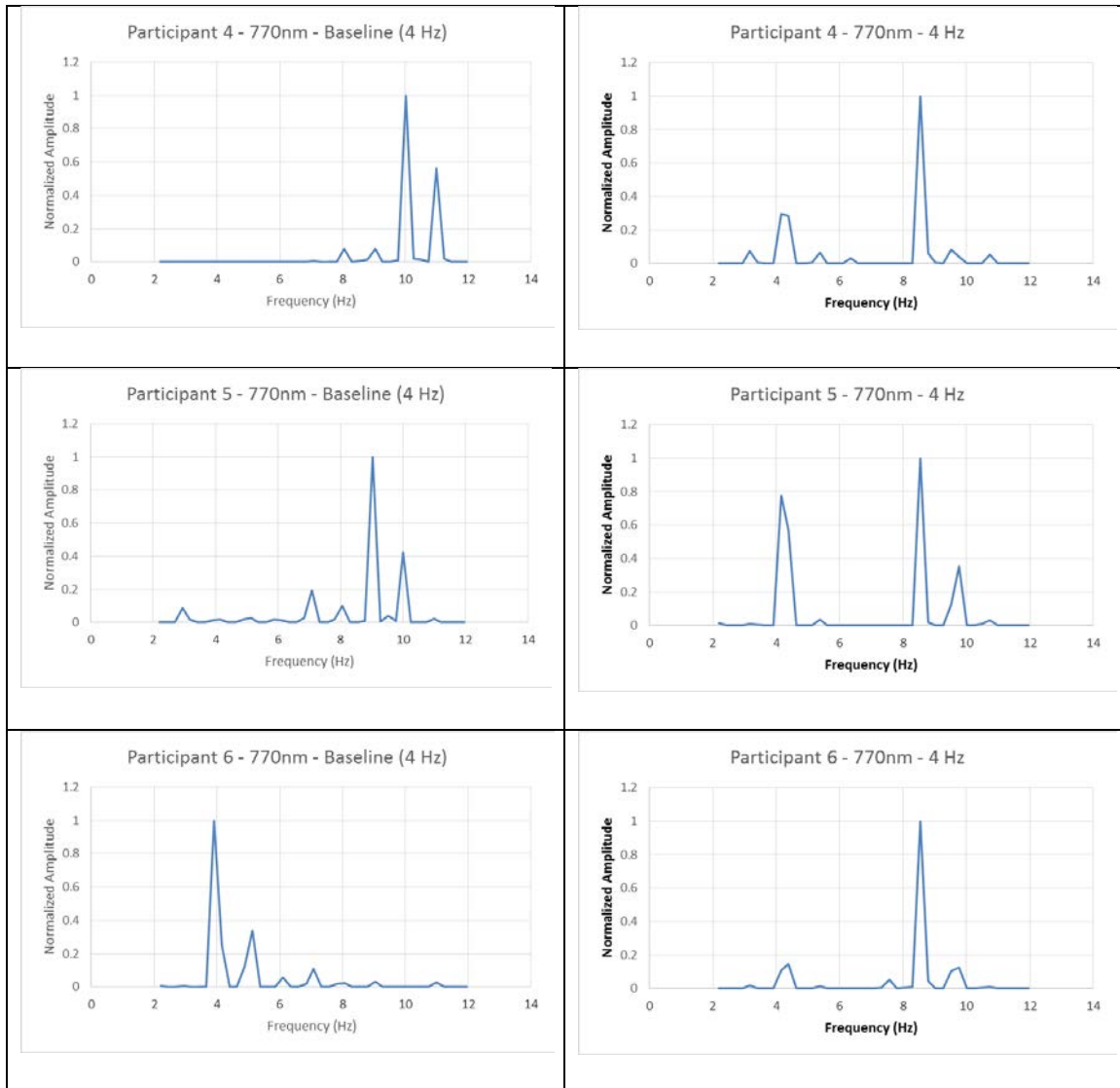
Figure 35 - Task 2: Normalized PSD for Participants 4 - 6 for the 4Hz 810nm target stimuli compared to baseline

Task 2 – 830 nm

Both flicker and illumination were observed by each participant in the 830nm portion of Task 2. The participant observations are annotated in Table 11.

Table 11: Participant observations of 830 nm target stimuli in Task 2

Participant Number	Observed Illumination	Observed Flicker
P001	Yes	Yes
P002	Yes	Yes
P003	Yes	Yes
P004	Yes	Yes
P005	Yes	Yes
P006	Yes	Yes

The only participants to see a predominant increase in power at the target frequency were participants 4 and 6; however, there was also a large increase in power at and the target frequency for Participant 3. Additionally, participants 1 and 3 had primary power increases at approximately 8.5 Hz. The observed power at approximately 8 Hz may represent harmonics of the 4 Hz target frequency because it occurs at approximately an integer multiple (approximately 8.5 Hz) of the target frequency of 4.3 Hz. Figures 36 and 37, below, compare the baseline measures of frequency band power at the same frequencies from the 1 Hz task to the 4 Hz task. The baseline measures were epoched and averaged in the same manner as the 4 Hz task period. The intent of this figure is to show the target frequencies are not present in other trials for the participant. The baseline, again, reflects that no occurrences of either the target frequency or its harmonic exist before the 4 Hz target stimuli were presented.
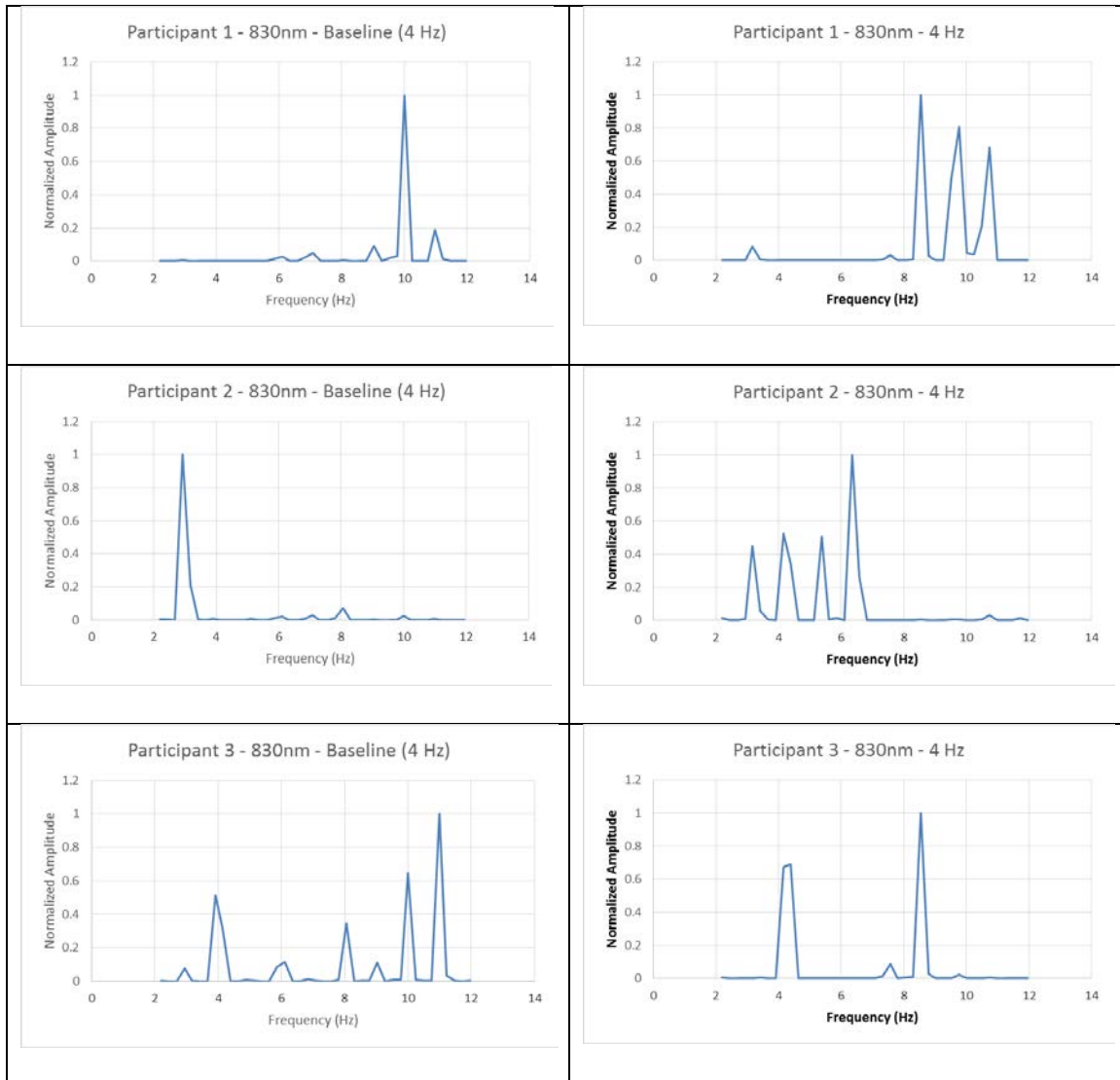
Figure 36 - Task 2: Normalized PSD for Participants 1 - 3 for the 4Hz 830nm target stimuli compared to baseline
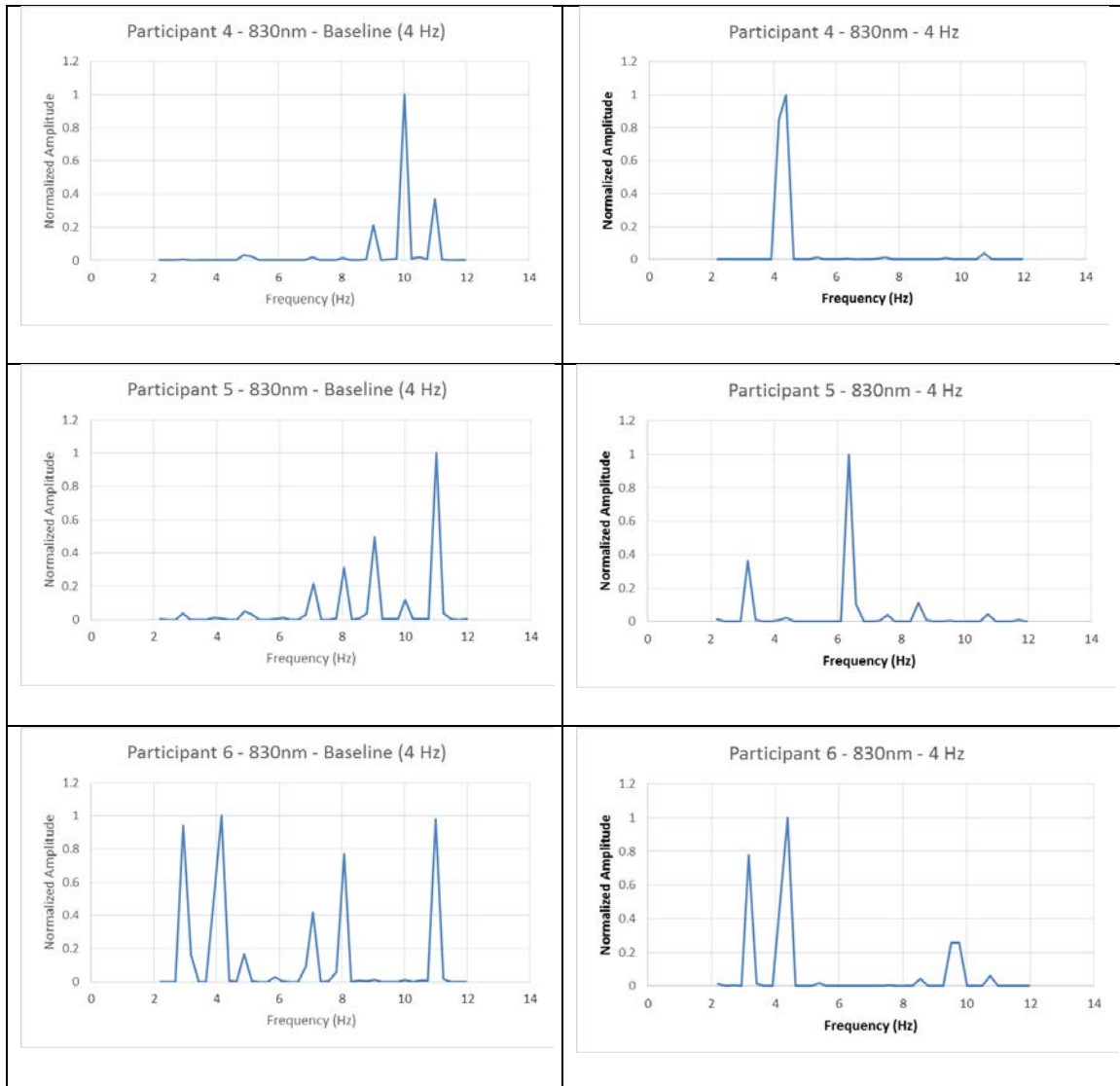
Figure 37 - Task 2: Normalized PSD for Participants 3 - 6 for the 4Hz 830nm target stimuli compared to baseline

Task 2 – 940nm

Neither flicker nor illumination were observed by any participant in the 940 nm portion of Task 2. The participant observations are annotated in Table 12.

Table 12: Participant observations of 940 nm target stimuli in Task 2

Participant Number	Observed Illumination	Observed Flicker
P001	No	No
P002	No	No
P003	No	No
P004	No	No
P005	No	No
P006	No	No

The only participant to see a predominant increase in power at the target frequency was Participant 2; however, there was predominant increase in power at approximately 8 Hz for Participant 3. Additionally, participants 2 and 5 had secondary increases in 8 Hz power. The observed power at approximately 8 Hz may represent harmonics of the 4 Hz target frequency because it occurs at approximately an integer multiple (approximately 8.5 Hz) of the target frequency of 4.3 Hz. Figures 38 and 39, below, compare the baseline measures of frequency band power at the same frequencies from the 1 Hz task to the 4 Hz task. The baseline measures were epoched and averaged in the same manner as the 4 Hz task period. The intent of this figure is to show the target frequencies are not present in other trials for the participant. The baseline, again, reflects that no occurrences of either the target frequency or its harmonic exist before the 4 Hz target stimuli were presented.
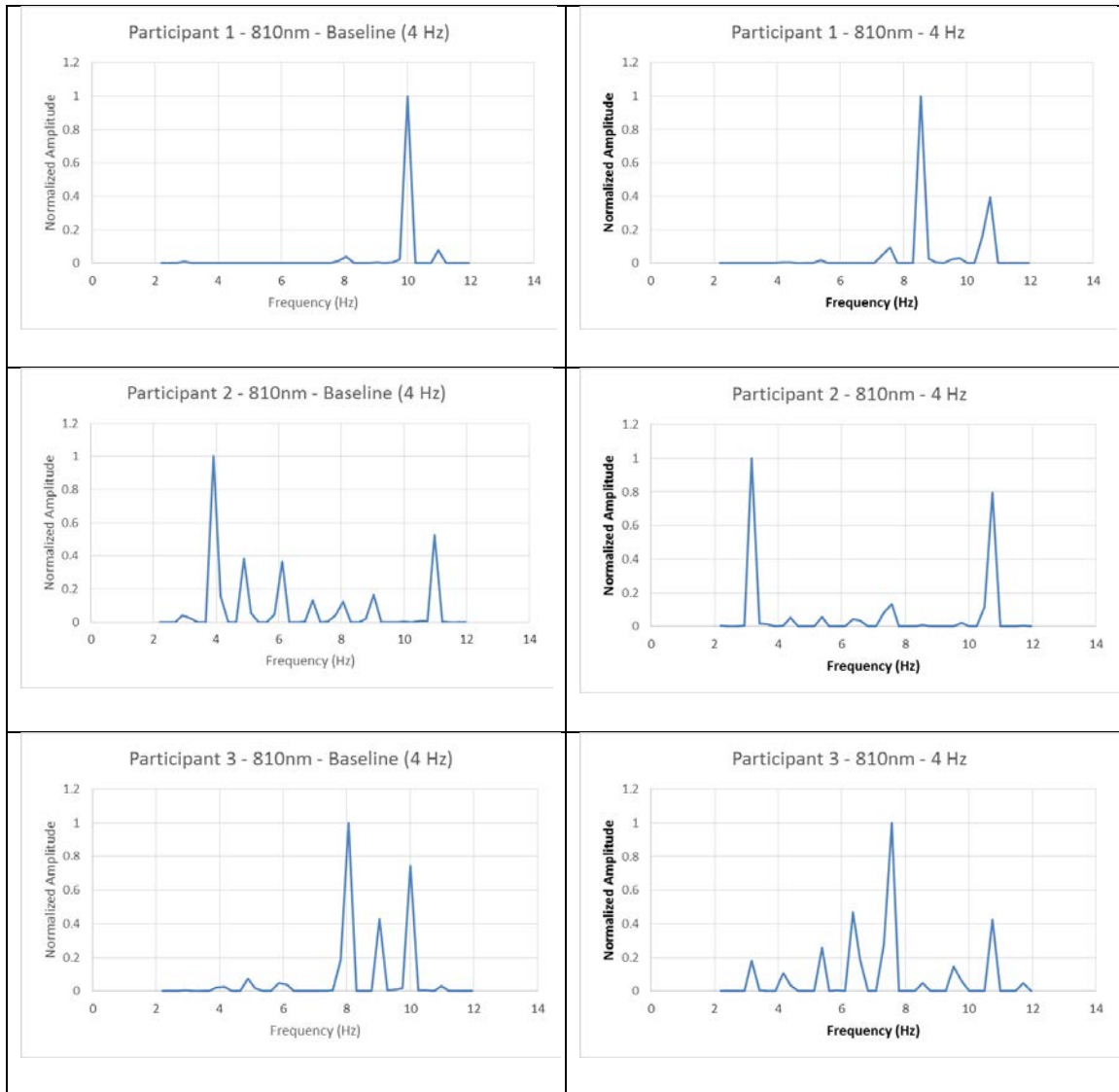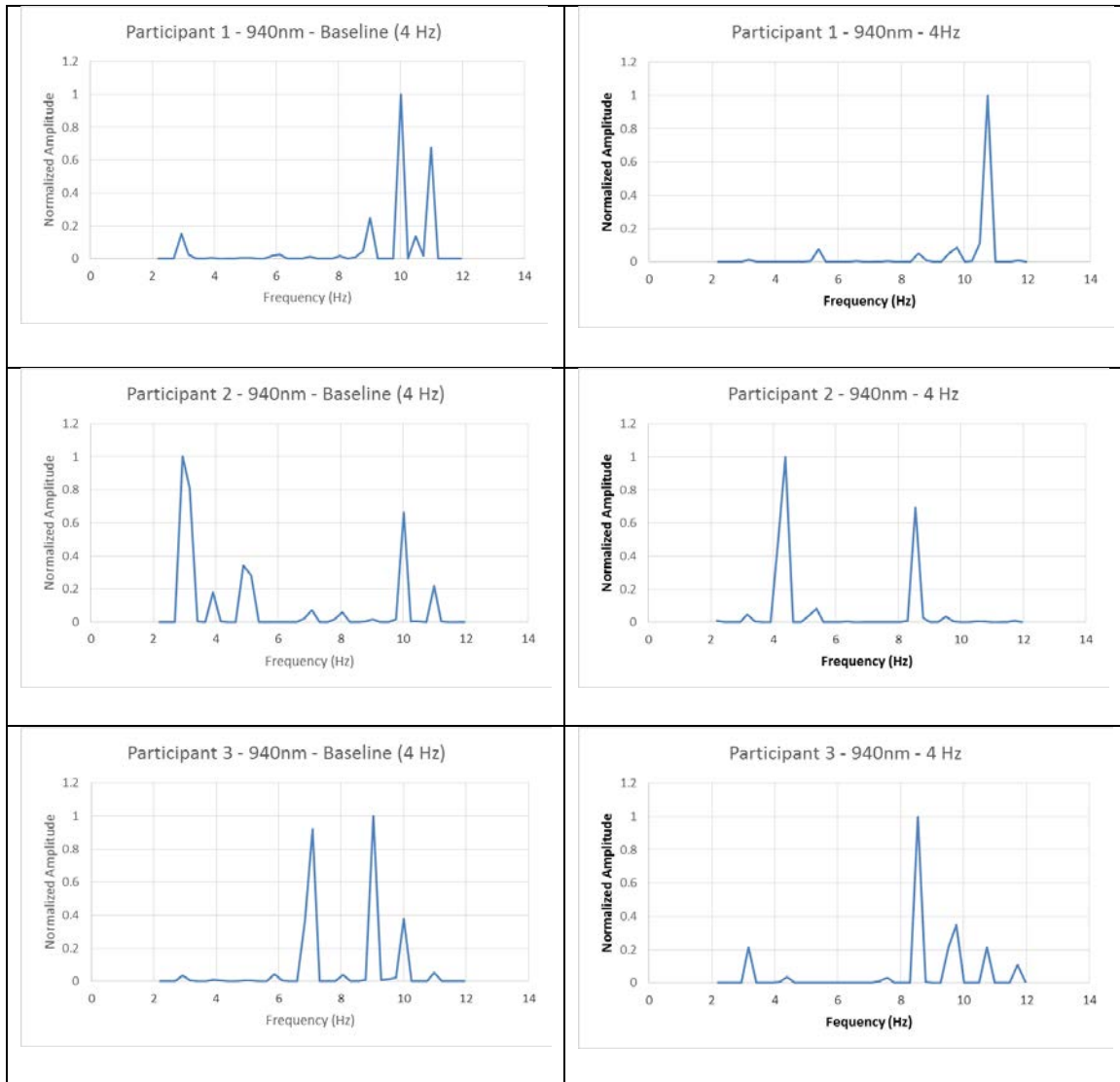
Figure 38 - Task 2: Normalized PSD for Participants 1 - 3 for the 4Hz 940nm target stimuli compared to baseline
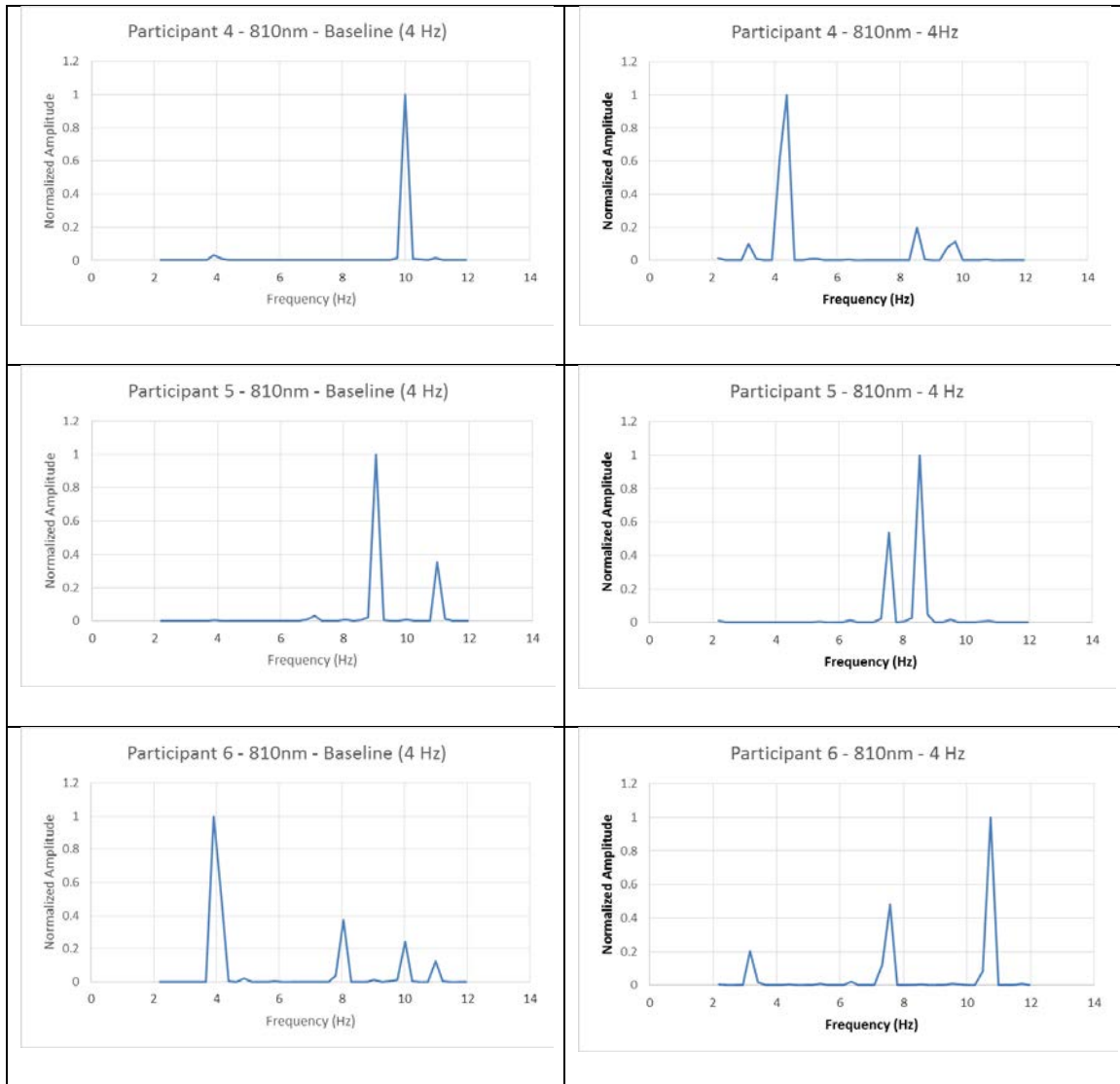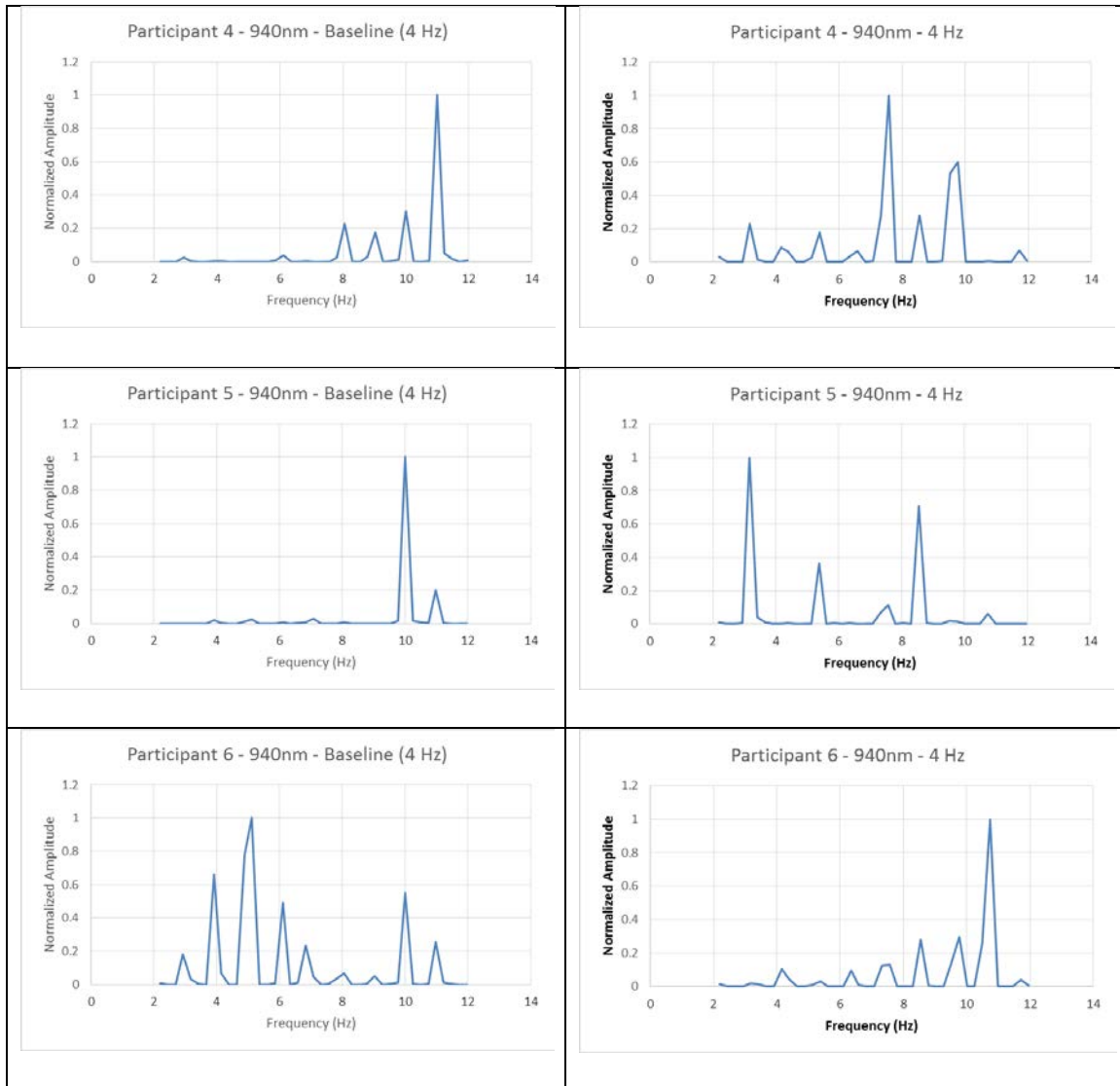
Figure 39 - Task 2: Normalized PSD for Participants 3 - 6 for the 4Hz 940nm target stimuli compared to baseline

Task 3 – 40 Hz Condition

The oscillatory responses for each participant, in Task 3, were calculated by using PSD analysis. The responses for each participant were plotted referencing a normalized amplitude against the frequency window extending from 30 Hz to 50 Hz. The normalized amplitude is used to extract the frequency containing the highest power

density occurring over the observed period of 65 seconds, and it is represented as the product of the measured power at O1 and O2, for each observed frequency, divided by the maximum observed power across the frequencies. The data collected from Task 3 was collected using a bandpass FIR filter with cutoff frequencies of 30 Hz to 50 Hz. The first and last 3 epochs were removed from the collected data to capture a centralized period in which the participant was most attentive to the task, and no epochs were removed because of blinks. Table 13 identifies the target frequency measured in this task and observed frequency response near the target frequency. The frequency resolution of the spectral density windows provided in Task 3 are limited to .244 Hz, therefore, the observed frequencies may be off by $\pm$ .244 Hz. Although it was not always the predominant observed frequency band power, the observed frequency occurred at every wavelength of Task 3 across participants.

Table 13: Target and Observed Frequencies from Task 3

Target Frequency	Observed Frequency
39.76 Hz	39.795 Hz

Task 3 – 640nm

Only illumination, and not flicker, was observed by each participant in the 640nm portion of Task 3. The participant observations are annotated in Table 14.

Table 14: Participant observations of 640 nm target stimuli in Task 3

Participant Number	Observed Illumination	Observed Flicker
P001	Yes	No
P002	Yes	No
P003	Yes	No
P004	Yes	No
P005	Yes	No
P006	Yes	No

Figure 40 depicts the frequency band powers observed for each participant in the 640 nm portion of Task 3. The only participants to see an increase in power at the target frequency were participants 1, 2, 3, 5, and 6. Participant 2 was the only participant, who had a response at 40 Hz, to not have a predominant increase in power at the target frequency.

Figure 40 - Task 3: Normalized PSDs for each participant to the 40 Hz, 640nm target stimuli

Task 3 – 770 nm

Only illumination, and not flicker, was observed by each participant in the 770 nm portion of Task 3. The participant observations are annotated in Table 15.

Table 15: Participant observations of 770 nm target stimuli in Task 3

Participant Number	Observed Illumination	Observed Flicker
P001	Yes	No
P002	Yes	No
P003	Yes	No
P004	Yes	No
P005	Yes	No
P006	Yes	No

Figure 41 depicts the frequency band powers for the 770nm portion of Task 3. The only participants to see an increase in power at the target frequency were participants 1, 3, 4, 5, and 6, and participants 4 and 5 were the only participants to have their predominant response measured at 40 Hz. Participants 1, 3, and 6 had responses observed at 40 Hz; however, the responses were relatively low.
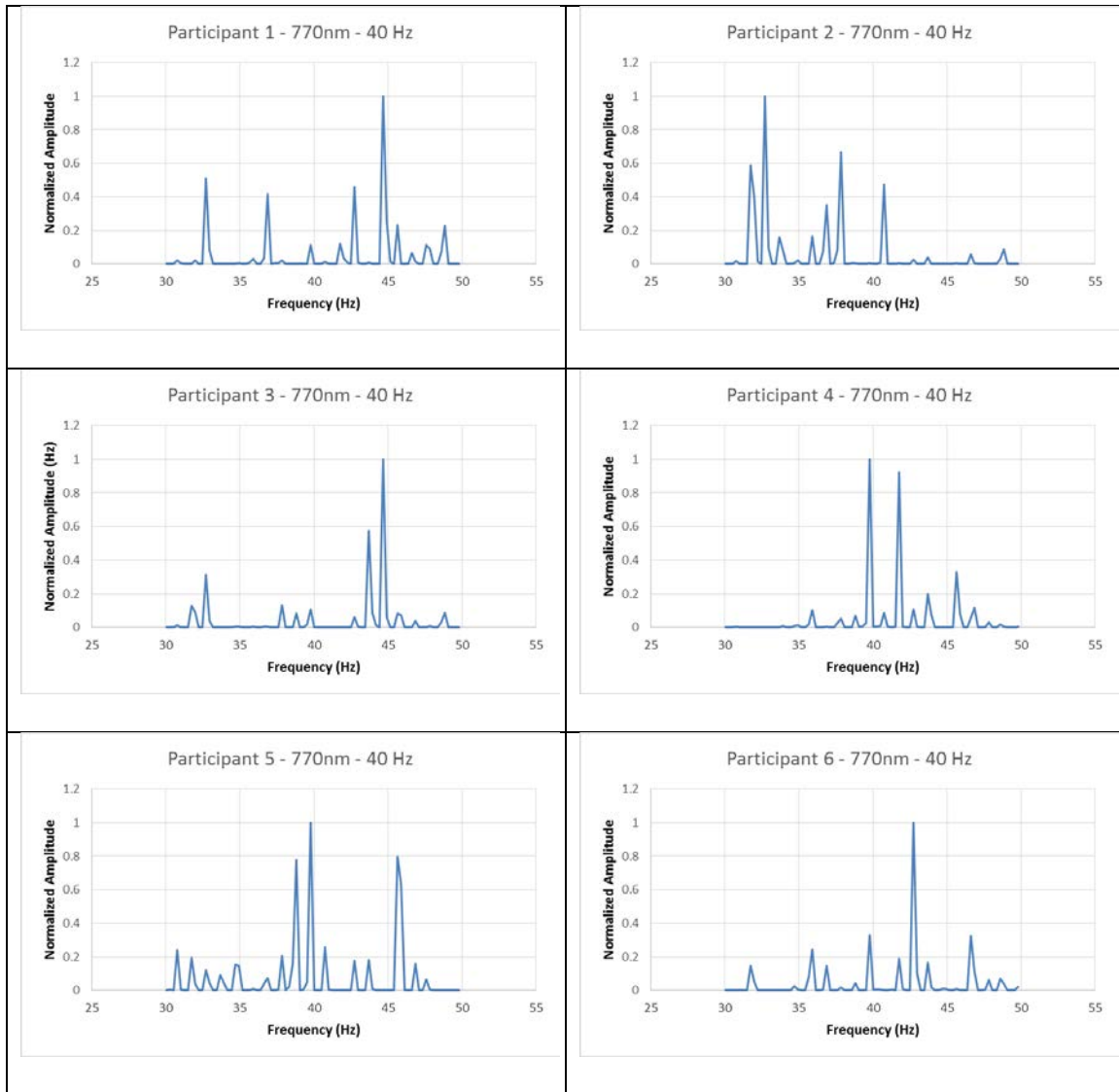
Figure 41 - Task 3: Normalized PSDs for each participant to the 40 Hz, 770nm target stimuli

Task 3 – 810nm

      Only illumination, and not flicker, was observed by participants 1, 2, and 4 in the 810 nm portion of Task 3. Participants 3, 5, and 6 did not observe illumination from the target stimuli. The participant observations are annotated in Table 16.

Table 16: Participant observations of 810 nm target stimuli in Task 3

Participant Number	Observed Illumination	Observed Flicker
P001	Yes	No
P002	Yes	No
P003	No	No
P004	Yes	No
P005	No	No
P006	No	No

      Figure 42 depicts the frequency band powers for each participant from the 810 nm portion of Task 3. The only participants to see an increase in power at the target frequency were participants 1, 2, 3, and 6. No participants had a predominant response observed at the target frequency. Participants 1, 3, and 6 had responses observed at the target frequency; however, the responses were relatively low.
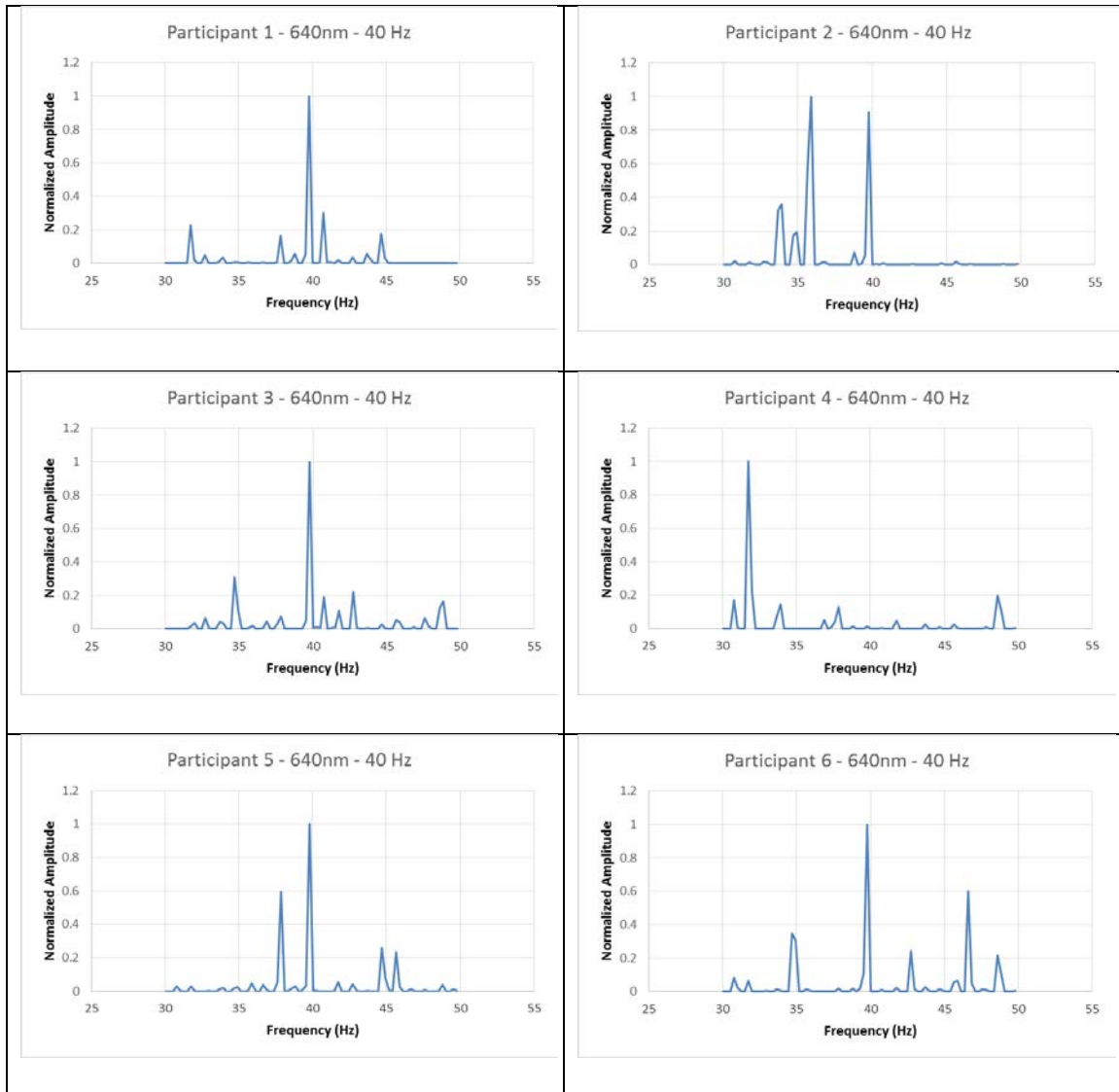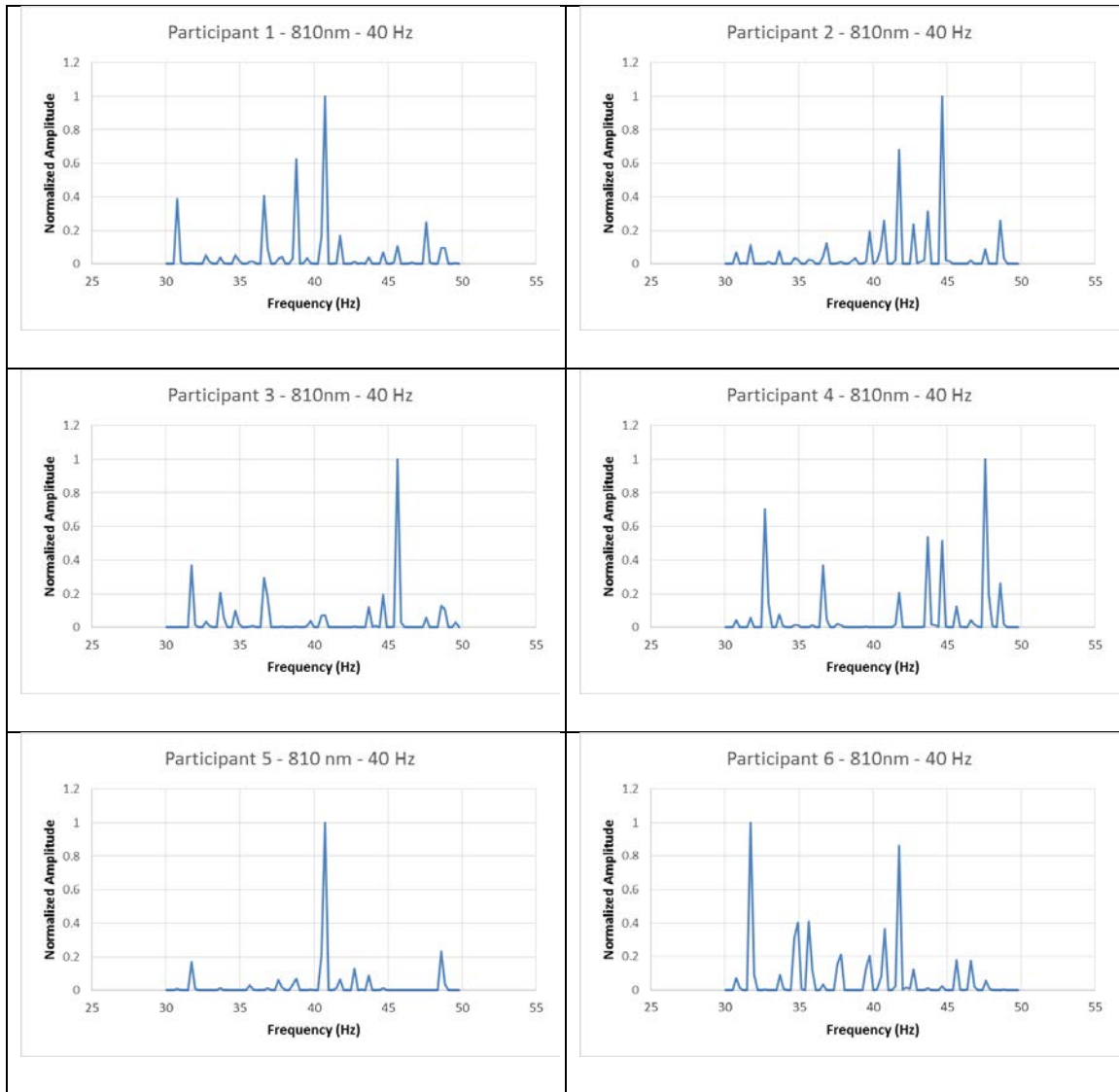
Figure 42 - Task 3: Normalized PSDs for each participant to the 40 Hz, 810nm target stimuli

Task 3 – 830 nm

Only illumination, and not flicker, was observed by participants 1, 2, 3, 4, and 5 in the 830nm portion of Task 3. Participant 6 observed both illumination and flicker from the target stimuli. The participant observations are annotated in Table 17.

Table 17: Participant observations of 830 nm target stimuli in Task 3

Participant Number	Observed Illumination	Observed Flicker
P001	Yes	No
P002	Yes	No
P003	Yes	No
P004	Yes	No
P005	Yes	No
P006	Yes	Yes

Figure 43 depicts the frequency band powers for each participant from the 830nm portion of Task 3. The only participants to see an increase in power at the target frequency were participants 1, 2, 4, and 5. Only Participant 5 had a predominant response observed at the target frequency, and Participant 2 also had a strong response at the target frequency. Participants 1 and 4 had responses observed at 40 Hz; however, the responses were relatively low.
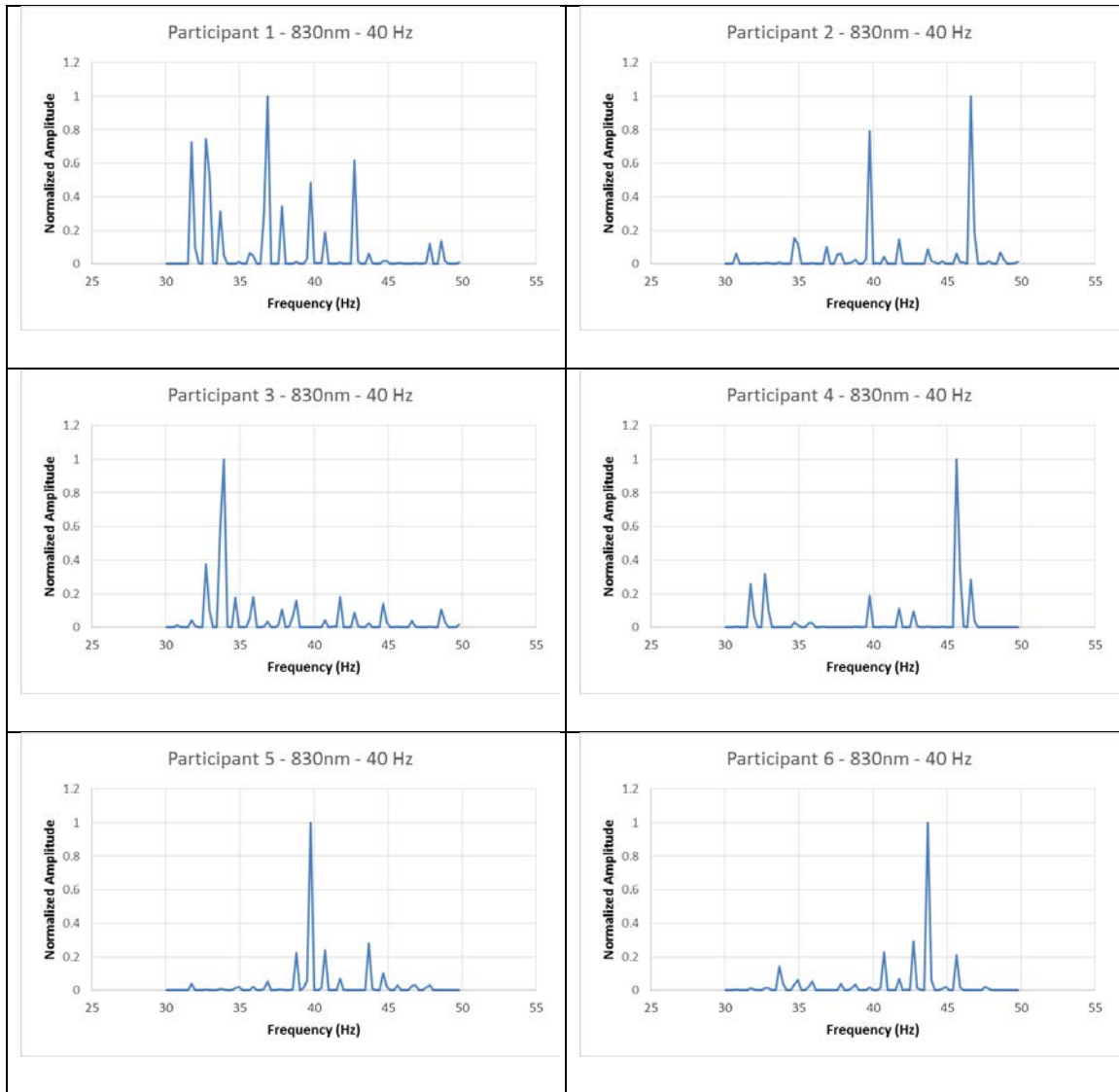
Figure 43 - Task 3: Normalized PSDs for each participant to the 40 Hz, 830nm target stimuli

Task 3 – 940nm

No participant observed either illumination or flicker in the 940nm portion of Task 3. The participant observations are annotated in Table 18.

Table 18: Participant observations of 940 nm target stimuli in Task 3

Participant Number	Observed Illumination	Observed Flicker
P001	No	No
P002	No	No
P003	No	No
P004	No	No
P005	No	No
P006	No	No

Figure 44 depicts the frequency band powers for each participant from the 940 nm portion of Task 3. The only participants to see an increase in power at approximately 40 Hz were participants 2, 3, and 4. No participants had a predominant response at 40 Hz, and participants 2, 3, and 4 had relatively low responses observed at 40 Hz.
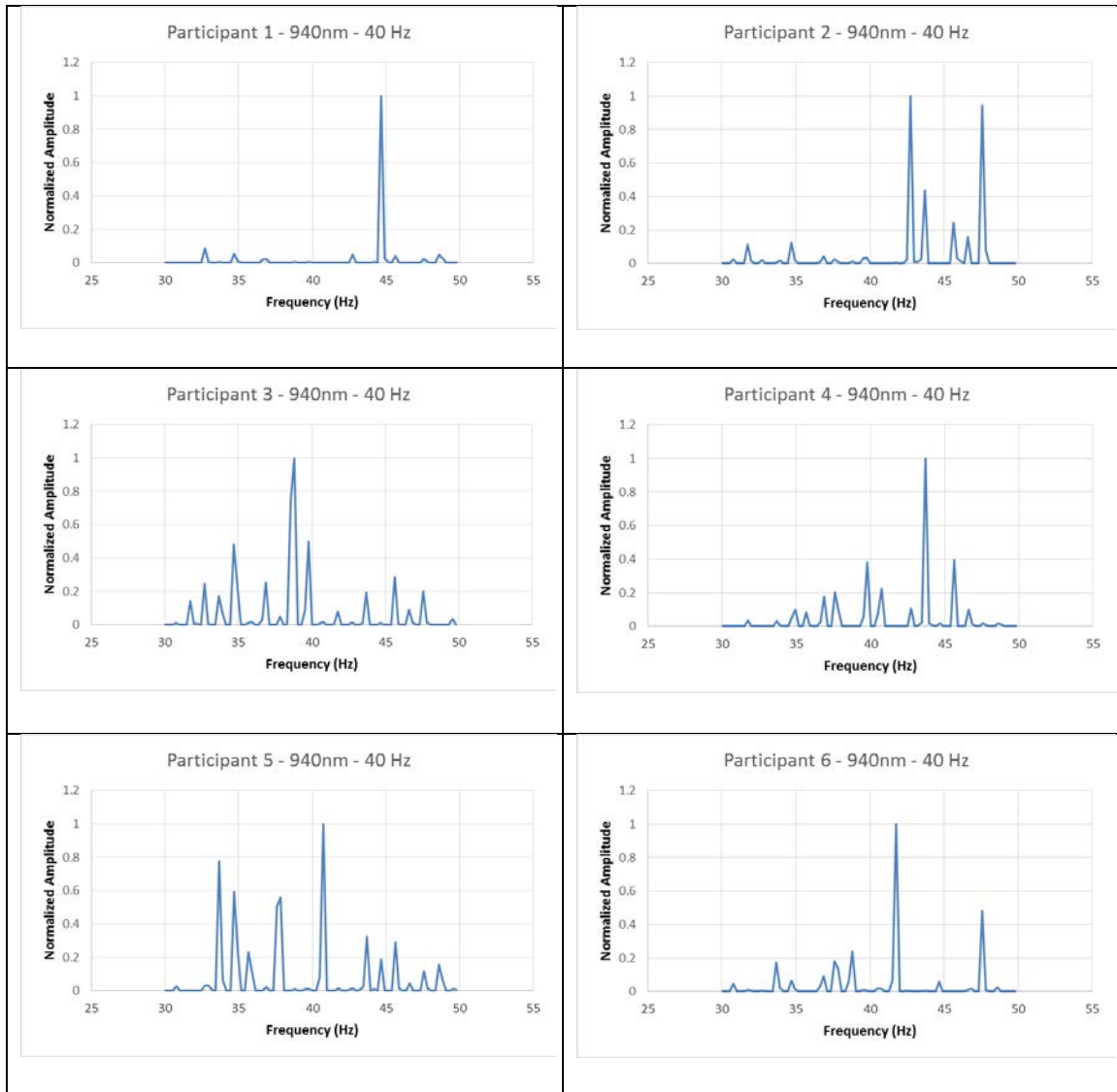
Figure 44 - Task 3: Normalized PSDs for each participant to the 40 Hz, 940nm target stimuli

Summary

In analyzing the time-locked ERPs for across the group of participants it is apparent that ERPs can be generated in the visual cortex by using stimuli of increasing wavelengths up to approximately 830 nm. However, the production of these ERPs appears to be related to the observer's observance of the stimuli as evidenced by the

reduction in signal-to-noise ratios of responses in tasks for which the participant could

not detect the onset of the target stimuli. There is variation between participants and an

LED condition which produces a response in one participant does not necessarily produce

an equivalent response in another participant. Figure 45 shows the variation in SNR

observations for each participant and each wavelength in Task 1. Additionally, Figure 46

highlights the overlap between the signal-to-noise ratios at both O1 and O2 across

participants as well the negative trend associated with the signal-to-noise ratios across

wavelengths in Task 1.
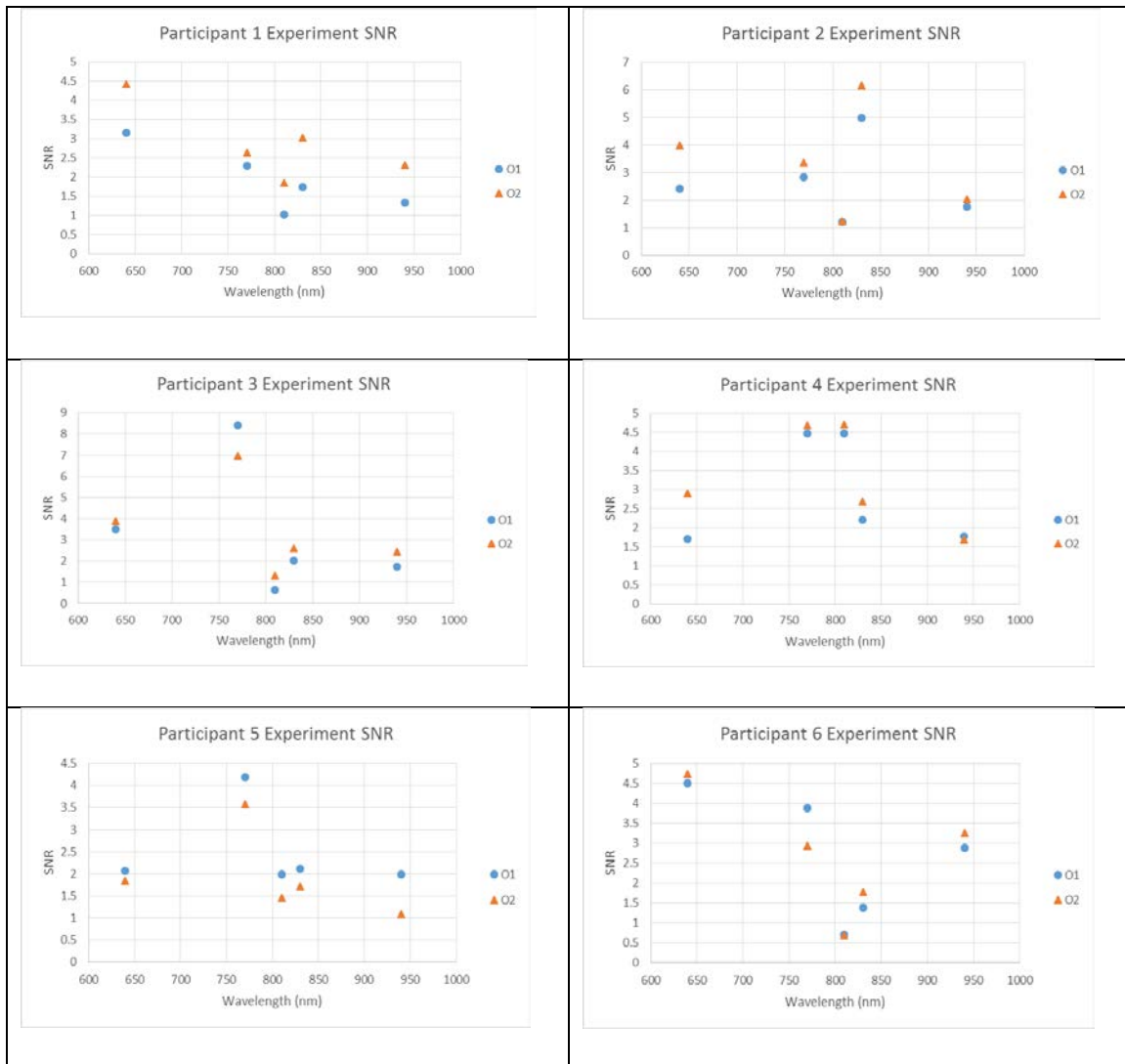
Figure 45 - SNRs across Task 1 for each participant
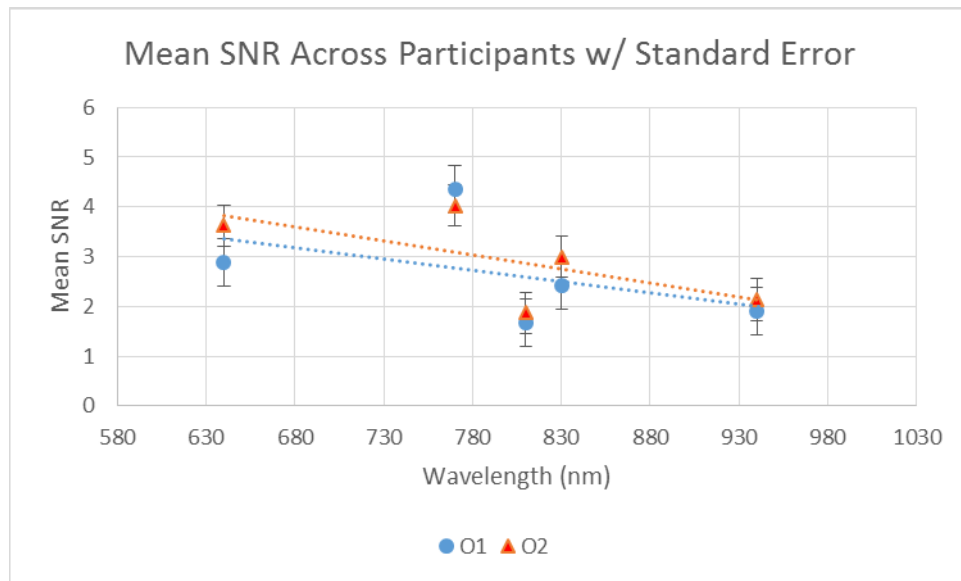
Figure 46 - Mean Signal-to-Noise Ratio across Participants in 1 Hz Task

It does not appear that frequency coded information can be consistently observed
in persons that do not observe either the onset or flicker of a visual stimulus as evidenced
by the observations of oscillatory responses at target frequencies in the 4 Hz task at 810
nm and 940 nm and lack of responses at both wavelengths in the 40 Hz task. It appears
dim stimuli oscillating at frequencies beyond the participant's CFF can negatively impact
our ability to capture and interpret frequency band powers at the relative frequency of the
dim stimuli. In multiple participants, across all of the target stimuli, the target
frequencies or their harmonics can be identified by using the methods outlined in
chapters II and III. However, there is variation in the location of the dominant
frequencies across participants for each wavelength and task. Figures 47 and 48 highlight
the variation between both subjects and frequencies across trials. Figure 47 provides
evidence that there was a high density of responses to the target stimuli. However, the

preponderance of the responses were captured at the first harmonic frequency and not the

target frequency in the 4 Hz trial (70% rate of identification).
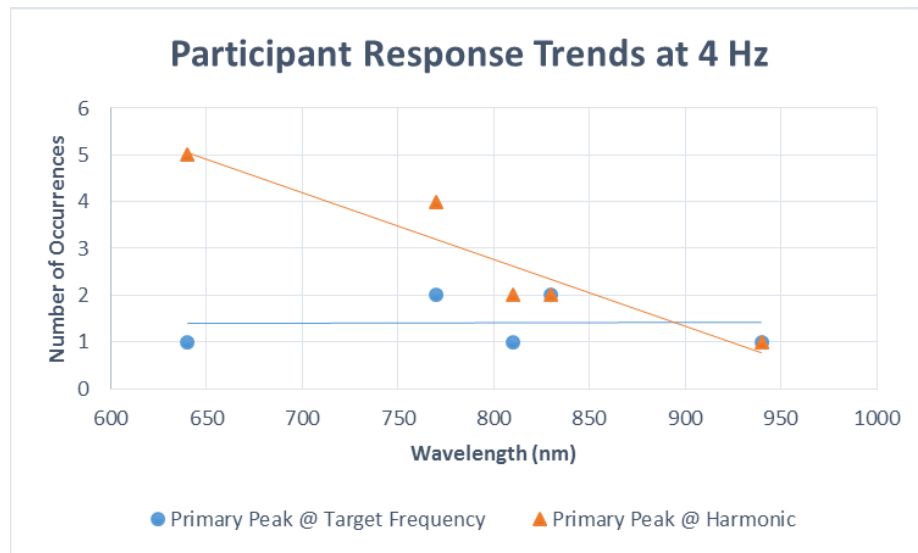
Figure 47 - Participant responses against 4 Hz task

Figure 48 provides evidence that there was a reduction in the number of responses

to the target stimuli in the 40 Hz task relative to the 4 Hz task. Additionally, the

responses follow a negative trend as the peak wavelength of the target stimuli increases. (30% identification rate of target stimuli).
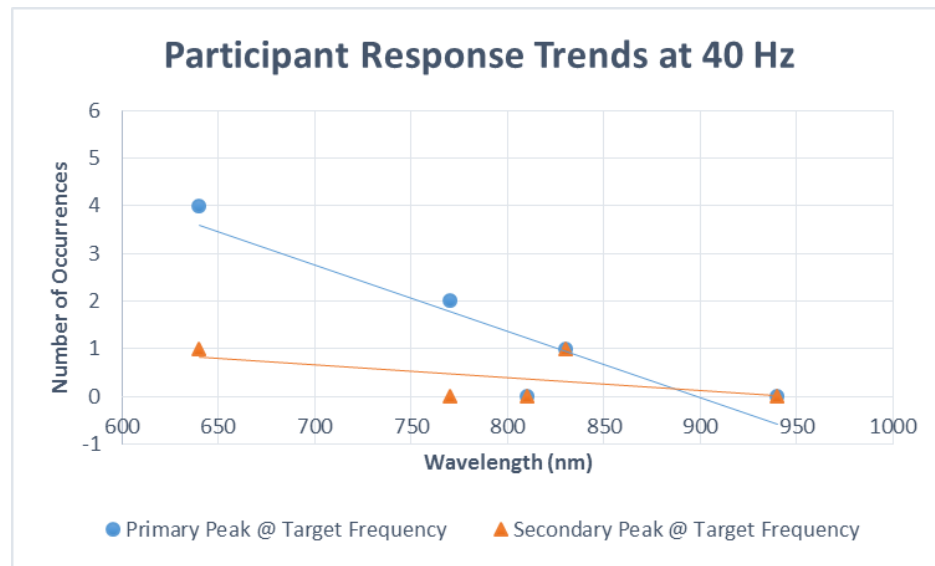
Figure 48 - Participant responses against 40 Hz task

The results from each task in the experiment are summarized in Table 19. Based on the findings, it is evident that the visibility of the stimuli may have contributed to the ability to identify responses via the prescribed approach. Additionally, it is clear that the percentage of responses is concentrated at the shorter peak wavelength target stimuli versus the longer peak wavelength stimuli. However, there were a considerable number of responses noted in the 4 Hz task (Task 2) when compared to tasks 1 and 3. There may have been more responses in Task 2 because higher power responses occur at the lower frequency range of 4 – 12 Hz when compared to the higher frequency associated with Task 3. Also, the effects of dim stimuli on the amplitude of voltage responses in the 1 Hz task (Task 1) contributed to lower responses when compared to Task 2.

Table 19: Summary of results across tasks

Wavelength (nm)	Task 1	Task 2	Task 3	% by Stimuli
640	83%	100%	83%	89%
770	83%	100%	33%	72%
810	17%	50%	0%	22%
830	33%	67%	33%	44%
940	0%	33%	0%	11%
% by Task	43%	70%	30%	

V. Conclusions and Recommendations

Introduction of Research

This research provides a concept for the use of long wavelength stimuli and frequencies beyond the human CFF as an alternative to obtrusive LEDs used in common BCI applications. Using aspects common to existing BCI research, it was hypothesized that long wavelength LEDs operating at varying frequencies could be a feasible method for replacing current visual stimuli in BCI applications.

Research Questions Answered

The basis of this research can be captured in the following research questions:

1. **How does the wavelength of light emitted from Light-Emitting Diodes affect the signal characteristics of Event-Related Potentials produced in the human brain? More specifically, which wavelengths of light-emitting diodes can be used to elicit VECPs in the visual cortex?**

   When considering the appearance of time-locked ERPs and SNRs, the increasing wavelength of target stimuli appear to reduce the measured amplitudes of ERPs across participants (Woodman, 2010). Additionally, there appears to be an associated decrease in the SNR observed across participants as the wavelength increases. Although more obscured by noise when stimuli exist outside the visible range, ERPs can be observed in the visual cortex at wavelengths up to approximately 940nm.

2. **How does the frequency of light produced by Light-Emitting Diodes affect the characteristics of Event-Related Potentials produced in the human brain? More specifically, can oscillatory frequencies above the human CFF be used to elicit oscillatory responses in the visual cortex without producing the visual perception of flicker?**
   It has been demonstrated that LEDs oscillating at 4 Hz (observed flicker) and 40 Hz (unobserved flicker) can be used to elicit oscillatory responses in the human brain. Additionally, the observation of the oscillatory responses may be made when using stimuli of increasing wavelengths from 640nm to 940nm at 4 Hz and 640nm to 830nm at 40 Hz in some cases.

Recommendations for Future Research

There are several limitations that were not addressed in this research. If possible, this research could be improved by identifying more experimental controls for the population of the experiment. The obscure nature of brain activity occurring across subjects creates uncertainty around why a response may be encountered with one subject

and not another in the same experiment environment. There are countless processes occurring in the brain at any given time and identifying many of those processes could facilitate a better understanding of the process that drives the occurrence of cortical responses. Additionally, understanding why a response can be measured in a subject in one scenario and not another could be valuable to the expansion of this research.

Noise is a confounding factor in the area of EEG research. Noise can be generated by a number of environmental elements such as power lines, computer monitors, other electronics, ongoing brain activity, etc. Efforts to expand the noise identification and filtering capabilities of the analysis process can increase the effectiveness of future research. Additionally, a more robust data acquisition system could reduce the effects of environmental noise in future EEG research. Data acquisition systems could include systems which do not require external amplification, wet electrodes, direct (wired) connection to amplifiers or computers, or AC power supplies.

BCI applications for DoD users will need to be more compact and mobile than the system used in this research in order to be useful in cockpits (which have limited space available for additional equipment) or to provide feedback on attention in training scenarios. By using unobtrusive stimuli oscillating at specific frequencies to elicit responses based on overt attention to time-locked stimuli, trainers could review attention at specific points in time to make corrections to human behaviors in specific scenarios. Steps taken to remove the confounding elements of EEG-based ERP experiments can increase the understanding of the aspects of these experiments that are relevant to the elicitation of specific responses consistently and can move DoD toward understanding how to build and implement systems based on this technology. Any Future research

should address the following three areas not evaluated in the current research effort: 1) Analysis of mobile systems to determine the usability of the current systems 2) evaluation of robust signal analysis methods to improve signal-to-noise ratios of targeted responses 3) evaluation of factors affecting the variability of observed ERP (in both time and frequency domains) within and across participants. To address these areas of concern, research should focus on ERP experiments that are component independent, if possible. Also, the research should use a small group (1-3) of participants who are willing to participate in an experiment multiple times so the research can explore the repeatability of observations. Demonstrating the repeatability of observations is much less disputable than the measures which rely on knowledge of EEG and typical ERPs to make determinations about the validity and meaning of responses.

Summary or Significance of Research

As the systems increasingly require cohesion and communication between the human-machine team, the means for increasing the bandwidth of that communication must be expanded. BCIs could be used to increase the bandwidth within the human-machine team; however, the use of stimuli which may be a distraction and impede task completion make it unlikely that BCIs would be used in military operations.

This research takes steps to successfully demonstrate the potential for using non-disruptive stimuli in BCI applications and lays the groundwork for developing more robust systems by demonstrating the following:

1. ERPs can be observed in humans when using LEDs that emit long wavelength energy as visual stimuli; however, the ratio of signal to noise continues to decrease as the wavelength of the target stimuli is increased.

2. Oscillatory responses can be observed, in the human brain, in response to LEDs emitting energy at oscillating frequencies below the rate at which the human observes flicker when using stimuli emitting energy at peak wavelengths between 640 nm and 940 nm and above the rate at which the human observes the flicker from peak wavelengths of 640 nm to 830 nm respectively.

Appendix A: MATLAB Code

Contents

```matlab
clearvars -except collection
trial=5;
task=4;
participant=1:6;
channels=4:5;

frequency_range=[30 50];

srate=2000;


for part=participant
clearvars -except collection trial task participant channels srate collection640 part
temp_collection frequency_range
```

get EEG data

```matlab
    data       = collection(part,trial,task).data(:,channels);      %EEG data
    digital    = collection(part,trial,task).data(:,end);           %All three
digital channels


FILTER=designfilt('bandpassfir','FilterOrder',2000,'CutoffFrequency1',frequency_range(
1),'CutoffFrequency2',frequency_range(2),'SampleRate',2000);
    data=filtfilt(FILTER,data);
```

find digital events

```matlab
    digital(2:end+1,2)  =   digital(:,1);              %create second column equal to
first shifted down one row
    digital(end,:)      =   [];                        %chop off extra data points at
the end
    digital(1,2)        =   digital(1,1);              %copy fist data point to make
sure it is not confused for a switch
    switches            =   digital(:,1)-digital(:,2); %this returns a negative
number wherever it was swithced off, and positive wherever it was turned on

    zeroI               =   find(switches>0);          %index values of the positive
edges (time zeros) in the digital signal
    zeroI(1:3)=[];
```

create epochs

```
    boundsT=[0 3]; %bounds (in seconds) of the epochs

    boundsI    =    round(boundsT*srate);                 %convert time bounds to
index bounds
    epochsI    =    [zeroI+boundsI(1), zeroI+boundsI(2)];   %index values of the epoch
bounds
    [r,c]      =    find(epochsI>size(data,1) | epochsI<1); %find the epochs which
reach outside the limits of the EEG data
    epochsI(r,:)=    [];                                  %remove the epochs which
reach outside the limits of the EEG data

    % the following extracts the epochs from the EEG signal. In the epochs
    % matrix, time descends down the rows, each column is a channel, and each
    % page (in the third dimension) is an epoch
    for ep=1:size(epochsI,1)
        epochs(:,:,ep)=data(epochsI(ep,1):epochsI(ep,2),:);
    end
```

zero mean all epochs

```
    avgs=mean(epochs,1);

    avgs=repmat(avgs,size(epochs,1),1,1);




    epochs=epochs-avgs;
```

Average epochs

```
    epochAVG=mean(epochs,3); %this averages all epochs together for each channel
```

compute power spectrum

```
    [pxx,fxx]=periodogram(epochAVG,[],[],srate);




    [r,c]=find(fxx>=frequency_range(1) & fxx<=frequency_range(2)); %select only
freqencies withen the range selected
    fxx=fxx(r,:);
    pxx=pxx(r,:);

%    array(:,1)=fxx; %this is used when writing to Excell
%    array(:,2:3)=pxx; %this is used when writing to Excell

    pxx=prod(pxx,2); %multiply two channels together
    pxx=pxx.*fxx; %frequency correction
```

```
%      array(:,4)=pxx; %this is used when writing to Excell


%      % write to Excel
%      epochNum=size(epochs,3);
%      path='C:\Users\tdyuser\Desktop\LEDfreq\SSVEP\';
%      file=['Trial_',num2str(trial)];
%
%      header={'Frequency (Hz)','O1 (uV^2)','O2 (uV^2)','(O1*O2)*frequency/max
(normalized)','',num2str(epochNum)};
%
%
%      xlswrite([path,file],array,part,'A2:D83');
%      xlswrite([path,file],header,part,'A1:F1');


    temp_collection(:,part)=pxx;
end
```

plot figures

```
figure

plot(fxx,temp_collection)

legend('1','2','3','4','5','6')
xlim([frequency_range(1) frequency_range(2)])
grid on

figure
plot(fxx,mean(temp_collection,2))
legend('1','2','3','4','5','6')
xlim([frequency_range(1) frequency_range(2)])
grid on
```

Published with MATLAB® R2015a

105

Appendix B: LED Data Sheets

Overview

The LEDs used during the experimental data collection were a central part of the research effort. There were aspects of the research that were affected by the specific technical specifications of each LED used in the experiment. The data sheets describing the operation and performance of the LEDs are included in this appendix.

DESCRIPTION

Need some really bright LEDs? We are big fans of these clear red LEDs, in fact we use them exclusively in our kits. They are very bright and have about 20degree LED beam. They go easily into a breadboard and will add that extra zing to your project.

- Pack of 25 clear red LEDs
- 5mm diameter
- 640 nm wavelength
- 1.8-2.2V Forward Voltage, at 20mA current
- 1500 mcd typical brightness
- Viewing Angle : ±10 degrees
- Maximum continuous current: 30mA

If you need some help using LEDs, please read our "Introduction to using LEDs" tutorial for any electronics project.

TECHNICAL DETAILS

Peak Emission Wavelength: 770nm

The MTE1077N1-R is a red T 1 3/4, 5mm water clear emitter designed for applications requiring high power output and high reliability in a narrow angle package.

FEATURES

> High Reliability

> Narrow Beam Angle

> High Output Power

APPLICATIONS

> Optical Sensors

> Optical Switches

> Medical Application

Absolute Maximum Ratings (Ta=25°C)

ITEMS	SYMBOL	RATINGS	UNIT
Forward Current (DC)	IF	50	mA
Forward Current (Pulse)*1	IFP	0.5	A
Reverse Voltage	VR	5	V
Power Dissipation	PD	100	mW
Operating Temperature Range	Topr	-20 ~ +80	°C
Storage Temperature Range	Tstg	-30 ~ +100	°C
Junction Temperature	Tj	100	°C
Lead Soldering Temperature*2	Tls	260	°C

*1: Tw=10µsec, T=10msec; *2: Time 3 Sec max, Position: Up to 2mm from the body.

Electrical & Optical Characteristics (Ta = 25°C)

ITEMS	SYMBOL	CONDITIONS	MIN	TYP	MAX	UNIT
Power Output	PO	IF=20mA	--	5.5	--	mW
Forward Voltage	VF	IF=20mA	--	1.55	1.96	V
Reverse Current	IR	VR=5V	--	--	100	µA
Peak Emission Wavelength	λp	IF=20mA	--	770	--	nm
Spectral Line Half Width	Δλ	IF=20mA	--	25	--	nm
Half Intensity Beam Angle	Θ	IF=20mA	--	±12	--	deg
Rise Time	Tr	IFP=20mA	--	--	--	nS
Fall Time	Tf	IFP=20mA	--	--	--	nS
Junction Capacitance	Cj	1MHz, V=0V	--	35	--	pF
Temperature Coefficient of PO	P/T	IF=10mA	--	-0.6	--	%/°C
Temperature Coefficient of VF	V/T	IF=10mA	--	-2.0	--	mV/°C

2012-05-17

1

Peak Emission Wavelength: 810nm

The MTE2081-OH5 consists of a 810nm high output infrared die in a water-clear 5mm plastic molded package. Custom package solutions and sorting are available.

FEATURES

> High Output Power
> Narrow Beam Angle
> High Reliability
> Excellent Optical / Mechanical Axis Alignment

APPLICATIONS

> Optical Switches & Sensors
> Optical Position Sensing / Security Systems
> Medical Applications / Optical Communication
> Currency Validation / Light Curtain

Absolute Maximum Ratings (Ta=25ºC)

ITEMS	SYMBOL	RATINGS	UNIT
Forward Current (DC)	IF	100	mA
Forward Current (Pulse)*1	IFP	1	A
Reverse Voltage	VR	5	V
Power Dissipation	PD	180	mW
Operating Temperature Range	Topr	-20 ~ +80	ºC
Storage Temperature Range	Tstg	-30 ~ +100	ºC
Junction Temperature	Tj	100	ºC
Lead Soldering Temperature*2	Tls	260	ºC

*1: Tw=10µsec, T=10msec. *2: Time 5Sec max, Position: Up to 3mm from the body.

Electrical & Optical Characteristics (Ta = 25ºC)

ITEMS	SYMBOL	CONDITIONS	MIN	TYP	MAX	UNIT
Power Output	PO	IF=50mA	--	20.0	--	mW
Forward Voltage	VF	IF=50mA	--	1.55	1.9	V
Reverse Current	IR	VR=5V	--	--	100	µA
Peak Emission Wavelength	λp	IF=50mA	--	810	--	nm
Spectral Line Half Width	Δλ	IF=50mA	--	40	--	nm
Half Intensity Beam Angle	Θ	IF=50mA	--	±7	--	deg

2011-02-16

1

# High Speed Infrared Emitting Diode in T-1¾ Package

Description

TSHG8200 is a high speed infrared emitting diode in GaAlAs double hetero (DH) technology, molded in a clear, untinted plastic package.

The new technology combines high speed with high radiant power at wavelength of 830 nm.

Features

- High modulation bandwidth
- Extra high radiant power and radiant intensity
- Low forward voltage
- Suitable for high pulse current operation
- Standard package T-1¾ ($\varnothing$ 5 mm)
- Angle of half intensity $\varphi = \pm 10°$
- Peak wavelength $\lambda_p = 830$ nm
- High reliability
- Good spectral matching to Si photodetectors
- Lead (Pb)-free component
- Component in accordance to RoHS 2002/95/EC and WEEE 2002/96/EC

94 8390
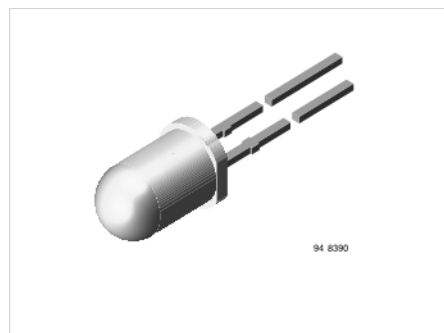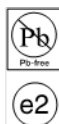
Applications

Infrared radiation source for CMOS cameras (illumination). High speed IR data transmission.

Parts Table

Part	Remarks
TSHG8200	MOQ: 4000 pc

Absolute Maximum Ratings

$T_{amb} = 25 °C$, unless otherwise specified

Parameter	Test condition	Symbol	Value	Unit
Reverse Voltage		V_R	5	V
Forward current		I_F	100	mA
Peak Forward Current	$t_p/T = 0.5$, $t_p = 100$ µs	I_{FM}	200	mA
Surge Forward Current	$t_p = 100$ µs	I_{FSM}	1	A
Power Dissipation		P_V	250	mW
Junction Temperature		T_j	100	°C
Operating Temperature Range		T_{amb}	- 40 to + 85	°C
Storage Temperature Range		T_{stg}	- 40 to + 100	°C
Soldering Temperature	$t \leq 5$ sec, 2 mm from case	T_{sd}	260	°C
Thermal Resistance Junction/Ambient		R_{thJA}	300	K/W

TSHG8200

Vishay Semiconductors

Basic Characteristics

T_{amb} = 25 °C, unless otherwise specified

Parameter	Test condition	Symbol	Min	Typ.	Max	Unit
Forward Voltage	I_F = 100 mA, t_p = 20 ms	V_F		1.5	1.8	V
	I_F = 1 A, t_p = 100 µs	V_F		2.3		V
Temp. Coefficient of V_F	I_F = 100 mA	TK_{VF}		-2.1		mV/K
Reverse Current	V_R = 5 V	I_R			10	µA
Junction capacitance	V_R = 0 V, f = 1 MHz, E = 0	C_j		125		pF
Radiant Intensity	I_F = 100 mA, t_p = 20 ms	I_e	80	160	400	mW/sr
	I_F = 1 A, t_p = 100 µs	I_e		1600		mW/sr
Radiant Power	I_F = 100 mA, t_p = 20 ms	Φ_e		50		mW
Temp. Coefficient of Φ_e	I_F = 100 mA	$TK_{\Phi e}$		-0.35		%/K
Angle of Half Intensity		φ		±10		deg
Peak Wavelength	I_F = 100 mA	λ_p		830		nm
Spectral Bandwidth	I_F = 100 mA	$\Delta\lambda$		40		nm
Temp. Coefficient of λ_p	I_F = 100 mA	$TK_{\lambda p}$		0.25		nm/K
Rise Time	I_F = 100 mA	t_r		20		ns
Fall Time	I_F = 100 mA	t_f		13		ns
Cut-Off Frequency	I_{DC} = 70 mA, I_{AC} = 30 mA pp	f_c		20		MHz
Virtual Source Diameter		$\varnothing$		3.7		mm

Typical Characteristics

(T_{amb} = 25 °C unless otherwise specified)
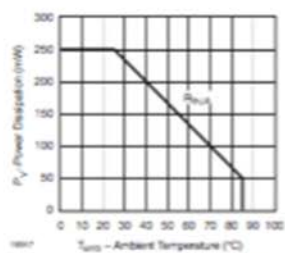
Figure 1. Power Dissipation vs. Ambient Temperature
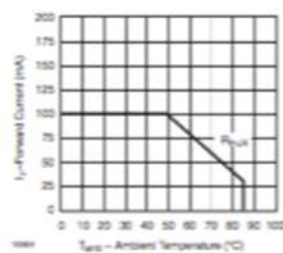
Figure 2. Forward Current vs. Ambient Temperature

110

EVERLIGHT

Technical Data Sheet
5mm Infrared LED , T-1 3/4

IR333-A

Features
- High reliability
- High radiant intensity
- Peak wavelength λ p=940nm
- 2.54mm Lead spacing
- Low forward voltage
- Pb free
- The product itself will remain within RoHS compliant version.

Descriptions
- EVERLIGHT'S Infrared Emitting Diode(IR333-A) is a high intensity diode , molded in a blue transparent plastic package.
- The device is spectrally matched with phototransistor , photodiode and infrared receiver module.

Applications
- Free air transmission system
- Infrared remote control units with high power requirement
- Smoke detector
- Infrared applied system

Device Selection Guide

LED Part No.	Chip Material	Lens Color
IR	GaAlAs	Blue

EVERLIGHT

Package Dimensions
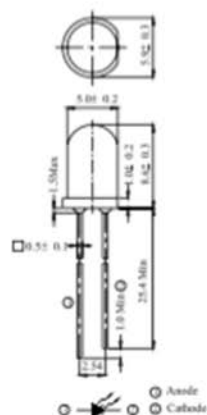
Notes: 1.All dimensions are in millimeters
2.Tolerances unless dimensions ±0.25mm

Absolute Maximum Ratings (Ta=25℃)

Parameter	Symbol	Rating	Units
Continuous Forward Current	I_F	100	mA
Peak Forward Current	I_{FP}	1.0	A
Reverse Voltage	V_R	5	V
Operating Temperature	T_{opr}	-40 ~ +85	℃
Storage Temperature	T_{stg}	-40 ~ +85	℃
Soldering Temperature	T_{sol}	260	℃
Power Dissipation at(or below) 25℃ Free Air Temperature	P_d	150	mW

Notes: *1:I_{FP} Conditions--Pulse Width≦100μs and Duty≦1%.
*2:Soldering time≦5 seconds.

EVERLIGHT

Electro-Optical Characteristics (Ta=25℃)

Parameter	Symbol	Condition	Min.	Typ.	Max.	Units
Radiant Intensity	Ee	I_F=20mA	7.8	20	--	mW/sr
		I_F=100mA Pulse Width ≤ 100 μs ,Duty ≤ 1%	--	85	--	
		I_F=1A Pulse Width ≤ 100 μs ,Duty ≤ 1%.	--	750	--	
Peak Wavelength	λ p	I_F=20mA	--	940	--	nm
Spectral Bandwidth	Δ λ	I_F=20mA	--	45	--	nm
Forward Voltage	V_F	I_F=20mA		1.2	1.5	V
		I_F=100mA Pulse Width ≤ 100 μs ,Duty ≤ 1%	--	1.4	1.8	
		I_F=1A Pulse Width ≤ 100 μs ,Duty ≤ 1%.	--	2.6	4.0	
Reverse Current	I_R	V_R=5V	--	--	10	μ A
View Angle	2 θ 1/2	I_F=20mA	--	20	--	deg

Rank

Condition：I_F=20mA

Unit：mW/sr

Bin Number	M	N	P	Q
Min	7.80	11.0	15.0	21.0
Max	12.5	17.6	24.0	34.0

113

Appendix C: Institutional Review Board Approval for Protocol

DEPARTMENT OF THE AIR FORCE
AIR FORCE RESEARCH LABORATORY
WRIGHT-PATTERSON AIR FORCE BASE OHIO 45433

MEMORANDUM FOR AFIT/ENV (MICHAEL MILLER)   JAN 1 0 2017

FROM: 711 HPW/IR

SUBJECT: IRB Approval for the Use of Human Volunteers in Research

1. Protocol title: Event Related Potential Evocation Using Unobtrusive Stimuli

2. Protocol number: FWR20170014H

3. Protocol version: v1.00

4. Risk: Minimal

5. Approval date: 10 January 2017

6. Expiration date: 9 January 2018
   Your renewal submission date is *one month prior* to your expiration date. The renewal is due
   9 December 2017

7. Expedited Review Category:
   ☐ 32CFR219.110(b)(1)   ☐ 32CFR219.110(b)(2)   ☐ 32CFR219.110(b)(3)

   ■ 32CFR219.110(b)(4)   ☐ 32CFR219.110(b)(5)   ☐ 32CFR219.110(b)(6)

   ☐ 32CFR219.110(b)(7)   ☐ 32CFR219.109: Full Board

8. Assurances and Agreements with Expiration Dates:
   a. AFIT DoD Assurance 50301: 5 October 2017
   b. Wright State University Assurance FWA00002427: 10 April 2017

9. The study objective is to determine if Event-Related Potentials (ERPs) and Visual Evoked
Cortical Potentials (VECPs) can be elicited and interpreted with minimal intrusiveness to the
human participant by using visual stimuli that are not perceived as flickering or stimuli which
emit light near or outside the human visible range. The stimuli of concern in this research are
near-infrared, infrared, and visible Light Emitting Diodes (LED).

114

10. All inquiries and correspondence concerning this protocol should include the protocol number and name of the primary investigator. Please contact the 711 HPW/IR office using the organizational mailbox at AFRL.IR.ProtocolManagement@us.af.mil or calling 937-904-8094 [DSN 674].

KIM E. LONDON, JD, MPH, CIP
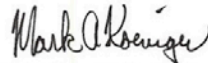Chair, AFRL IRB

1st Indorsement to AFIT/ENV (MICHAEL MILLER), 10 January 2017, Approval for Use of Humans in Research, Initial Review, FWR20170014H

MEMORANDUM FOR AFMSA/SGE-C

This protocol has been reviewed and approved by the AFRL IRB. I concur with the recommendation of the IRB and approve this research.

MARK A. KOENIGER
Brigadier General, USAF, MC, CFS
Commander
711th Human Performance Wing

Bibliography

Burle, B., Spieser, L., Roger, C., Casini, L., Hasbroucq, T., & Vidal, F. (2015). Spatial and temporal resolutions of EEG: Is it really black and white? A scalp current density view. *International Journal of Psychophysiology*, *97*(3), 210–220. http://doi.org/10.1016/j.ijpsycho.2015.05.004

Cheng, M., Gao, X., Gao, S., & Xu, D. (2002). Design and implementation of a brain-computer interface with high transfer rates. *IEEE Transactions on Biomedical Engineering*, *49*(10), 1181–1186. http://doi.org/10.1109/TBME.2002.803536

Cilliers, P. J., & Van Der Kouwe, A. J. W. (n.d.). A System for VEP Detection and Stimulus Phase Discrimination.

Citi, L., Poli, R., Cinel, C., & Sepulveda, F. (2008). P300-based BCI mouse with genetically-optimized analogue control. *IEEE Transactions on Neural Systems and Rehabilitation Engineering*, *16*(1), 51–61. http://doi.org/10.1109/TNSRE.2007.913184

Cohen, M. X. (2014). *Analyzing Neural Time Series Data: Theory and Practice*. *MIT Press*. http://doi.org/10.1017/CBO9781107415324.004

Diez, P. F., Torres M??ller, S. M., Mut, V. A., Laciar, E., Avila, E., Bastos-Filho, T. F., & Sarcinelli-Filho, M. (2013). Commanding a robotic wheelchair with a high-frequency steady-state visual evoked potential based brain-computer interface. *Medical Engineering and Physics*, *35*(8), 1155–1164. http://doi.org/10.1016/j.medengphy.2012.12.005

Donchin, E., Spencer, K. M., & Wijesinghe, R. (2000). The mental prosthesis: Assessing the speed of a P300-based brain- computer interface. *IEEE Transactions on Rehabilitation Engineering*, *8*(2), 174–179. http://doi.org/10.1109/86.847808

Endsley, M. R. (2015a). *Autonomous Horizons: System Autonomy in the Air Force - A Path to the Future* (Vol. 1). Retrieved from http://www.af.mil/Portals/1/documents/SECAF/AutonomousHorizons.pdf?timestamp=1435068339702

Endsley, M. R. (2015b). *Autonomous Horizons: System Autonomy in the Air Force - A Path to the Future* (Vol. 1).

Ferreira, A. L. S., Miranda, L. C., Miranda, E. E. C., & Sakamoto, S. G. (2013). A survey of interactive systems based on brain-computer interfaces. *SBC J Interact Syst*, *4*(1), 3–13.

Gao, S., Wang, Y., Gao, X., & Hong, B. (2014). Visual and auditory brain-computer interfaces. *IEEE Transactions on Biomedical Engineering*, *61*(5). http://doi.org/10.1109/TBME.2014.2300164

Graimann, B., Allison, B., & Pfurtscheller, G. (2010). Brain-Computer Interfaces, 1–27. http://doi.org/10.1007/978-3-642-02091-9

Herrmann, C. S. (2001). Human EEG responses to 1-100 Hz flicker: Resonance phenomena in visual cortex and their potential correlation to cognitive phenomena. *Experimental Brain Research*, *137*(3–4), 346–353. http://doi.org/10.1007/s002210100682

Hwang, H.-J. J., Ferreria, V. Y., Ulrich, D., Kilic, T., Chatziliadis, X., Blankertz, B., & Treder, M. (2015). A Gaze Independent Brain-Computer Interface Based on Visual Stimulation through Closed Eyelids. *Sci Rep*, *5*(October), 15890. http://doi.org/10.1038/srep15890

Hwang, H. J., Kim, S., Choi, S., & Im, C. H. (2013). EEG-Based Brain-Computer Interfaces: A Thorough Literature Survey. *International Journal of Human-Computer Interaction*, *29*(12), 814–826. http://doi.org/10.1080/10447318.2013.780869

iMotions. (2016). *EEG Pocket Guide*.

Kraemer, M., Abrahamsson, M., & Sjostrom, A. (1997). The neonatal development of the light flash evoked response. *Investigative Ophthalmology & Visual Science*, *38*(4), 302.

Kuś, R., Duszyk, A., Milanowski, P., Łabecki, M., Bierzyńska, M., Radzikowska, Z., … Durka, P. J. (2013). On the Quantification of SSVEP Frequency Responses in Human EEG in Realistic BCI Conditions. *PLoS ONE*, *8*(10). http://doi.org/10.1371/journal.pone.0077536

Landa, Leos; Krpoun, Zdenek; Kolarova, Martina; Kasparek, T. (2014). Homepage : E VENT - RELATED P OTENTIALS AND T HEIR, *56*(1), 17–23.

Lee, P.-L., Hsieh, J.-C., Wu, C.-H., Shyu, K.-K., Chen, S.-S., Yeh, T.-C., & Wu, Y.-T. (2006). The Brain Computer Interface Using Flash Visual Evoked Potentials and Independent Component Analysis. *Annals of Biomedical Engineering*, *34*(10), 1641–1654. http://doi.org/10.1007/s10439-006-9175-8

Lenhardt, A., Kaper, M., & Ritter, H. J. (2008). An adaptive P300-based online brain-computer interface. *IEEE Transactions on Neural Systems and Rehabilitation Engineering*, *16*(2), 121–130. http://doi.org/10.1109/TNSRE.2007.912816

Luck, S. J. (2005a). An Introduction to the Event-Related Potential Technique. *Monographs of the Society for Research in Child Development*, *78*(3), 388. http://doi.org/10.1118/1.4736938

Luck, S. J. (2005b). Ten Simple Rules for Designing ERP Experiments. *Event-Related Potentials: A Methods Handbook*, 408. http://doi.org/10.1371/journal.pcbi.0020012

Middendorf, M., McMillan, G., Calhoun, G., & Jones, K. S. (2000). Brain-computer interfaces based on the steady-state visual-evoked response. *IEEE Transactions on Rehabilitation Engineering*, *8*(2), 211–214. http://doi.org/10.1109/86.847819

Nakanishi, M., Wang, Y., Wang, Y.-T., Mitsukura, Y., & Jung, T.-P. (2014a). Generating visual flickers for eliciting robust steady-state visual evoked potentials at flexible frequencies using monitor refresh rate. *PloS One*, *9*(6), e99235. http://doi.org/10.1371/journal.pone.0099235

Norcia, A. M., Appelbaum, L. G., Ales, J. M., Cottereau, B. R., & Rossion, B. (2015). The steady-state visual evoked potential in vision research: A review. *Journal of Vision*, *15*(6), 4. http://doi.org/10.1167/15.6.4.doi

Prueckl, R., & Guger, C. (2009). A Brain-Computer Interface Based on Steady State Visual Evoked Potentials for Controlling a Robot. *Lecture Notes in Computer Science*, *5517*, 690–697. http://doi.org/10.1007/978-3-642-02478-8_86

Sakurada, T., Kawase, T., Komatsu, T., & Kansaku, K. (2015). Use of high-frequency visual stimuli above the critical flicker frequency in a SSVEP-based BMI. *Clinical Neurophysiology*, *126*(10), 1972–1978. http://doi.org/10.1016/j.clinph.2014.12.010

Singla, R., Khosla, A., & Jha, R. (2014). Influence of stimuli colour in SSVEP-based BCI wheelchair control using support vector machines. *Journal of Medical Engineering & Technology*, *38*(3), 125–34. http://doi.org/10.3109/03091902.2014.884179

Sur, S., & Sinha, V. K. (2009). Event-related potential: An overview. *Ind.Psychiatry J*. http://doi.org/10.4103/0972-6748.57865

Tartaglione, A., Spadavecchia, L., Maculotti, M., & Bandini, F. (2012). Resting state in Alzheimer's disease: a concurrent analysis of Flash-Visual Evoked Potentials and quantitative EEG. *BMC Neurology*, *12*, 145. http://doi.org/10.1186/1471-2377-12-145

Teplan, M. (2002). Fundamentals of EEG measurement. *Measurement Science Review*, *2*, 1–11. http://doi.org/10.1021/pr070350l

Treder, M. S., & Blankertz, B. (2010). (C)overt attention and visual speller design in an ERP-based brain-computer interface. *Behavioral and Brain Functions : BBF*, *6*, 28. http://doi.org/10.1186/1744-9081-6-28

Urigüen, J. A., & Garcia-Zapirain, B. (2015). EEG artifact removal-state-of-the-art and guidelines. *Journal of Neural Engineering*, *12*(3), 31001. http://doi.org/10.1088/1741-2560/12/3/031001

Wang, Yijun; Gao, Xiaorong; Hong, Bo; Gao, S. (2010). Practical Designs of Brain-Computer Interfaces Based on the Modulation of EEG Rhythms. In B. Braiman (Ed.), *Brain-Computer Interfaces* (pp. 137–154). Heidelberg: Springer-Verlag. http://doi.org/10.1007/978-3-642-02091-9

Wang, Y., Gao, X., Hong, B., Jia, C., & Gao, S. (2008). Brain-Computer Interfaces Based on Visual Evoked Potentials. *Ieee Engineering in Medicine and Biology Magazine*, *27*(5), 64–71. http://doi.org/10.1109/MEMB.2008.923958

Wang, Y., Wang, R., Gao, X., & Hong, B. (2006). A Practical VEP-Based Brain – Computer Interface, *14*(2), 234–240.

Wolpaw, J. R., Birbaumer, N., McFarland, D. J., Pfurtscheller, G., & Vaughan, T. M. (2002). Brain Computer Interfaces for communication and control. *Frontiers in Neuroscience*, *4*(113), 767–791. http://doi.org/10.3389/conf.fnins.2010.05.00007

Wu, C. H., Chang, H. C., Lee, P. L., Li, K. S., Sie, J. J., Sun, C. W., … Shyu, K. K. (2011). Frequency recognition in an SSVEP-based brain computer interface using empirical mode decomposition and refined generalized zero-crossing. *Journal of Neuroscience Methods*, *196*(1), 170–181. http://doi.org/10.1016/j.jneumeth.2010.12.014

Wu, Z. (2016). Physical connections between different SSVEP neural networks. *Scientific Reports*, *6*(April 2015). http://doi.org/10.1038/srep22801

Wu, Z., & Su, S. (2014). A dynamic selection method for reference electrode in SSVEP-based BCI. *PLoS ONE*, *9*(8). http://doi.org/10.1371/journal.pone.0104248

Yin, E., Zhou, Z., Jiang, J., Chen, F., Liu, Y., & Hu, D. (2013). A novel hybrid BCI speller based on the incorporation of SSVEP into the P300 paradigm. *Journal of Neural Engineering*, *10*(2), 26012. http://doi.org/10.1088/1741-2560/10/2/026012

Zhang, Y., Jin, J., Qing, X., Wang, B., & Wang, X. (2012). LASSO based stimulus frequency recognition model for SSVEP BCIs. *Biomedical Signal Processing and Control*, *7*(2), 104–111. http://doi.org/10.1016/j.bspc.2011.02.002

Zhang, Y., Xu, P., Cheng, K., & Yao, D. (2014). Multivariate synchronization index for frequency recognition of SSVEP-based brain-computer interface. *Journal of Neuroscience Methods*, *221*, 32–40. http://doi.org/10.1016/j.jneumeth.2013.07.018

Zhang, Y., Zhou, G., Jin, J., Wang, X., & Cichocki, A. (2015). SSVEP recognition using common feature analysis in brain-computer interface. *Journal of Neuroscience Methods*, *244*, 8–15. http://doi.org/10.1016/j.jneumeth.2014.03.012

REPORT DOCUMENTATION PAGE				Form Approved OMB No. 074-0188

The public reporting burden for this collection of information is estimated to average 1 hour per response, including the time for reviewing instructions, searching existing data sources, gathering and maintaining the data needed, and completing and reviewing the collection of information. Send comments regarding this burden estimate or any other aspect of the collection of information, including suggestions for reducing this burden to Department of Defense, Washington Headquarters Services, Directorate for Information Operations and Reports (0704-0188), 1215 Jefferson Davis Highway, Suite 1204, Arlington, VA 22202-4302. Respondents should be aware that notwithstanding any other provision of law, no person shall be subject to an penalty for failing to comply with a collection of information if it does not display a currently valid OMB control number.
PLEASE DO NOT RETURN YOUR FORM TO THE ABOVE ADDRESS.

1. REPORT DATE (DD-MM-YYYY) 06-03-2017	2. REPORT TYPE Master's Thesis	3. DATES COVERED (From – To) August 2015 – March 2017

TITLE AND SUBTITLE Alternate Stimuli for the Elicitation of Event-Related Potentials	5a. CONTRACT NUMBER
	5b. GRANT NUMBER
	5c. PROGRAM ELEMENT NUMBER
6. AUTHOR(S) Jackson, Bryan V., Captain, USAF	5d. PROJECT NUMBER 2015-189
	5e. TASK NUMBER
	5f. WORK UNIT NUMBER

7. PERFORMING ORGANIZATION NAMES(S) AND ADDRESS(S) Air Force Institute of Technology Graduate School of Engineering and Management (AFIT/EN) 2950 Hobson Way, Building 640 WPAFB OH 45433-7765	8. PERFORMING ORGANIZATION REPORT NUMBER AFIT-ENV-MS-17-M-195
9. SPONSORING/MONITORING AGENCY NAME(S) AND ADDRESS(ES) National Aeronautics and Space Administration Langley Research Center Hampton, VA 23681-2199 kellie.d.kennedy@nasa.gov and chad.l.stephens@nasa.gov ATTN: Kellie Kennedy and Chad Stephens	10. SPONSOR/MONITOR'S ACRONYM(S) NASA Langley
	11. SPONSOR/MONITOR'S REPORT NUMBER(S)

12. DISTRIBUTION/AVAILABILITY STATEMENT DISTRUBTION STATEMENT A. APPROVED FOR PUBLIC RELEASE; DISTRIBUTION UNLIMITED.

13. SUPPLEMENTARY NOTES This material is declared a work of the U.S. Government and is not subject to copyright protection in the United States.

14. ABSTRACT Brain-Computer Interfaces (BCIs) are systems that leverage user-brain activity to identify and perform specific functions. In applications requiring overt visual attention, focusing on visual stimuli with known temporal variation can elicit measurable changes in brain activity. However, elements of BCI applications can be intrusive. This research was designed to determine if Event-Related Potentials (ERPs), to include Steady-State Visually-Evoked Potentials (SSVEPs), could be elicited and interpreted from less obtrusive stimuli. Specifically, this research explores the use of variable frequency and long-wavelength (infrared) stimuli for SSVEP interpretation to explore the application of less obtrusive stimuli for application in BCIs. It was determined that increasing the primary wavelength of visual stimuli into the near infrared portion of the electromagnetic spectrum negatively impacts the observation of ERPs in human subjects. Additionally, the longer primary wavelengths of visual stimuli have a negative impact on the observation of target frequency band powers in SSVEP experiments. However, each of these signals were detected across the majority of participants for Light-Emitting Diodes (LEDs) with center frequencies as high as 770 nm and across some participants and conditions for LEDs with center frequencies as high as 830 nm.

15. SUBJECT TERMS Brain-Computer Interface, Event-Related Potential, Steady-State Visual Evoked Potential, Visual Evoked Potential

16. SECURITY CLASSIFICATION OF:			17. LIMITATION OF ABSTRACT	18. NUMBER OF PAGES	19a. NAME OF RESPONSIBLE PERSON Michael E. Miller, AFIT/ENV
a. REPORT	b. ABSTRACT	c. THIS PAGE	UU	121	19b. TELEPHONE NUMBER (Include area code) (937) 255-6565, ext 4651 (michael.miller@afit.edu)
U	U	U			